Measurement of Radioactivity Concentrations and Analysis of Radiation Hazards for Environmental and Industrial Samples Collected from Different Parts of Ethiopia

By

Yared Birhane Kidane

A DISSERTATION

SUBMITTED TO THE GRADUATE PROGRAMS OF
COLLEGE OF NATURAL AND COMPUTATIONAL SCIENCES
ADDIS ABABA UNIVERSITY
IN FULFILLMENT OF THE REQUIREMENTS FOR THE DEGREE OF

DOCTOR OF PHILOSOPHY
(NUCLEAR PHYSICS)

ADDIS ABABA, ETHIOPIA
JANUARY 2025

ADDIS ABABA UNIVERSITY

GRADUATE PROGRAMS

MEASUREMENT OF RADIOACTIVITY CONCENTRATIONS AND ANALYSIS OF RADIATION HAZARDS FOR ENVIRONMENTAL AND INDUSTRIAL SAMPLES COLLECTED FROM DIFFERENT PARTS OF ETHIOPIA

By
Yared Birhane Kidane
Department of Physics
Addis Ababa University

Approved by the Examining Board:

Dr. Tilahun Tesfaye Deressu Signature _____
Advisor

TBA Signature _____
Examiner

TBA Signature _____
Examiner

Dated: January 2025

ADDIS ABABA UNIVERSITY

DATE: **January 2025**

AUTHOR:	**Yared Birhane Kidane**
TITLE:	**Measurement of Radioactivity Concentrations and Analysis of Radiation Hazards for Environmental and Industrial Samples Collected from Different Parts of Ethiopia**
DEPARTMENT:	**Department of Physics**
DEGREE:	**PhD**
SUBMISSION:	**October 2024**
CONVOCATION YEAR:	**2024**

Permission is herewith granted to Addis Ababa University to circulate and to have copied for non-commercial purposes, at its discretion, the above title upon the request of individuals or institutions.

Signature of Author

This Work is Dedicated

to My beloved Parents, Birhane Kidane and Letemeskel Negash

CONTENTS

List of Tables

List of Figures

ACKNOWLEDGEMENTS

Above all, I want to express my gratitude to “God Almighty,” whose generosity made it possible for this work to advance and be successful.

I would like to extend my sincere gratitude to Dr. Tilahun Tesfaye, Nuclear Physics at the Department of Physics, Addis Ababa University, for overseeing this research study, provoking discussions, insightful remarks, ongoing support, and reviewing the entire article and for facilitating fruitful discussions that will benefit me for the rest of my life.

My Sincere thanks to Messebo cement factory and the staff members for their collaboration in sample collection. Also, I would like to thank Ethiopian Technology Authority (ETA) and the staff members for their technical support at the time of the experimental work and for allowing me to use their experimental facility.

I’m indebted to the financial support rendered to me by my alma matter Addis Ababa University and my employer Assosa University. I’m also grateful to the physics department chairperson Professor Fekadu Gashaw, W/o Tsilat Adinew (secretary), and the staff members of Physics Department (AAU), for giving me all the support I need during my study time.

Finally, I would like to forward my special thanks to my family and family relatives for there support through out my studding. Specially, I would like to thank my mother Letemeskel Negash for her encouragement and support to my study. I am very grateful for my friends, classmates and workfellow in Assosa University, specially physics department staff members.

Addis Ababa University — Yared Birhane Kidane

October 2024

ABBREVIATIONS AND ACRONYMS

A	mass number
AEDE	Annual Effective Dose Equivalent
AGDE	annual gonadal dose equivalent
Bq	Becquerel
$Bq\,kg^{-1}$	Becquerel per kilogram
CAT	Computed Axial Tomography
CB	conduction band
Ci	Curie
CNSC	Canadian Nuclear Safety Commission
CT	Computerized tomography
D_{eff}	annual effective dose equivalent
D_R	absorbed dose rate
DAP	di-ammonium phosphate
DNA	Deoxyribonucleic acid
DSA	digital signal analyzer
EC	electron capture
ELCR	Excess Life time Cancer Risk
ETA	Ethiopian Technology Authority
FDA	Food and Drug Adminstration
FWHM	Full Width at Half maximum
GCR	Galactic Cosmic Rays
GENIE	General Electric Network for Information Exchange
Gy	Gray
H_{ex}	external hazard index
HPGe	High purity germanium
Hz	hertz
rem	roentgen equivalent man
IAEA	International Atomic Energy Agency
IBM	International Business Machines Corporation
IC	internal conversion
ICRP	International Commission on Radiological Protection
ICRU	International Commission on Radiation Units
IT	isomeric transition

keV	kilo-electron volt
LET	Linear Energy Transfer
MCA	multi channel analyser
MDA	minimum detectable activity
MDC	minimum detectable concentration
MeV	Mega electron volt
mg/kg	milligram per kilogram
mg/L	milligram per liter
mL	milliliter(10^{-3}L)
$mSv\,y^{-1}$	millisievert per year
NaI (Tl)	Thallium activated sodium Iodide
$nGy\,h^{-1}$	nano Gray per hour
NORM	Natural Occurring Radioactivity Materials
NPP	Nuclear power plant
NRPB	National Radiological Protection Board (NRPB)
pCi/g	picocurie per gram
R	Roentgen
SEP	Solar energetic particles
Sf	spontaneous fission
SPSS	Statistical Package for Social Sciences
Sv	Sievert
TENORM	Technological Enhanced Natural Occurring Radioactivity Materials
UNSCEAR	United Nation Scientific Commission Effects of Atomic Radiation
USEPA	United States Environmental Protection Agency
USNRC	United States Nuclear Regulatory Commission
VB	valence band

ABSTRACT

In this study, the activity concentrations of ^{238}U, ^{226}Ra, ^{232}Th, and ^{40}K in various environmental and industrial product samples were determined using a gamma detection system. The industrial samples analyzed included cement raw materials and finished products, while the environmental samples comprised soil samples and medicinal plants. The measured mean activity concentrations of ^{226}Ra, ^{232}Th, and ^{40}K in the cement raw materials and products were found to be 21.1 ± 0.995, 53.2 ± 2.9, and $304 \pm 13.8\,\mathrm{Bq\,kg^{-1}}$, respectively. For soil samples from Mekelle City, the corresponding mean activity concentrations were 25.035 ± 1.788, 53.091 ± 4.22, and $371.34 \pm 14.26\,\mathrm{Bq\,kg^{-1}}$, respectively.

The mean specific activity concentrations of ^{238}U, ^{232}Th, and ^{40}K in soil samples from the districts of Menge, Sherkole, Assosa, and Bambasi were determined as follows: for Menge, 24 ± 1.2, 36.15 ± 2, and $275.5 \pm 13.3\,\mathrm{Bq\,kg^{-1}}$; for Sherkole, 35.14 ± 1.77, 47.3 ± 2.7, and $146 \pm 7.2\,\mathrm{Bq\,kg^{-1}}$; for Assosa, 45.2 ± 2.3, 70 ± 3.8, and $238.8 \pm 11.6\,\mathrm{Bq\,kg^{-1}}$; and for Bambasi, 61 ± 3.2, 89.2 ± 5.3, and $237.7 \pm 12.7\,\mathrm{Bq\,kg^{-1}}$. Regarding the medicinal plants, the mean activity concentrations of ^{238}U, ^{232}Th, and ^{40}K were found to be 7.82 ± 0.04, 28.67 ± 2.66, and $579.4 \pm 1.37\,\mathrm{Bq\,kg^{-1}}$, respectively.

The study also estimated the absorbed dose rate ($D\,(\mathrm{nGy\,h^{-1}})$), the annual effective dose rate ($E\,(\mathrm{mSv\,y^{-1}})$), the gamma index ($I_\gamma$), the hazard indices ($H_{\mathrm{ex}}$ and H_{in}), and the excessive lifetime cancer risk (ELCR). Notably, the specific activity concentration of ^{40}K in *Moringa oleifera* exceeded the recommended safe limit. Meanwhile, the measured mean radioactivity concentrations in the Mekelle soil, Messebo cement raw materials, and cement products were below the safe values of 35, 30, and $400\,\mathrm{Bq\,kg^{-1}}$ for ^{226}Ra/^{238}U, ^{232}Th, and ^{40}K, respectively. However, the mean concentrations in soil samples from the Assosa, Bambasi, Menge, and Sherkole districts exceeded these safe values. Consequently, such elevated concentrations pose potential health risks, and continuous monitoring is recommended.

Keywords: Cement ·HPGe Detector ·Gamma-ray ·Medicinal Plant ·Radioactivity ·Radionuclide ·Soil

CHAPTER 1

INTRODUCTION

1.1 Background and Motivation of the Study

Radioactivity is a natural phenomenon that has existed since the Earth's formation. It originates from both natural sources, such as the decay of uranium, thorium, and potassium isotopes, as well as from anthropogenic activities, including industrial processes, medical applications, and nuclear power generation [3]. In many regions, exposure to natural sources of radiation contributes significantly to the overall radiation dose received by populations. However, industrial activities, particularly mining and energy production, have the potential to elevate levels of radiation exposure, making it a growing concern [2].

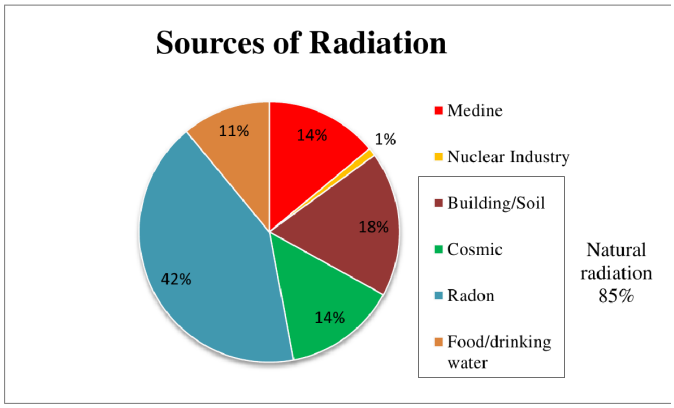

Figure 1.1: Sources of natural and anthropogenic radioactivity in the environment [2].

Ethiopia, like many other countries, features diverse geological formations, industrial activities, and environmental conditions that can lead to varying levels of natural and artificial radioactivity. Regions with significant mineral deposits, industrial complexes, and energy production facilities may exhibit elevated concentrations of radionuclides in the environment. For instance, activities such as coal combustion and mining can increase the levels of naturally occurring radioactive materials (NORMs), which may be further elevated by industrial processes into Technologically Enhanced Naturally Occurring Radioactive Materials (TENORMs) [4]. These conditions raise concerns about potential radiation hazards affecting both environmental and public health.

The primary motivation for this study arises from the need to gain a thorough understanding of radioactivity levels across various regions of Ethiopia. Considering the nation's economic growth and industrial expansion, it is crucial to evaluate how these activities may impact environmental radioactivity and the potential radiation hazards they present. This evaluation is especially important because radiation exposure, even at low levels, poses health risks, including an increased likelihood of cancer and genetic mutations with prolonged exposure periods [5].

Moreover, international standards set by organizations such as the International Atomic Energy Agency (IAEA) and the World Health Organization (WHO) provide guidelines for safe radiation

exposure levels [5]. For effective regulatory control, however, it is essential to have localized data on radioactivity concentrations to inform decision-making and ensure public and environmental safety. Figure 1.2 illustrates the potential pathways through which radiation can impact humans and the environment.

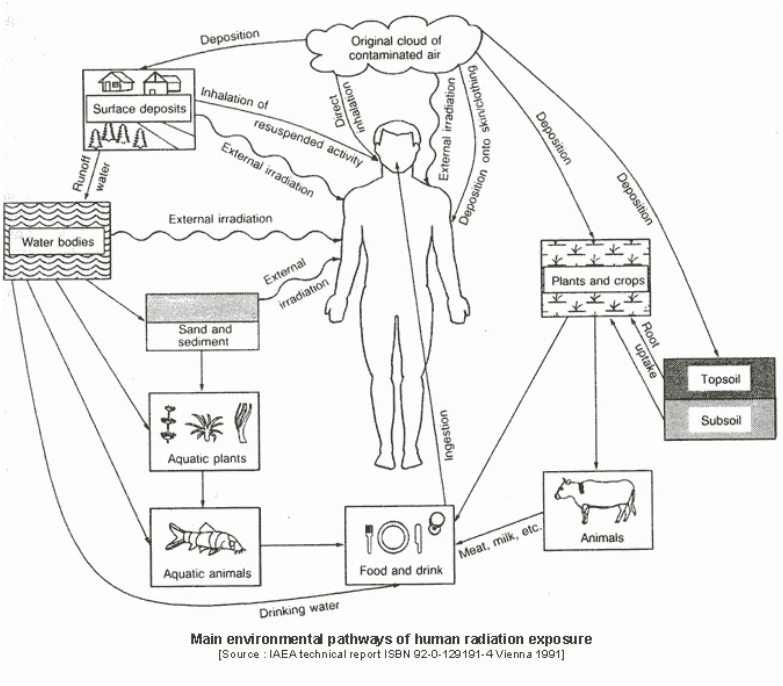

Figure 1.2: Potential pathways of radiation exposure and its impact on humans and the environment [3].

The absence of detailed studies on radioactivity concentrations and the associated hazards in Ethiopia further drives this research. This study aims to address this gap by measuring radioactivity levels in environmental and industrial samples from various regions of Ethiopia, analyzing the data, and assessing potential radiation hazards. The findings will provide essential insights into the impact of industrial activities on the local environment and help inform regulatory bodies about necessary safety measures.

1.2 Objectives of the Study

The objectives of this study are:

- To measure radioactivity concentrations in environmental and industrial samples from different parts of Ethiopia.
- To assess potential radiation hazards based on the measured data, using internationally recognized hazard indices.
- To compare the results with internationally accepted NORM guidelines to evaluate compliance with safety standards.
- To make recommendations for mitigating potential radiation hazards in both industrial and environmental contexts.

This research will enhance understanding of radioactivity in Ethiopia, providing critical data for ensuring public health and environmental protection while aligning with global safety standards.

1.3 Research Questions

The study is guided by the following research questions:

1. What are the radioactivity levels in the sampled areas across Ethiopia?
2. How do these levels compare to international safety standards for radiation exposure?
3. What potential hazards do these radioactivity levels pose to humans and the environment?

1.4 Scope of the Study

This study focuses on measuring radioactivity concentrations and assessing radiation hazards in environmental and industrial samples collected from various regions of Ethiopia, specifically Mekelle City, Assosa, Bambasi, Menge, and Sherkole. The study targets two main types of samples: raw materials used in cement production and finished cement products.

A thorough comparison of measured radioactivity levels with internationally accepted safety standards is undertaken to assess whether the concentrations of radioactive materials pose significant health risks to the environment, industrial workers, or the general public. Additionally, the study evaluates the effectiveness of existing safety regulations and monitoring protocols in Ethiopia, aiming to provide evidence-based recommendations for improving radiation safety in both environmental and industrial contexts.

The geographic focus encompasses both industrial activities (Mekelle City) and regions with environmental concerns (Assosa, Bambasi, Menge, and Sherkole), ensuring that both natural and industrial sources of radioactivity are comprehensively addressed.

1.5 Significance of the Study

This study provides a comprehensive assessment of environmental and industrial radioactivity in several Ethiopian regions, including Mekelle City, Assosa, Bambasi, Menge, and Sherkole. By measuring the concentrations of natural radionuclides in these regions and evaluating associated radiation hazards, the study makes crucial contributions:

1. **Contribution to Environmental Radiation Studies**: The research adds to the existing body of knowledge on naturally occurring radioactive materials (NORM) across various Ethiopian settings. The findings will serve as a baseline for future radiation monitoring in the country, informing environmental safety practices and public health policies.
2. **Impact on Industrial Safety and Public Health**: Evaluating radioactivity in cement production materials and final products is critical for ensuring the safety of workers and the general public. The study assesses the radiological hazards faced by workers handling raw materials in cement production and provides an evaluation of the safety of cement products used in construction.
3. **Regulatory and Policy Implications**: The study's results will contribute to the development and refinement of radiation safety regulations in Ethiopia. By comparing the measured

radioactivity levels with internationally accepted standards, the research offers evidence-based recommendations for setting safety limits and implementing radiation protection guidelines.

4. **Supporting Sustainable Development**: Ensuring the safety of industrial processes, such as cement production, is vital for sustainable industrial growth in Ethiopia. This study's findings can help industries adopt safer practices while supporting government efforts to balance economic development with public and environmental health protection.

Overall, the study provides a scientific foundation for informed decision-making on environmental protection, industrial safety, and public health in Ethiopia. Its outcomes have the potential to enhance both environmental and occupational radiation safety standards.

1.6 Structure of the Dissertation

The dissertation is organized as follows:

- **Chapter 1**: Provides the background, objectives, research questions, and structure of the study.
- **Chapter 2**: Reviews the literature on natural and artificial radioactivity, health effects of radiation, and previous studies relevant to the topic.
- **Chapter 3**: Describes the materials and methods used for sample collection, preparation, and analysis, including gamma spectrometry techniques.
- **Chapter 4**: Presents the results of measurements, including radioactivity concentrations and hazard indices, and compares them to safety standards. The presentation of the findings in the context of their implications for public health, environmental safety, and regulatory practices in Ethiopia.
- **Chapter 5**: Concludes the study, summarizing key findings and offering recommendations for future research and policy-making.

CHAPTER 2

LITERATURE REVIEW

2.1 Radiation Dose Conversion Methods

In the study of radioactivity concentration for different types of materials or substances, measurements are often expressed in various SI units. Some of the basic radioactive dose conversion units are given below [1, 6]:

1. 1 gray (Gy) = 100 rad
2. 1 rad = 10 milligray (mGy)
3. 1 sievert (Sv) = 1,000 millisieverts (mSv) = 1,000,000 microsieverts (μSv)
4. 1 sievert = 100 rem
5. 1 becquerel (Bq) = 1 count per second (cps)
6. 1 curie (Ci) = 37,000,000,000 becquerels (Bq) = 37 gigabecquerels (GBq)

For x-rays and gamma rays, 1 rad = 1 rem = 10 mSv. For neutrons, 1 rad = 5 to 20 rem (depending on the energy level) = 50-200 mSv [7]. For alpha radiation (helium-4 nuclei), 1 rad = 20 rem = 200 mSv. The primary unit for measuring radioactivity is the curie, which historically was defined as the disintegration rate of 1 g of radium-226, equaling exactly 3.7×10^{10} disintegrations per second (dis/sec) [8].

In recent years, the becquerel (Bq) has become the standard unit for disintegration rate, where 1 Bq = 1 dis/sec. The gray (Gy) is used as the unit of absorbed dose in radiation exposure, representing the joules deposited per kilogram. Due to the high ionization density, alpha particles are less penetrating than beta or gamma radiation but cause greater localized damage in biological tissue [9].

Table 2.1: Conversion factors for radiation dose measurements [1].

Unit Conversion	Factor
1 Gy to rad	100
1 Sv to mSv	1000
1 Bq to cps	1
1 Ci to Bq	37 GBq

Table 2.1 provides conversion factors for various radiation dose units commonly used in measurements and safety guidelines.

2.1.1 Absorbed Dose Units

Absorbed dose rate refers to the rate at which ionizing radiation is absorbed per unit of time. The absorbed dose (D) is defined as the mean energy (e) imparted by ionizing radiation to matter of

mass m, divided by the mass, $D = e/m$. This expresses the energy deposition in any substance by all types of ionizing radiation [1]. The traditional unit of absorbed dose is the rad, equal to 100 erg g^{-1} or 0.01 J kg^{-1}. The SI unit is the gray (Gy), where 1 Gy = 1 J kg^{-1} [8].

2.2 Monitoring of Naturally Occurring Radiation in the World

The average effective background radiation dose rate is approximately 2.4 mSv per year, with 1.1 mSv attributed to terrestrial and cosmic radiation and another 1.3 mSv from radon exposure [2, 10]. In regions with a substantial radioactive component in the earth's crust, background radiation can be 10-20 times higher than average. Studies indicate that radiation exposures from mineral extraction and processing are relatively low compared to those from natural ionizing radiation sources [3].

Globally, the average annual effective dose from mineral extraction is about 20 μSv [8]. For example, mining assessments in Australia have shown that those living near facilities may receive over 1 mSv annually, primarily from external irradiation due to scattered heavy minerals [11]. The highest estimated doses from dust inhalation reach about 2.5 mSv/year for individuals residing within 2 km of processing plants.

The average radioactivity concentrations globally are 35 Bq kg^{-1} for ^{238}U, 30 Bq kg^{-1} for ^{232}Th, and 400 Bq kg^{-1} for ^{40}K [2]. Population-weighted absorbed dose rates from terrestrial gamma radiation range from 50 to 59 nGy h^{-1}, with an upper annual dose equivalent limit of 5 mSv [10].

2.2.1 Outdoors

The primary source of outdoor external exposure is terrestrial radionuclides present in trace levels in soil. Higher radiation levels are found in igneous rocks like granite, while sedimentary rocks typically have lower concentrations, except for certain shales and phosphate rocks [7]. Surveys reveal that the activity concentration of ^{40}K in soil is an order of magnitude higher than that of ^{238}U or ^{232}Th [2].

2.2.2 Indoors

Indoor exposure to gamma rays is generally higher due to the use of earth materials in building construction. Occupancy factors further amplify indoor exposure, with population-weighted average exposure rates of 58 nGy h^{-1} outdoors and 81 nGy h^{-1} indoors [8]. Using a conversion coefficient of 0.7 Sv Gy^{-1} from absorbed dose in air to effective dose for adults, the average annual indoor and outdoor effective dose is calculated as follows:

For indoor exposure:

$$84 \text{ nGy h}^{-1} \times 8,760 \text{ h} \times 0.8 \times 0.7 \text{ Sv Gy}^{-1} = 0.41 \text{ mSv} \tag{2.1}$$

For outdoor exposure:

$$59 \text{ nGy h}^{-1} \times 8,760 \text{ h} \times 0.2 \times 0.7 \text{ Sv Gy}^{-1} = 0.07 \text{ mSv} \tag{2.2}$$

The resulting global average of the annual effective dose is approximately 0.48 mSv, with individual country values generally ranging between 0.3-0.6 mSv [2].

2.2.3 Internal Exposures

Internal exposure arises from the intake of terrestrial radionuclides through inhalation and ingestion [9]. The dose rate from ^{40}K can be directly and accurately determined from its concentration in the human body. However, the assessment of uranium and thorium series radionuclides requires complex chemical analysis of body tissues or bioassay measurements. Annual equivalent doses due to ^{40}K amount to approximately 165 μSv y^{-1} for adults and 185 μSv y^{-1} for children [12].

2.3 Radon Exposure and Associated Hazards

Radon (^{222}Rn) and thoron (^{220}Rn), both inert radioactive gases, are products of the decay of ^{226}Ra and ^{232}Th, respectively. They contribute significantly to internal exposure through inhalation, depositing their short-lived decay products in the respiratory tract. The isotopes belong to three natural decay series: ^{219}Rn (from the ^{235}U series), ^{220}Rn (from the ^{232}Th series), and ^{222}Rn (from the ^{238}U series), with half-lives of 3.96 s, 55.6 s, and 3.82 days, respectively [13].

Radon release involves three steps: emanation from mineral grains into pore spaces, transport through diffusion or advection, and exhalation into the atmosphere. The emanation coefficient, or emanating power, represents the fraction of radon atoms released from a radium-bearing grain into the pore space. The presence of radon and its progeny contributes to the inhalation dose, leading to bronchial irradiation from alpha particles emitted by decay products.

2.4 Cosmic Rays and Altitude Effects

Cosmic radiation, originating from space, is another significant source of natural exposure, varying with altitude. The population-weighted average dose rates are estimated to be 1.25 times that at sea level for directly ionizing and photon components, and 2.5 times higher for neutrons. As a result, the estimated world average effective dose from cosmic rays is approximately 380 μSv a^{-1}, with significant variations based on altitude [2].

2.5 Radionuclides in Industrial Products

Many industrial products contain naturally occurring radioactive materials (NORM), as raw materials are often mined, transported, and processed for use. The cement industry, for example, uses raw materials such as limestone, silica, and alumina, which can contain radionuclides. The concentration of these radionuclides can contribute to radiation exposure in both workers and end-users.

2.5.1 Cement Production and Building Materials

Cement, an essential component of concrete, is manufactured from calcareous raw materials, predominantly limestone, silica, alumina, and iron oxide. The material composition of clinker, the primary component of Portland cement, is shown in Table 2.2.

During cement production, the prepared raw materials are heated in a kiln at temperatures up to 1450°C to form clinker, which is then ground with additives to produce cement. Coal is often used as a fuel in this process, which can contribute to the release of radionuclides into the air.

Table 2.2: Material composition of clinker, the primary component of Portland cement

No	Raw Material	Source	Percentage by Mass
1	Limestone	Limestone, shells, chalk	60-70
2	Silica	Sand, fly ash	17-25
3	Alumina	Clay, shale, fly ash	2-8
4	Iron Oxide	Iron ore	0-6

The primary emissions from cement production are ^{222}Rn and ^{210}Pb. Industrial plants such as phosphate industries and gas-fired power production can also release radon and its progeny. Worldwide annual exposure to natural radiation sources is estimated to be between 1-10 mSv, with 2.4 mSv being the current average estimate [2].

2.5.2 Pozzolanic Cement and Radiation Hazards

Pozzolanic Portland cement (PPC) is produced by mixing Portland clinker with natural pozzolana. While pozzolana contributes to the durability and chemical resistance of the cement, its addition can also influence the radioactivity levels. Figure 2.1 illustrates the process of cement production.

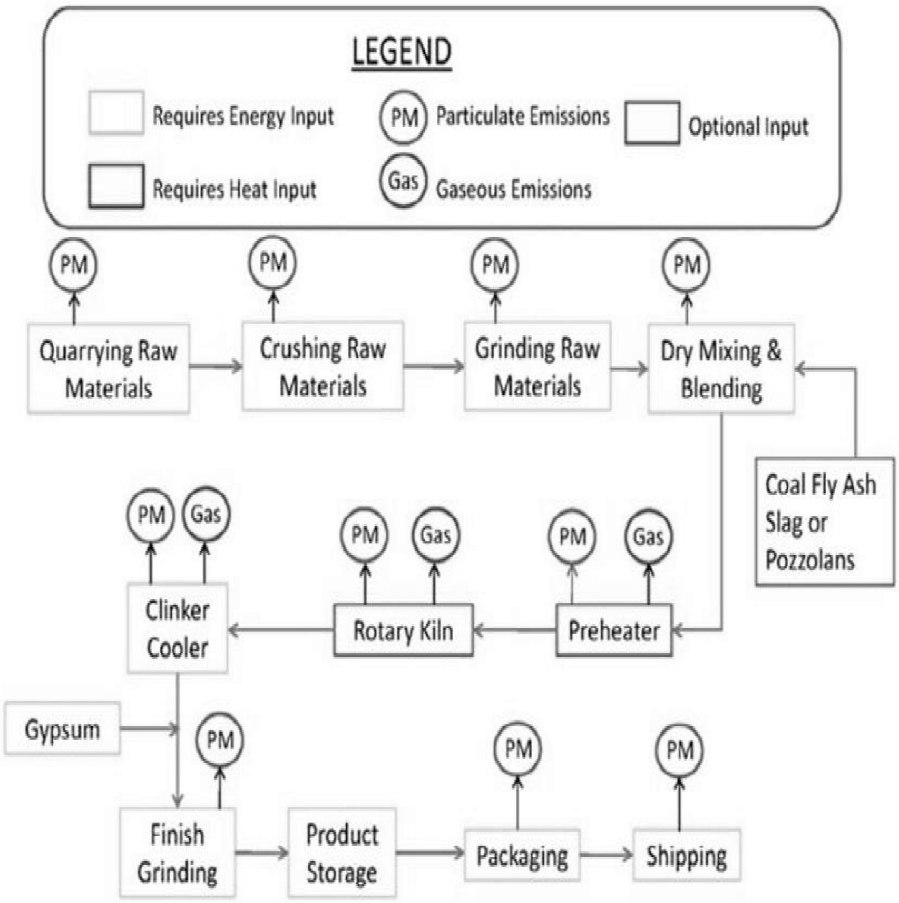

Figure 2.1: Process of cement production

In Ethiopia, the radioactivity concentrations in raw materials used for cement production, including limestone and additives, are investigated to assess potential radiation hazards to workers and

consumers. By analyzing the levels of radionuclides such as ^{238}U, ^{232}Th, and ^{40}K, the study aims to compare the results with international standards for radiation safety.

In summary, the presence of natural radionuclides in environmental and industrial samples is a global phenomenon, contributing to varying degrees of radiation exposure. Understanding the dose conversion units, monitoring exposure levels, and analyzing the concentration of radionuclides in both outdoor and indoor settings are critical to ensuring public and environmental safety. Furthermore, the evaluation of radiation hazards in industrial products like cement, as well as in building materials and medicinal plants, is essential for establishing effective regulatory controls and mitigating health risks.

In Ethiopia, there is a need for comprehensive research to assess radioactivity levels in various contexts, from industrial processes to environmental settings. The findings will provide essential data for public health and safety standards, and support efforts to align with global best practices in radiation protection.

CHAPTER 3

RESEARCH METHODOLOGY

3.1 Sample Collection and Preparation

The procedures followed for sample collection, sample preparation, measurement instruments, and data analysis are presented. Samples of the soils, cement, and medicinal plants were randomly and selectively obtained from different separate places. The samples are given code names during collection, and the following factors were put into consideration:

- The tools are cleaned when used against any possible contaminants.
- Care was taken to get soils above 30 cm separately from that of below this depth.
- Samples were collected from the all-over cross section of each area to ensure proper presentation.
- Checking the top hummus and other vegetation if they are removed from the sampling point before the sample collection.
- All the collected samples were labeled and stored in polyethylene bags and those samples were put in a shielded container to minimize radiation exposure levels during transportation.

3.1.1 Site selection and Instrumental setup for environmental samples

Lake and reservoir sediments give unique substrates for investigating the occurrence of many energy-related pollutants. They are the main sink for materials entering watersheds and may be dated by radioactive methods to provide a depositional past history. Also, accurate coring such as minimal disturbance of sediments, which is of great importance to paleolimnological investigations, especially those aimed at reconstructing the deposition history and inventories of pollutants deposited through atmospheric processes.

The very low sufficient performing coring system can cause mistakes or by taking sediment formation cores from locations in lakes that are not representative of atmospheric deposition, for example, In areas which are affected by sediment focusing (excessive erosion) can often lead to wrong interpretation of actual events. Using the sphincter corer with a tripod modification for taking the sediment cores [14].

The site or areas chosen should be flat and open area. Geographical landscapes that have obstractions such as boulders, large felled or standing trees, and any man-made materials should be avoided as these will prevent the flux from the underlying soil. When the ground is not flat it will result in anomalies since the soil surface area close to the detector is increased, and then the surface contribution from large distances is reduced. For measurements of fallout radionuclides, the area must be undisturbed in that water and wind erosion as well as a human activity, such as cultivating,

would tend to upset the distribution of any deposited activity. Different mapping tools criteria can be used for site selection. The wind roses and atmospheric dispersion calculations provide useful guidance in selecting appropriate soil sampling locations.

3.1.2 Experimental procedures and sample preparation

The samples must be collected on purposeful means from the sampling sites and the samples will be air-dried at room temperature, The dried samples will be ground until homogenized. The powdered samples will be taken to the research laboratory using polyethylene capsules or vials and processed in such a way suitable for experimental gamma-ray detector.

The sampling of soil is a useful to determine the concentrated amounts of airborne long-lived radioactive and stable contaminants that accumulated on the ground. Soil sampling is mostly questionable value to estimate small increments of deposition over a few years or less. It is not recommended as a routine method of environmental monitoring except in pre-operational surveys. The purpose of the project such as deposit, resuspension, root uptake should express the type of sampling such as total inventory, surface sampling, depth profile. Site characteristics, such as soil type, topography, source, and current distribution of the contaminant must be taken into account when designing the study. Other factors to be considered in the design stage are first, the uniformity of the deposited contamination, second, the required accuracy necessary to provide reasonable results, and third one is a minimization of cross-contamination.

Another requirement needed for planning and carrying out the pretreatment of samples is, the reference state of the samples that will be used in reporting the results of the measurements. For example, samples of soil, vegetation or sediment are usually weighed before being analyzed, and the results are reported about unit weight and the unit area from which the samples were collected. Normally these types of samples are weighed directly after collection which is wet weight, by dried and measure the weight again and labeled as dry weight before those are analyzed. Under this procedures, the researcher must ensure that all samples are dried to the same extent to report results per unit dry weight. The restriction is lifted if results are reported per unit weight or unit area of sample collection. The pretreatment process to be used can have complicated decisions, if the process is such that it may alter the property of the sample that is to be measured. If a volatile component, for example iodine is to be measured in vegetation, the pretreatment of the vegetation sample must not be such as to volatilize that component using the procedure.

The soil may be crushed to reduce the size and sieved to remove sample content above the desired size, blended to obtain a more homogenous distribution of particle sizes, or milled to reduce the particle size of the soil. If the sample was sieved or split in the field or a small sample was taken, the preparation process may be eliminated. For some reason, it is possible to remove large size stones and not grind them, but they must be weighed separately. The samples were air-dried, crushed to break up large rocks, blended to allow a representative aliquot to be removed, and only this crushed sample is pulverized. The pulverizing reduces the soil to standard particle size.

As per procedures manual of Environmental Measurments Labratory (EML) 3.1, each sample was cleaned, dried, and crushed into fine powder by using a jaw crusher. The samples were dried in a temperature-controlled heat oven at $100^{\circ}c$ for about 10-24 hours depending on the soil moisture. The

dried soil samples were pulverized into fine powder by grind material, and the powdered samples were sieved through 0.25 mm mesh to keep uniform grain size and obtain homogeneous samples for measurements. About 500 g of weights of the samples were recorded using an electrical balance, the homogeneous samples were packed and sealed in well labeled airtight cylindrical Marinelli beaker and stored for four weeks (28 days) before gamma-ray analysis, this time allows to achieve secular equilibrium between progenies and their daughter's radionuclides.

The containers were sealed tightly with insulating tape around their opening for blocking the possibility of moisture contamination. To maintain the radioactive secular equilibrium between ^{226}Ra and its daughter products, the sealed containers were stored for four weeks. Measurement was performed with calibrated source samples, which contain a known activity and also have geometries identical to that of the evaluated samples. As shown in Figure 3.1, the samples were packed using Ethiopian Radiation Protection Authority (ERPA)/Ethiopian Technology Authority (ETA) Marinelli beakers, which have a sample geometry of 538 G-E.

Figure 3.1: Sealed samples in Marinelli beakers

3.2 Gamma Ray Spectrum Detector

Ionizing radiation can be measured in terms of the physical and chemical effects of its interaction with matter. Most laboratory methods are based mainly on the ionizing properties of radiation and the use of instruments that convert the emitting radiation to electrical signals. Ionization chambers, Proportional counters, Geiger-Muller tubes, Scintillation counters, Semiconductor detectors, Thermoluminescence detectors, and various mechanical and chemical track detectors are used to monitor and quantify the α, γ, and β, radiation of the environment. The nature of the radiation and its character govern the choice of a suitable detector.

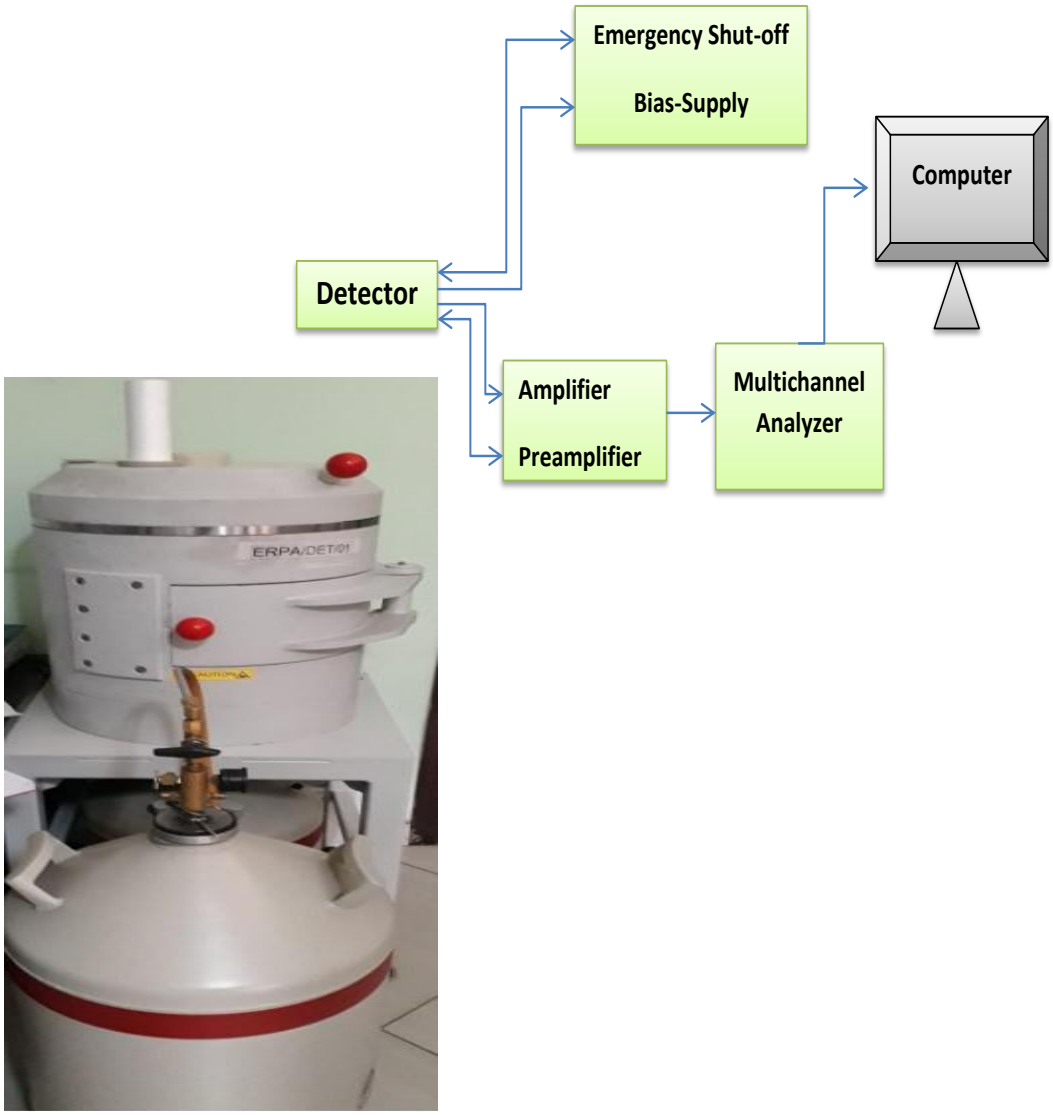

Figure 3.2: HPGe detector compound process line

High-purity germanium detector (HPGe) is designed to measure gamma radiation. The γ radiation has specific energies depending on which isotope it was emitted by, allowing for simple identification of the radionuclide content of a sample once the energy of the gamma radiation has been measured. A photon can get absorbed by an atom in a process called the photoelectric effect. If the photon isn't fully absorbed by the electron it may be detected by transferring a part of its energy into the

recoiling electron and this interaction is called Compton scattering. In this study, the measurement of radioactivity concentration has been done using gamma-ray spectra coupled with the HPGe detector of the Ethiopian Radiation Protection Authority (ERPA).

This research work was carried out using gamma spectrometry analysis. For each sample, it was counted for 28,800 seconds to achieve minimum counting error in an HPGe detector and which is coupled to a multichannel analyzer by a preamplifier base as shown in Figure 3.2. The detector has a resolution of about 1.8 keV which has the capability of identifying the gamma-ray energies used for the acquisition. The specific activity of ^{238}U was assessed from gamma-ray lines of ^{214}Pb at 351 keV and ^{214}Bi at 609.3 and 1764.5 keV, while the activity of ^{232}Th had been evaluated from gamma-ray lines of ^{228}Ac at 338.4, 911.1, and 968.9 keV, ^{212}Pb at 238.63 keV, and ^{208}Tl at 583.19 keV. The specific activity of ^{40}K was directly determined from its gamma-ray line at 1460.8 keV [15]. The detector of ERPA has 77% efficiency and calibration was done using IAEA reference samples, which was supplied by IAEA for the Ethiopian Radiation Protection Authority. The detector was calibrated by ^{60}Co and ^{137}Cs, which are the quality standard sources according to ISO 9001. The ISO/IEC 17025 quality standard was used to calibrate the detector.

The germanium crystal received a voltage of +4500 V, which has to be cooled by the liquid nitrogen beforehand. The electron and hole pairs are created after radiation interacts with the germanium crystal. The applied voltage causes these pairs to travel along a circuit and that can then be recorded as the detector's signal output because the energy deposited by the radiation is proportional to the number of electron-hole pairs. The pre-amplifier collects the charge deposited by the absorbed photons and used as the interface between the detector and the amplifier. The module which is bias supply that applies the voltage over the germanium crystal, that is to make sure that no voltage is applied before the germanium crystal cooled sufficiently. An emergency shut-off circuit is connected to the detector's cryostat. This used for the bias supply to be turned off if the crystal temperature exceeds a certain temperature. The MCA measures the pulse height of each event, which is proportional to the energy deposited in the detector and assigns each event into a channel.

Each channel represents a certain range of pulse heights. The amplifier used to amplify the signal, and allowing control of which energy ranges will be classified into which channels by the multi channel analyzer (MCA). Also, the amplifier allows for the manipulation of the pulse shape of the detector signal. The detector signal makes small imperfections that comes from system noise, which is caused by the electronics. The pile-up effects can happen which is caused by many pulse signals in a short time, it depends strongly on the length of each pulse. Amplifiers allow for adjustments to be made to the shaping time of the pulse, then it allows the user to balance noise and pulse pile-up effects to fit the application requirements.

The pulse signal of the detector may not return to its baseline after each pulse, but over or undershoot the baseline. This increases pileup effects in the multi channel analyzer. To counteract this the amplifier has a pole-zero (P/Z) adjustment, if properly set achieved then the pulse will immediately returns to the baseline. When radiation bombarded the shielding material, then the atom's inner electron shell can form vacancies. After vacancies are filled, the x-rays are emitted by the radiation and which are called a material characteristic x-ray and may show up as peaks in the pulse height spectrum of HPGe detector. The MCA sorts each event into a channel but does not indicate which event matches with what energy. By dividing the count rate with the intensity in percent we obtain a

measure of the detector's relative efficiency.

Sources such as ^{214}Bi, ^{214}Pb, ^{212}Pb, and ^{228}Ac are part of the decay chain of ^{238}U, ^{235}U, and ^{232}Th which are commonly found in the ground. ^{40}K can be found in humans as well as food like bananas. ^{137}Cs, accumulated in the environment by human activities such as atomic bomb testing and nuclear accidents. The ^{226}Ra content was not based on the 186 keV peak area of ^{226}Ra itself because this area is interfered by that of ^{235}U. Moreover, the abundance of this photon energy is limited (3.3%), which would result in a relatively high limit of detection for ^{226}Ra. Instead, the ^{226}Ra concentration is determined as the average of the equilibrium concentrations of ^{214}Pb and ^{214}Bi, likewise the ^{232}Th activity is calculated from ^{212}Pb and ^{228}Ac [16].

The efficiency of a detector is a measure of the probability that an incident photon will be absorbed in the detector. It is usually stated as the ratio of recorded counts over incident photons. The energy resolution of a detector is a measure of its ability to distinguish between two gamma rays of only slightly different energies. This is usually defined as the full width of a photo-peak at half the maximum amplitude (FWHM) divided by its energy. Instruments used in gamma-ray spectrometry are usually specified by the energy resolution of the ^{137}Cs photo peak at 662 keV. Dead-time refers to the finite time required for a detector to process an individual particle of radiation. During this time all incoming pulses are ignored. Dead-time should be as small as possible. Gamma-ray spectrometry uses the direct proportionality between the energy of an incoming gamma-ray and the pulse amplitude at the output of the detector. After amplification and digitization, the pulse amplitudes are analyzed, and the output of the spectrometer is an energy spectrum of detected radiation. Since individual radionuclides emit specific gamma-ray energies, gamma-ray spectra can be used to diagnose the source of the radiation.

3.2.1 Spectrum analysis

In order to analysis data on the gamma spectrum, the procedural manuals which have specific energy for specific radionuclides can be used. In many cases, the built-in peak area estimate features of state of the art analyzers are used in providing quick results in the field. Prominent peaks are identified in a benchmark spectrum and the appropriate regions of interest are set up. On certain analyzers, function keys are programmed using the net peak area, counting time, and calibration factor (N/I and N/A). They used to provide an instantaneous readout of exposure rate and concentration. For more complete data reduction a small computer is interfaced with the analyzer to run a spectrum analysis program. If desired a portable system may be configured using a battery-powered laptop computer.

The standard analysis program for specific gamma-ray spectrum was performed [17].
1. Based on a two point energy calibration as set by the operator, certain peaks which are characteristic of typical environmental spectra are identified, namely [13].

1. the 186, 295, 352, 609, 1120 and 1765 keV peaks in the ^{238}U series;

2. the 583, 911, 966 and 2615 keV peaks in the ^{232}Th series;

3. the 1460 keV peak of ^{40}K;

4. the 662 keV peak of ^{137}Cs.

These peaks are defined by set energy bands where the left and right channel markers are representative of the Compton continuum.
2. The counts between the energy boundaries for each of the above peaks are summed. The background counts in three channels on each side of a peak are averaged, and the result is used as an estimate of the baseline under the peak. This is multiplied by the number of channels in the peak and subtracted out from the total counts in the peak band to yield the net peak counts.
3. Detector specific calibration factors are applied to convert from peak count rate to exposure rate and concentration or inventory.
4. A printout is made listing count rates, converted quantities, and associated statistical counting errors.
5. Permanent storage of the spectrum is made on either magnetic tape or diskette.
6. There is a possibility that, an automated search is performed to identify any peaks present in the spectrum. Data such as nuclide, half-life, (γ-ray intensity and associated energy are printed out using a library of nearly 400 principal (γ-ray energies that are seen in the environment. Any peak can be quickly analyzed by using an optional automated continuum strip.
7. The program enters an interactive phase where the operator examines any additional peaks check the results of the automated routine or examining any new kinds of features of a spectrum [13].

In many conditions, the built in peak area examine features of the state of the art analyzers are used in providing quick results in the field. Before measurements are made energy calibration and efficiency calibration are applied to the detector.

γ-ray emission probability (Percentage Yield) Various methods can be used to obtain γ-ray emission Probabilities, for example ^{60}Co are calculated from the decay scheme using parameters (notably the internal conversion coefficients), rather than direct γ-ray measurement. The emission probabilities of the most prominent high energy γ-ray were determined by means of the weighted mean method in the case of consistent data sets.

Key Line Different radionuclides emit a number of gamma rays of unique abundances, usually at least one gamma ray has a significant abundance and is an interference free. If the key line is selected for a particular gamma ray in the data list (library), the software will not identify the radionuclide as being present if not that Key line(s) is found. Therefore, it has several terms that identify it, for example abundance, branching ratio, yield or intensity.
Two commonly used definitions are:
Abundance: the probability of emission of a given radiation during the decay of an atom of a given radionuclides.
Intensity: the probability of emission of a given radiation during the decay of one atom of a given radionuclides, sometimes called abundance.

As shown in Figure 3.3, the specific radionuclides energy spectrums were detected using the computer software analysis results.

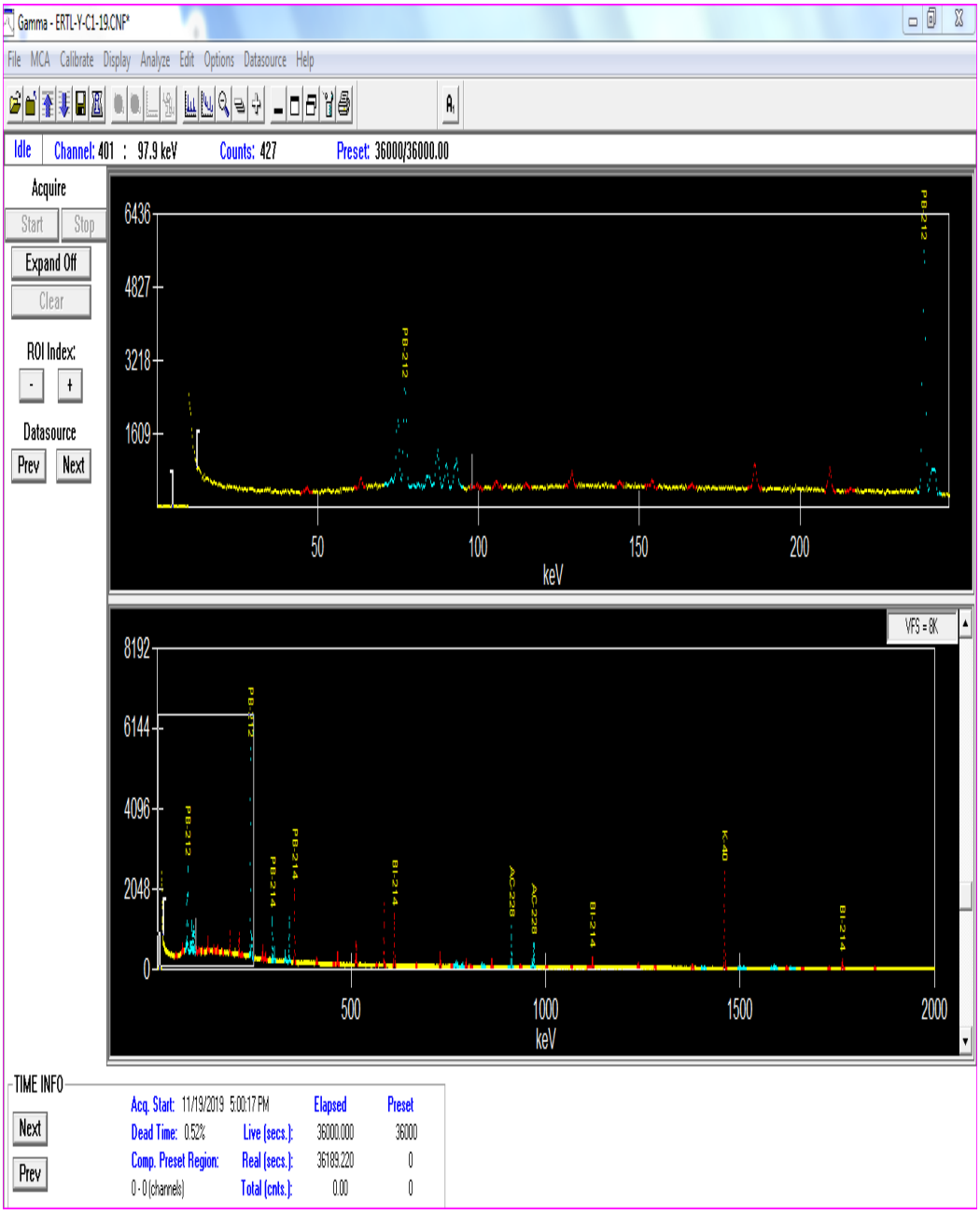

Figure 3.3: Energy spectrum out put graph for the cement sample

Efficiency calibration

Accurate efficiency calibration of the system is necessary to quantify radionuclides present in a

sample. This calibration must be performed with great care because the accuracy of all quantitative results will depend on it. It is also useful that all system settings and adjustments be made before determining the efficiencies and be maintained until a new calibration is undertaken see Figure 3.4 a. Slight changes in the settings of the system components may have small but direct effects on counting efficiency.

Energy calibration

An important requirement for the measurement of gamma emitters is the exact identity of photo peaks present in a spectrum produced by the detector system. The procedure for identifying the radionuclides within a spectrum depends upon methods that match the energies of the principal gamma rays observed in the spectrum to the energies of gamma rays emitted by known radionuclides. This method can be applied by manual inspection or by computer analysis. In both methods, it is expected that an accurate energy calibration for the germanium detector system should be done so that correct energies may be assigned to the centroid of each full energy peak in a sample spectrum as shown in Figure 3.4 b. The energy calibration of a germanium detector system is achieved by establishing the channel number of the MCA with gamma-ray energies, it is made by measuring mixed standards sources of known radionuclides with well-defined energies within the energy range of interest, usually 60 keV to 2000 keV [18].

a)

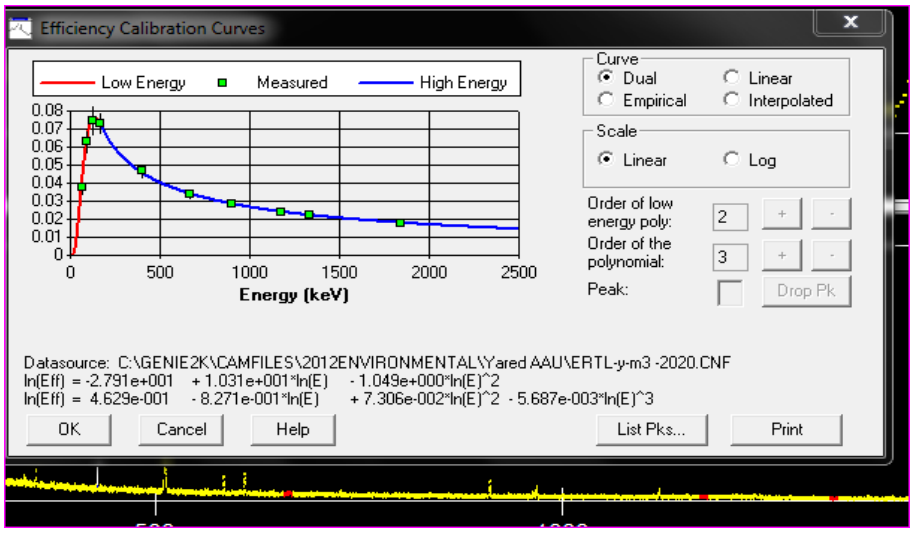

b)

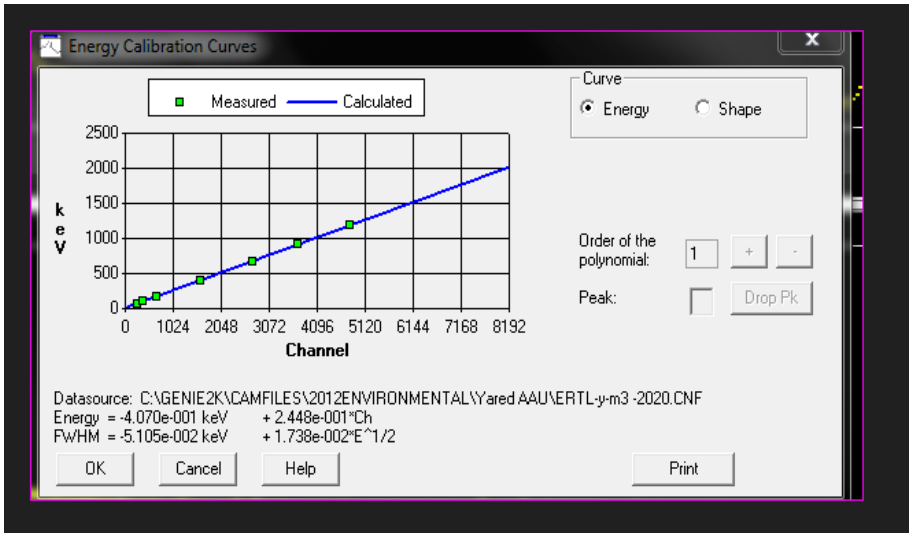

Figure 3.4: Curves for a) Efficiency calibration, b) Energy calibration

3.3 Measurements of activity concentration

Samples are measured using a high-resolution gamma-ray spectrometry consisting of 77% relative efficiency of the HPGe gamma-ray detectors in Ethiopian Radiation Protection Authority (ERPA), also with an energy resolution of approximately 1.8 keV. The absolute full-energy peak efficiency of the Multi-Channel Analyzer is connected to a computer having software of Genie 2000 and calibrated using certified reference materials of natural origin. The counting time of the emitted gamma spectrum was 28,800 s.

The counting geometry of the samples and the standard sources used for efficiency calibration were kept constant. That of ^{226}Ra emitted 186 keV gamma line but it has interference due to 185.7 keV of ^{235}U, and so the activity of ^{226}Ra can be determined indirect by using gamma-ray lines of ^{214}Pb at 351.92 and 295.21 keV and ^{214}Bi at 609.3, 1120.29, and 1764.5 keV, while the activity of ^{232}Th had been evaluated from gamma-ray lines of ^{228}Ac at 338.4, 911.1, and 968.9 keV, ^{212}Pb at 238.63 keV, and ^{208}Tl at 583.19 keV. The specific activity of ^{40}K was directly determined from its gamma-ray line at 1460.8

keV [15]. The specific activity concentrations A_c in (Bq kg^{-1}), of cement samples were calculated using the following formula [19].

$$A_c = \frac{N_c}{I\varepsilon M_s T_s} \tag{3.1}$$

where N_c : is the net count for packed sample ((N_s) count for packed sample minus count for the background (N_b)), I: is the abundance of the gamma-line in a radionuclide, ε: is the measured efficiency for each gamma line observed for the same number of channels either for the sample or the calibration source, and M_s: is the mass of the sample in kilograms, T_s: is the actual sample counting time. The error associated with each measured activity of the samples was calculated using standard deviation (σ_s) [20].

$$Count\ rate = \frac{N_c}{T_s} = \frac{N_s}{T_s} \pm \sigma_s \tag{3.2}$$

where, σ_s is the standard deviation of the measured sample and calculated as follow:

$$\sigma_s = \sqrt{\frac{N_t}{T_t^2} + \frac{N_b}{T_b^2}}, \tag{3.3}$$

where, N_t is the total count, T_t is the total count time, T_b is the background counts time.

3.3.1 Estimation of radiological dose and hazardous indexes

The mean radioactive concentrations of the samples and their radiological health hazards assessment are absorbed dose, annual effective dose rate, gamma index, external hazards index, internal hazard index, and excessive lifetime cancer risks these parameters are evaluated to measure and assess the risk of exposure due to natural radioactivity. The most important naturally occurring radionuclides Uranium-238, Thorium-232, and Potassium-40 are present in cement.

Absorbed Dose Rate (D)

It is the absorbed dose of ionizing radiation per unit time. The absorbed dose rate (D) in the air due to radionuclides at 1 m above the ground surface [2].

$$D(nGy\ h^{-1}) = 0.0417A_k + 0.462A_{Ra} + 0.602A_{Th} \tag{3.4}$$

The result found to be comparable to the world average of 59 nGy h^{-1} for outdoor and 84 nGy h^{-1} for indoor.

Annual Effective Dose Rate

The annual effective dose equivalent is the equivalent biological effect representing the deposit of a joule of radiation energy per kilogram of human body within a year. For people living in a certain area, the annual effective dose could be calculated using the equation given below. The absorbed dose rate (D) values are used to estimate the annual effective dose rate (AEDR) in $mSv\ y^{-1}$, considering that

the population spent, on average, 80% of their time indoors, and using a conversion coefficient for the absorbed doses in the air to the effective dose received by an adult of 0.7 $SvGy^{-1}$. These results are comparable with the world average annual effective dose rate of 0.41 mSv y^{-1} for indoor, 0.07 mSv y^{-1} for outdoor, and the worldwide average annual effective dose rate of 1 $mSv\ y^{-1}$ [2].

where D is the calculated dose rate in ($nGy\ h^{-1}$), T is the indoor occupancy time

$$0.8 \times 24\ h \times 365.25\ d \cong 7010\ hy^{-1} \tag{3.5}$$

and F is the conversion factor (0.7 $SvGy^{-1}$).
For people living in a certain area, the annual effective dose could be calculated as follow:

$$E(mSv/y) = D(nGy/h) \times 24\ h \times 365.25\ d \times 0.2 \times 0.7\ (Sv/Gy) \tag{3.6}$$

which is for outdoor occupancy

$$E(mSv/y) = D(nGy/h) \times 24\ h \times 365.25\ d \times 0.8 \times 0.7\ (Sv/Gy) \tag{3.7}$$

which is for indoor occupancy
where 0.7 is the absorbed dose conversion factor and 0.2 is the outdoor occupancy, 0.8 is indoor occupancy.

Radium Equivalent (Ra_{eq})

The radium equivalent (Ra_{eq}), is represent the combined activity concentration of ^{226}Ra, ^{232}Th, and ^{40}K, used to asses the radiation hazard of the material, which is given by the following equation [19].

$$Ra_{eq} = A_{Ra} + 1.43A_{Th} + 0.077A_k \tag{3.8}$$

The recommended maximum levels of radium equivalents values for building materials to be used for homes is less than 370 Bq kg^{-1} and for industries is between 370 and 740 Bq kg^{-1} [21]. From this all the examined materials should satisfies these conditions to have acceptable values, and can be used for building materials as defined by the UNSCEAR and OECD criterion [22].

Gamma Index I_γ

It is one of the measurements of a radiation hazard that comes from gamma radiation and the recommended maximum value must be less than one. The gamma index (I_γ) can be calculated as follow [23].

$$I_\gamma = \frac{A_{Ra}}{300} + \frac{A_{Th}}{200} + \frac{A_K}{3000} \leq 1 \tag{3.9}$$

Its permissible limit is I_γ = 1 corresponds to an absorbed gamma dose rate of 0.3 $mSv\ y^{-1}$, which implying that materials with $I_\gamma \geq 1$ should be avoided.

External Hazard Index (H_{ex}) and Internal Hazard Index (H_{in})

The External hazard index (H_{ex}) and the internal hazard index (H_{in}), which explain the external hazard index as expression for external exposure that comes from radioactive nuclide and internal hazard index from internal exposure that comes from radon and its short-lived progeny. External hazard index (H_{ex}) and internal hazard index (H_{in}) is calculated using the following equations [19].
External hazard index (H_{ex})

$$H_{ex} = \frac{A_{Ra}}{370} + \frac{A_{Th}}{259} + \frac{A_K}{4810} \leq 1 \tag{3.10}$$

The internal hazard index(H_{in}) also calculated using

$$H_{in} = \frac{A_{Ra}}{185} + \frac{A_{Th}}{259} + \frac{A_K}{4810} \leq 1 \tag{3.11}$$

The internal hazard index must be less than unity in order to provide safe levels for the respiratory organs of individuals living in the dwellings.

Excessive Lifetime Cancer Risk (ELCR)

This is associated with the probability of developing cancer over a lifetime at a given exposure level. An increase in the ELCR causes a proportionate increase in the rate at which an individual can get blood cancer, breast cancer, and prostate cancer [24]. Excessive lifetime cancer risk (ELCR) is calculated by using the following equation from [25].

$$ELCR = AEDE \times DL \times RF \tag{3.12}$$

AEDE stands for Annual Effective Dose Equivalent, DL for average life expectancy which is an average of 70 years. RF factor which is cancer risk per Sievert (Sv^{-1}) from the International Commission on Radiological Protection [3] the value of 0.05 Sv^{-1} is used for the public [25]. It is a value depicting the number of cancers expected in each number of people on exposure to a carcinogen at a given dose. The threshold values of ELCR is 0.29×10^{-3} [2].

3.3.2 Activity concentrations in medicinal plants

The specific activity concentrations in $Bq\,kg^{-1}$ of the collected medicinal plants were calculated by the following formula [19].

$$A_c = \frac{N_p}{I\varepsilon M_s} \tag{3.13}$$

Where A_c: radioactivity concentration of the samples (Bq/kg), N_p: is the total count within second for packed sample minus count for the background, the gamma-energy counting efficiency is labelled as ε, I is the gamma-ray absolute intensity and M: mass for packed sample(kg).

Average annual committed effective dose ($E_{ave}(mSv/yr)$)

The average annual committed effective dose (AACED) due to intake of naturally occurring radionuclides from the studied medicinal plants was obtained by [26].

$$E_{ave}(mSv/yr) = A_i \times C_r \times DCF_{ing} \tag{3.14}$$

DCF_{ing} is the dose conversion factor, for ingestion $4.5 \times 10^{-5} mSvBq^{-1}$, $2.3 \times 10^{-4}\ mSvBq^{-1}$ and $6.2 \times 10^{-6}\ mSvBq^{-1}$ were used for ^{238}U, ^{232}Th, and ^{40}K, respectively [27]. C_r represents the consumption rate from ingestion of naturally occurring radionuclides in medicinal plants, in the present study the consumption rate used is 5 kga^{-1}, one of the reasons to take small amount of consumption rate is that in the study area the community does not use them as a primary food source and occasionally use those plants as traditional medicinal plants in some amount within a month or weeks. The value of the consumption rate (C_r) was calculated by [27].

$$C_r = \frac{3E_{ave}}{\sum_{i=1}^{3}[DCF_i \times A_i]} \tag{3.15}$$

CHAPTER 4

RESULTS AND DISCUSSIONS

4.1 Radioactivity Concentrations in Soil Samples

Soil is formed through a complex and lengthy process that results from the interaction of various factors, including weathering of rocks, organic matter decomposition, and the influence of climate, organisms, topography, and time. The parent material, usually rock, is gradually broken down into smaller particles through mechanical, chemical, and biological weathering processes. Temperature fluctuations, water, wind, and biological activity all contribute to the disintegration.

The content of soil varies widely depending on its origin, environmental factors, and the presence of organic and inorganic materials. Generally, soil is composed of minerals, organic matter, water, and air. Mineral components, derived from the weathered parent material, make up about 45% of the soil and include essential nutrients like nitrogen, phosphorus, and potassium. Organic matter, which constitutes about 5% of the soil, is crucial for soil fertility, providing nutrients and improving soil structure by helping it retain water and air. Water and air fill the pore spaces between soil particles, making up approximately 50% of the soil's composition.

The study of radioactivity in soil is crucial for understanding environmental impacts, protecting public health, and supporting agricultural safety and geoscientific research. Investigating radionuclide concentrations in soil helps in monitoring radiation exposure and developing risk mitigation strategies. Human exposure to radiation arises from natural sources, including cosmic rays and radioactive elements in soil, rocks, and the atmosphere. Internal exposure also occurs through ingestion and inhalation of contaminated food, water, and air [28].

Radionuclides enter the soil through natural processes such as cosmic ray interactions, primordial deposits, and human activities. Measuring radioactivity in environmental materials is essential for assessing biological health risks [29]. Soil composition, including particle size and mineral content, influences radionuclide absorption by plants, which subsequently affects the food chain. The transfer factor of radionuclides from soil to plants and animals is vital for estimating radiation exposure and risk [12].

Terrestrial radiation is present due to naturally occurring radioactive nuclides, such as uranium-238, which decays into radium-226 and radon-222 [30]. The concentration of radionuclides varies based on geographical and geological conditions. Measuring natural radioactivity levels in soil samples provides insights into potential radiation hazards, which are especially important for long-term residents and agricultural practices.

In this study, the radioactivity concentrations and radiological hazard parameters in soil from selected districts are assessed and compared to global averages, providing valuable data for understanding the local impact of natural radiation

4.1.1 Radioactivity in Soil Samples: Assosa City

Study Area and Sample Collection

The measured natural radioactivity concentrations in different soil samples, from Assosa City, Benishangul Gumuz regional State (BGRS) are presented in this section. The BGRS is one of the eleven regional states comprising the Ethiopian federal structure Figure 4.1.

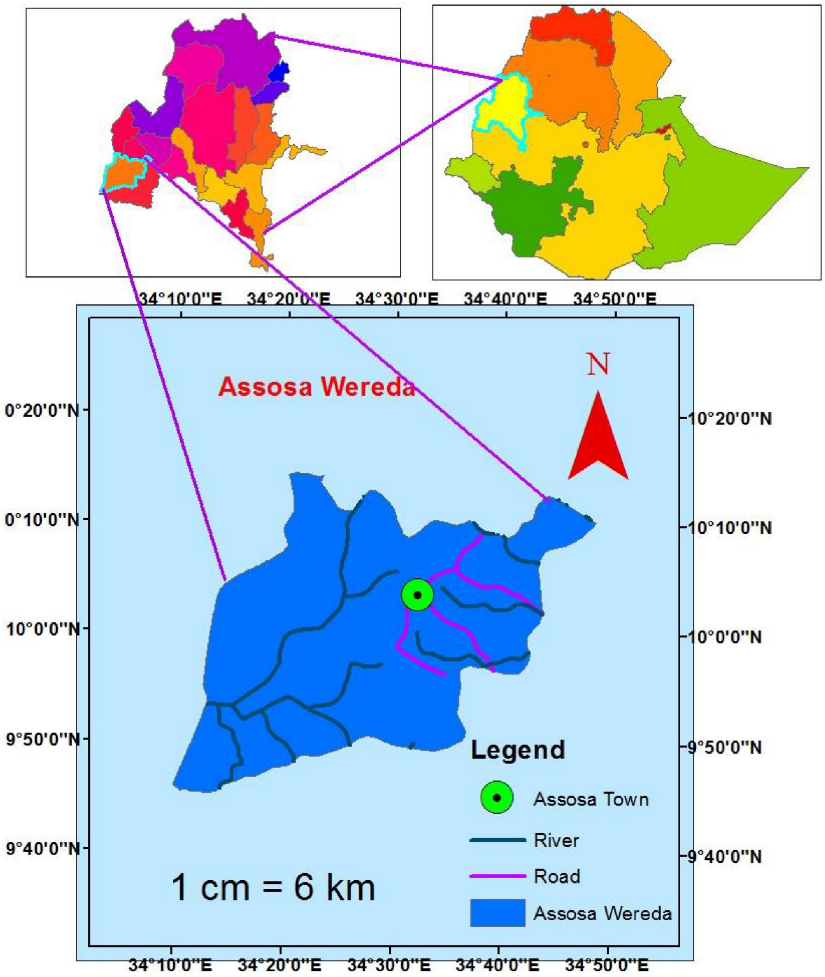

Figure 4.1: Map of Assosa City location in Benishangul Gumuz region

Assosa town is the capital of Benishangul Gumuz Regional State (BGRS), which is one of the eleven regional states comprising the Ethiopian federal structure. According to information obtained from the municipality of the town, Assosa is a town founded in 1984, It is located at a distance of 662 km South-West of the capital, Addis Ababa along with the main highway road. So, the town could be taken as one of the border towns in the country and located 90 km away from the Ethio-Sudanese border. It is situated on a flat plane at an average altitude of 1,550. The town is geographically located between $10°00'$ to $10°03'$ north and between $34°35'$ to $34°39'$ east and lies on an area of about 982.5 hectares [31]. All samples were collected carefully at 5cm-15cm depth from the soil surface land and each of the samples weighed approximately 1 kg.

Table 4.1 shows the samples collected and the codes given to name the samples and the respective GPS of the sampling sites.

Table 4.1: The GPS location of the collected Assosa City samples

No	Sample Code	Location (GPS)North	Location (GPS)East
1	Assosa-S1	10.066981°	34.556967°
2	Assosa-S2	10.071328°	34.559092°
3	Assosa-S3	10.077333°	34.558828°
4	Assosa-S4	10.084292°	34.569458°
5	Assosa-S5	10.058986°	34.553344°
6	Assosa-S6	10.054631°	34.5558°
7	Assosa-S7	10.072486°	34.548783°
8	Assosa-S8	10.075719°	34.544672°
9	Assosa-S9	10.071539°	34.539628°
10	Assosa-S10	10.088636°	34.560456°

Presentation of Measured Radioactivity Results

The measured radioactivity concentrations in the soil samples collected from Assosa city are presented in Table 4.2. As can be seen from table 4.2, the average radioactivity concentration of ^{238}U,

Table 4.2: Specific activity concentration of radionuclides in soil samples: Assosa City

No	Sample Code	A_U(Bq kg^{-1})	A_{Th}(Bq kg^{-1})	A_K(Bq kg^{-1})
1	Assosa-S1	39.25 ± 1.93	73.65 ± 4.13	196.01 ± 9.45
2	Assosa-S2	51.05 ± 2.65	118.55 ± 5.05	193.36 ± 10.07
3	Assosa-S3	46.58 ± 2.32	71.34 ± 4.07	173.27 ± 8.65
4	Assosa-S4	37.06 ± 1.78	64.405 ± 3.57	174.66 ± 8.35
5	Assosa-S5	57.80 ± 3.09	83.48 ± 4.71	183.88 ± 9
6	Assosa-S6	25.61 ± 1.29	30.52 ± 1.8	116.30 ± 5.96
7	Assosa-S7	53.75 ± 2.7	73.45 ± 4.23	173.72 ± 8.76
8	Assosa-S8	26.02 ± 1.9	35.35 ± 2.05	342 ± 16.55
9	Assosa-S9	58.74 ± 2.83	76.9 ± 4.32	371.64 ± 17.42
10	Assosa-S10	56.15 ± 2.76	72.75 ± 4.14	463.32 ± 22.03
11	**Mean value**	45.2 ± 2.3	70 ± 3.8	238.8 ± 11.6

^{232}Th, and ^{40}K for 10 soil samples are 45.2 ± 2.3 Bq kg^{-1}, 70 ± 3.8 Bq/kg^{-1}, and 238.8 ± 11.6 Bq kg^{-1}, respectively.

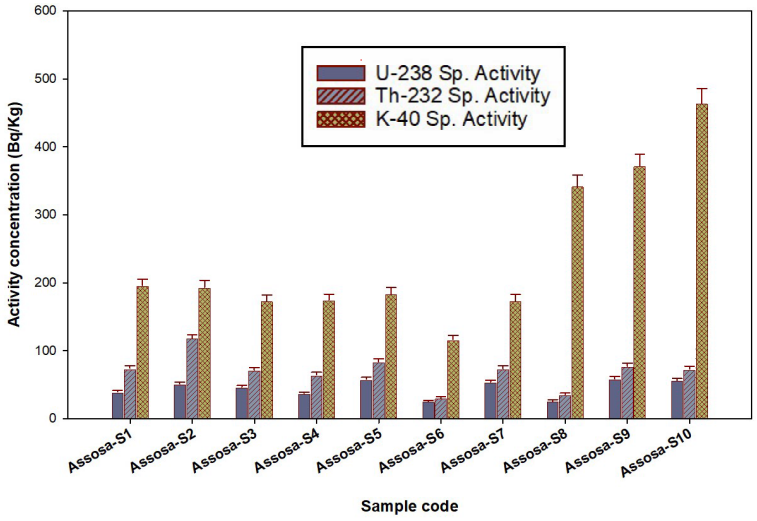

Figure 4.2: Specific activity concentration of radionuclides: Assosa soil samples

Comparison With Global Average and Safety Thresholds

The mean activity concentration of ^{238}U and ^{232}Th in Assosa City soil samples exceeds the recommended safe values of 35 and 30 Bq kg^{-1} for ^{238}U and ^{232}Th, respectively. As shown in Figure 4.2, the high radioactivity concentration of ^{238}U is found in sample Assosa-S9 and the lowest is in Assosa-S8. The high radioactivity concentration of ^{232}Th is observed on sample Assosa-S2 and the lowest one is in Assosa-S6. For ^{40}K high radioactivity concentration is found in Assosa-S10 and the lowest value in Assosa-S6. The results indicate that the radioactivity concentration in Assosa soil can cause significant health problems.

Table 4.3: Comparison of mean activity concentration of ^{238}U, ^{232}Th, and ^{40}K found in Assosa soil with other countries

No	Country	A_U(Bq kg^{-1})	A_{Th}(Bq kg^{-1})	A_K(Bq kg^{-1})	Reference
1	Ethiopia (Assosa)	45.2 ± 2.3	70 ± 3.8	238.8 ± 11.6	Present study
2	Algeria (Mila)	46.7	26.7	246.5	[32]
3	Belgium	26	27	380	[2]
4	China (Guangdong)	79.3	101	535.8	[33]
5	Georgia (Kharami)	38.57	53.18	879.76	[34]
6	India (Panipat)	30.2 ± 0.5	29.89 ± 0.6	291.06 ± 0.5	[35]
7	Italy (Lombardia)	72	48	617	[36]
8	Malaysia (Kedah)	102.08 ± 3.9	133.9 ± 2.9	325.8 ± 9.8	[15]
9	Nigeria (Imo State)	4.15	1.64	134.13	[37]
10	South Africa (Richards)	28.2 ± 11.4	29.6 ± 11.5	146.7 ± 63.3	[38]
11	Turkiye (Ardahan)	29.9 ± 6.2	36.7 ± 6.8	435.1 ± 24	[39]
12	Russia Federation	19	30	520	[2]
13	United States	40	35	370	[2]
14	UNSCEAR	35	30	400	-

A comparison of the radioactivity concentration of Assosa town soils with the similar studies in other countries is presented in Table 4.3. From the result, Assosa City soils have an average activity concentration of 45.2 ± 2.3 Bq kg^{-1}, 70 ± 3.8 Bq kg^{-1}, and 238.8 ± 11.6 Bq/kg^{-1} for ^{238}U, ^{232}Th, and ^{40}K, respectively. The mean activity concentration of ^{238}U, ^{232}Th, and ^{40}K for Assosa City soils are lower than soils from the Guangdong province of China [33], Panipat region of India [35], Lombardia region of Italy [36], Kedah region of Malaysia [15], and Ardahan province of Türkiye [39]. However, as shown in Figure 4.3, in comparison with similar studies the measured mean activity concentration of ^{238}U, ^{232}Th, and ^{40}K in Assosa soil are higher than soils from Mila region of Algeria [32], Imo state of Nigeria [37], and Richard Bay of South Africa [38] (see Table 4.3).

The radium equivalent activity Ra_{eq} values for the investigated soils varied from 78.16 ± 4.24 to 235.35 ± 10.62 Bq kg^{-1} with a mean value of 163.6 ± 8.6 Bq kg^{-1} and it is less than 370Bq kg^{-1}, and so it is within safe values. As shown in Table 4.4, the absorbed dose rate values are varied from 34.9 ± 1.74 to 102.8 ± 4.6 nGy h^{-1} with an average value of 72.865 ± 3.72 nGy h^{-1} which is above the recommended safe value of 59 nGy h^{-1}. The calculated values of outdoor annual effective dose equivalent obtained in this study varies from 0.254 ± 0.01 to 0.75 ± 0.0003 mSv y^{-1} with an average value of 0.52 ± 0.02 mSv y^{-1} and indoor annual effective dose rate ranged from 1.01 ± 0.05 to 2.98 ± 0.13 mSv y^{-1} with an average value of 2.11 ± 0.1 mSv y^{-1} (see Table 4.4). The mean value of indoor annual effective dose rate exceeds the world average annual effective dose rate value of 1 mSv y^{-1} [2]. The values of H_{in} and H_{ex} for all soil samples are below the safe value of one, so that the soils have the safest value see Figure 4.4.

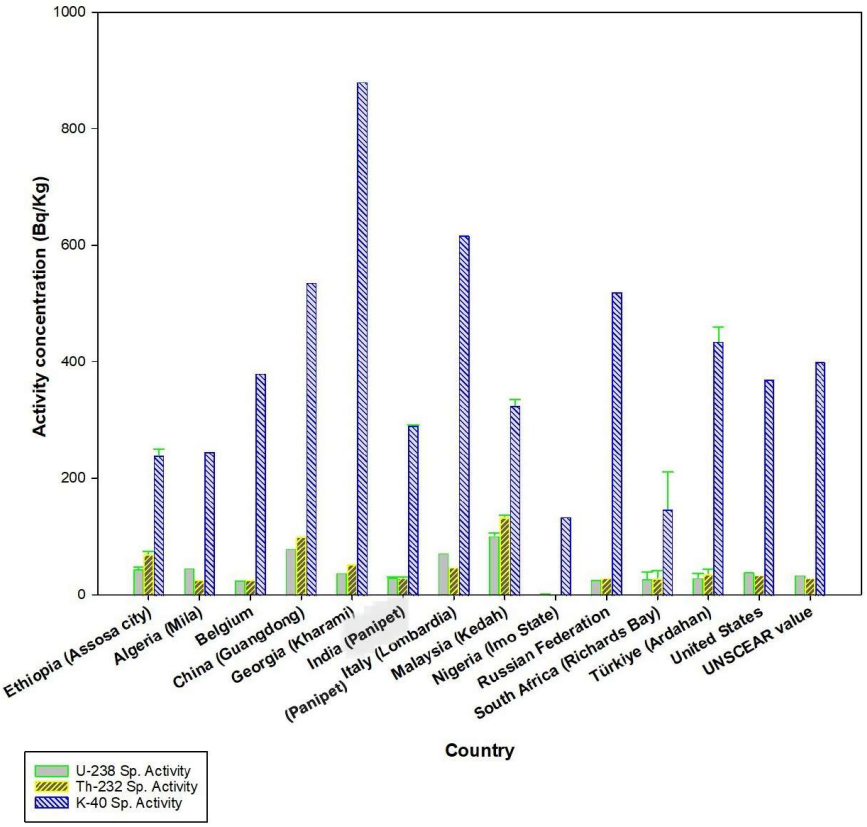

Figure 4.3: The comparison of radioactivity concentration in soil samples across different countries with Assosa City in Benishangul Gumuz region, Ethiopia

Table 4.4: Values of the radiological doses

No	Sample Code	Ra_{eq}	$D(nGy\ h^{-1})$	$E(mSv/y)_{Outdoor}$	$E(mSv/y)_{Indoor}$
1	Assosa-S1	159.55 ± 8.55	70.5 ± 3.58	0.519 ± 0.02	2.07 ± 0.1
2	Assosa-S2	235.35 ± 10.62	102.8 ± 4.6	0.75 ± 0.0003	2.98 ± 0.13
3	Assosa-S3	161.89 ± 8.78	71.6 ± 3.75	0.52 ± 0.027	2.07 ± 0.1
4	Assosa-S4	142.46 ± 7.52	63 ± 3.24	0.45 ± 0.023	1.82 ± 0.09
5	Assosa-S5	191.2 ± 10.5	84.5 ± 4.5	0.61 ± 0.032	2.45 ± 0.13
6	Assosa-S6	78.16 ± 4.24	34.9 ± 1.74	0.254 ± 0.01	1.01 ± 0.05
7	Assosa-S7	172.12 ± 9.41	76.24 ± 4.1	0.55 ± 0.029	2.21 ± 0.11
8	Assosa-S8	102.8 ± 6.09	47.42 ± 2.63	0.3 ± 0.01	1.37 ± 0.076
9	Assosa-S9	197.25 ± 10.34	88.79 ± 4.62	0.648 ± 0.033	2.57 ± 0.133
10	Assosa-S10	195.78 ± 10.35	88.9 ± 4.51	0.64 ± 0.03	2.57 ± 0.13
11	**Mean value**	163.6 ± 8.6	72.865 ± 3.72	0.52 ± 0.02	2.11 ± 0.1

Table 4.5: Values of the radiation hazard indexes

No	Sample Code	I_γ	H_{ex}	H_{in}	ELCR(10^{-3})
1	Assosa-S1	0.56 ± 0.02	0.42 ± 0.016	0.53 ± 0.01	1.81 ± 0.07
2	Assosa-S2	0.82 ± 0.026	0.63 ± 0.02	0.77 ± 0.024	2.625 ± 0.001
3	Assosa-S3	0.56 ± 0.02	0.43 ± 0.01	0.56 ± 0.02	1.82 ± 0.09
4	Assosa-S4	0.50 ± 0.019	0.38 ± 0.014	0.48 ± 0.016	1.57 ± 0.08
5	Assosa-S5	0.67 ± 0.02	0.51 ± 0.02	0.67 ± 0.024	2.135 ± 0.1
6	Assosa-S6	0.27 ± 0.01	0.21 ± 0.007	0.28 ± 0.009	0.88 ± 0.035
7	Assosa-S7	0.60 ± 0.023	0.46 ± 0.01	0.61 ± 0.02	1.92 ± 0.1
8	Assosa-S8	0.37 ± 0.01	0.27 ± 0.01	0.34 ± 0.013	1.05 ± 0.035
9	Assosa-S9	0.7 ± 0.024	0.53 ± 0.01	0.69 ± 0.022	2.26 ± 0.11
10	Assosa-S10	0.7 ± 0.023	0.52 ± 0.018	0.68 ± 0.022	2.24 ± 0.105
11	**Mean value**	0.5 ± 0.01	0.43 ± 0.013	0.56 ± 0.01	1.8 ± 0.07

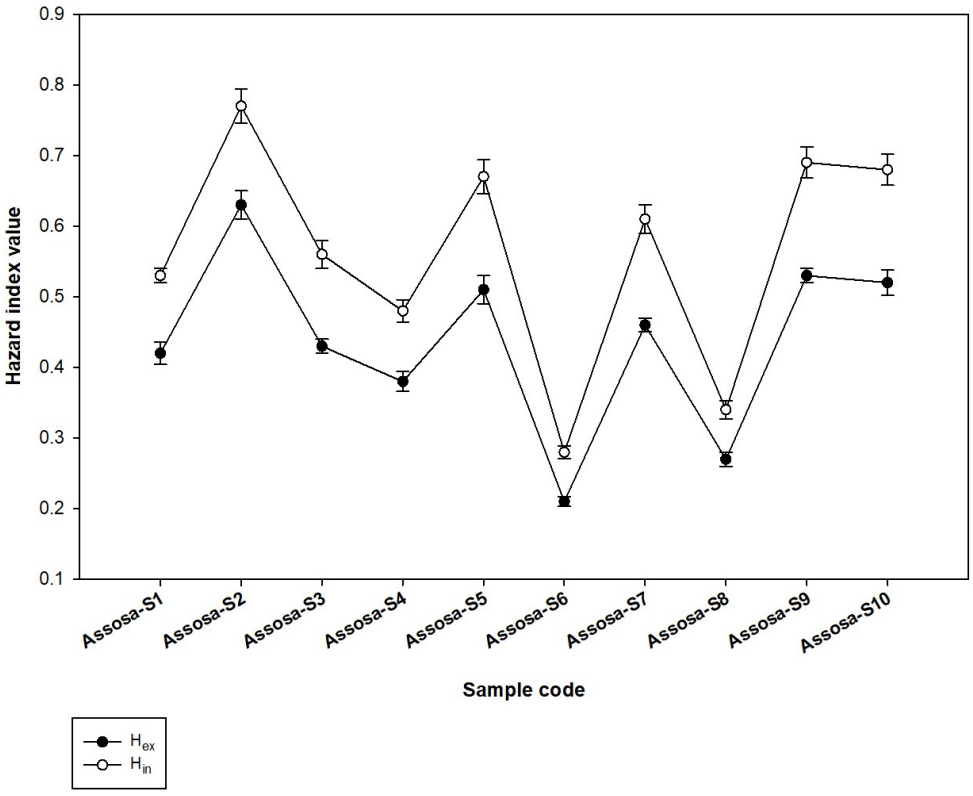

Figure 4.4: Hazard Indexes values of the Assosa soil samples

Discussion

Radioactive concentration measurement has been applied to geological, environmental, medicinal, and industrial samples. The measurement of radionuclide activity concentration of environmental soil samples will contribute to the baseline of the health risk that comes from radiation exposure. Thorium and Uranium may be redistributed during igneous, sedimentary, and metamorphic cycles of geological evolution, which might have resulted in small concentrations of deposits under favorable geological processes [40]. The natural sources of ionizing gamma radiation in the environment can be classified into terrestrial and cosmogenic radiation sources. Terrestrial radioactivity comes from the ground and cosmogenic radioactivity from the interaction of atmospheric gases with cosmic rays. Cosmic radiation-induced radionuclides (for example ^{14}C) and terrestrial radionuclides contribute to both external and internal exposures. External exposure from these radionuclides is mostly due to their emitted γ-rays and internal exposure is due to their deposition in the human body followed by emission of α, β, and γ radiations. The levels of radioactivity can be used to assess public dose rates, radioactive contamination, and also to predict changes in environmental radioactivity caused by nuclear accidents, industrial activities, and other human activities [2].

4.1.2 Radioactivity in Soil Samples: Bambasi District

Study Area and Sample Collection

Bambashi is a town in western Ethiopia. The town is named after the highest point in the Assosa Zone of the Benishangul-Gumuz Region. The natural radioactivity level of different soil samples from the town of Bambasi is studied and the results are presented in this section. Bambasi wereda is located in Ethiopia at 614 km from the capital City Addis Ababa and it is found between latitude 9°-10°N and longitude 034°-035° [41].

Soil samples were collected from the sampling sites based on the population density of the district/Woreda. Soil samples were collected from the selected eight sites of Bambasi town. All samples were collected carefully at a 5 cm-30 cm depth from the surface soil land and each of the samples weighed approximately 1 kg. The samples were coded with Bambasi-S1 to Bambasi-S8, with locations listed in Table 4.6.

Table 4.6: The GPS location of the collected Bambasi district samples

No	Sample Code	Location (GPS)North	Location (GPS)East
1	Bambasi-S1	9.751911°	34.726703°
2	Bambasi-S2	9.751736°	34.729544°
3	Bambasi-S3	9.753097°	34.73175°
4	Bambasi-S4	9.756256°	34.730528°
5	Bambasi-S5	9.757667°	34.728025°
6	Bambasi-S6	9.760117°	34.726661°
7	Bambasi-S7	9.761314°	34.728581°
8	Bambasi-S8	9.759558°	34.731228°

Presentation of Measured Radioactivity Results: Bambasi Soil Samples

The measured radioactivity concentrations in the soil samples collected from Bambasi city are presented in Table 4.7.

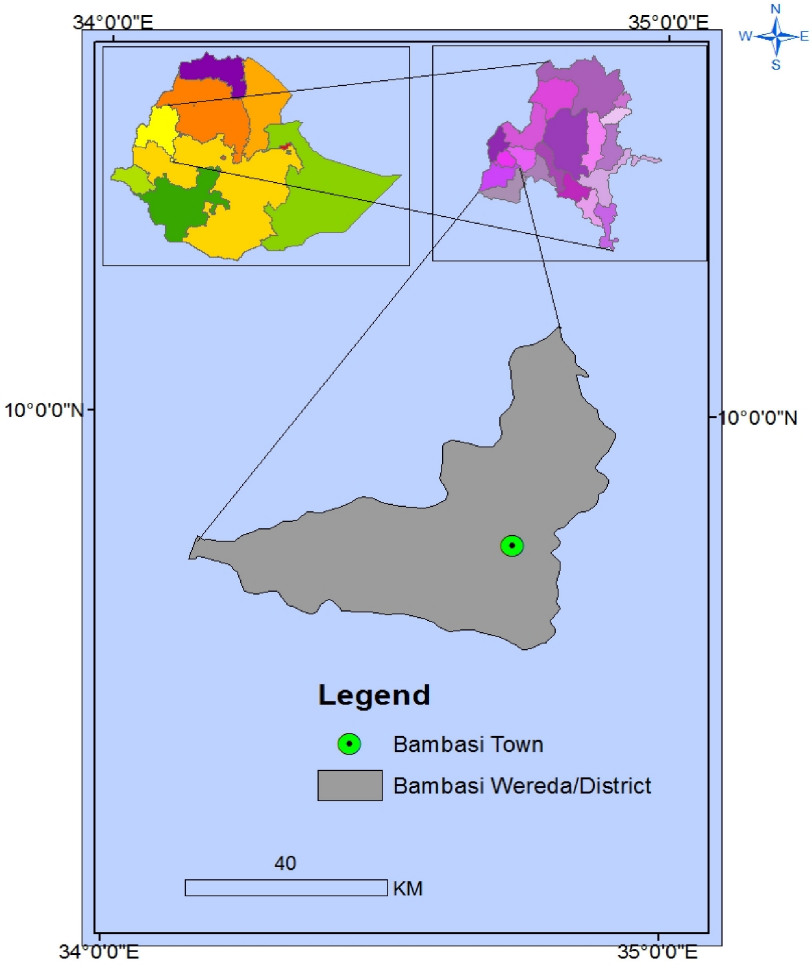

Figure 4.5: Map of Bambassi town in Benishangul Gumuz region

Table 4.7: Mean specific activity concentration of radionuclides in soil samples

No	Sample Code	A_U (Bq kg^{-1})	A_{Th} (Bq kg^{-1})	A_K (Bq kg^{-1})
1	Bambasi-S1	88.49 ± 5.73	119.65 ± 8.45	396.71 ± 25.39
2	Bambasi-S2	54.39 ± 2.85	82.83 ± 4.91	225.27 ± 11.73
3	Bambasi-S3	62.78 ± 3.09	90.87 ± 5.17	165.12 ± 8.29
4	Bambasi-S4	53.88 ± 2.68	83.2 ± 4.76	233.92 ± 11.58
5	Bambasi-S5	56.05 ± 2.99	86.6 ± 5.2	216.08 ± 11.6
6	Bambasi-S6	60.95 ± 3.14	85 ± 5.01	235.93 ± 12.13
7	Bambasi-S7	46.2 ± 2.25	73.4 ± 4.12	176.78 ± 8.63
8	Bambasi-S8	65.49 ± 3.30	92.25 ± 5.33	252.39 ± 12.54
9	**Mean value**	61 ± 3.2	89.2 ± 5.3	237.7 ± 12.7

Comparison with Global Average and Safety Thresholds: Bambasi Soil

The average radioactivity concentrations for eight soil samples are 61 ± 3.2 Bq kg^{-1} for ^{238}U, 89.2 ± 5.3 Bq kg^{-1} for ^{232}Th, and 237.7 ± 12.7 Bq kg^{-1} for ^{40}K (see Table 4.7). The mean activity concentration of ^{238}U and ^{232}Th in Bambasi district soil samples exceeds the recommended safe values of 35, and 30 Bq kg^{-1} for ^{238}U and ^{232}Th, respectively. The high radioactivity concentration of ^{238}U is found in sample Bambasi-S1 and the lowest is in Bambasi-S7 see Figure 4.6. The high radioactivity concentration of ^{232}Th is observed on sample Bambasi-S1 and the lowest one is in Bambasi-S7. For

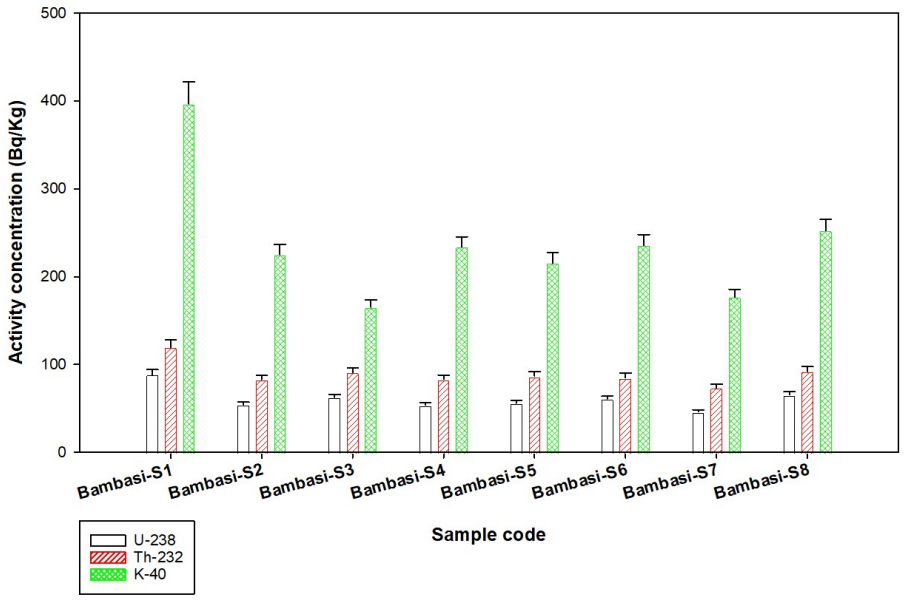

Figure 4.6: Specific activity concentration of radionuclides in Bambasi soil samples

^{40}K high radioactivity concentration is found similarly in Bambasi-S1 and the lowest value in Bambasi-S7. The results indicate that the radioactivity concentration in Bambasi soil can cause significant health concerns.

Table 4.8: Comparison of mean activity concentration of ^{238}U, ^{232}Th, and ^{40}K found in Bambasi soil with other countries

No	Country	A_U(Bq kg^{-1})	A_{Th}(Bq kg^{-1})	A_K(Bq kg^{-1})	Reference
1	Ethiopia (Bambasi)	61 ± 3.2	89.2 ± 5.3	237.7 ± 12.7	Present study
2	Algeria (Mila)	46.7	26.7	246.5	[32]
3	Brazil (Espirito Santo)	30	94	48	[42]
4	China (Guangdong)	79.3	101	535.8	[33]
5	Georgia (Mtskheta)	25.4	26.9	464	[43]
6	India (Panipet)	30.2 ± 0.5	29.89 ± 0.6	291.0 ± 0.5	[35]
7	Ireland	60	26	350	[2]
8	Iraq (Baba Gurgur dome)	57.8	25.4	479.9	[44]
9	Italy (Lombardia)	72	48	617	[36]
10	Nigeria (Imo State)	4.15	1.64	134.13	[37]
11	Poland (Kampinoski)	8.54	6.65	206	[45]
12	Russia Federation	19	30	520	[2]
13	South Africa (Richards)	28.2 ± 11.4	29.6 ± 11.5	146.7 ± 63.3	[38]
14	Türkiye (Rize province)	24.5	51.8	344.9	[46]
15	Türkiye (Ardahan)	29.9 ± 6.2	36.7 ± 6.8	435.1 ± 24	[39]
16	United States	40	35	370	[2]
17	UNSCEAR	35	30	400	-

A comparison of the radioactivity concentration of Bambasi district soil with similar studies of other countries is presented in Table 4.8. The mean activity concentration of ^{238}U, ^{232}Th, and ^{40}K for Bambasi district soil are lower than soils from the Guangdong province of China [33], and Lombardia region of Italy [36]. However, as shown in Figure 4.7, the measured mean activity concentration of ^{238}U, ^{232}Th, and ^{40}K in Bambasi district soil are higher than soils from Mila region of Algeria [32], Panipat region of India [35], Richard Bay of South Africa [38], and Ardahan province of Turkiye [39].

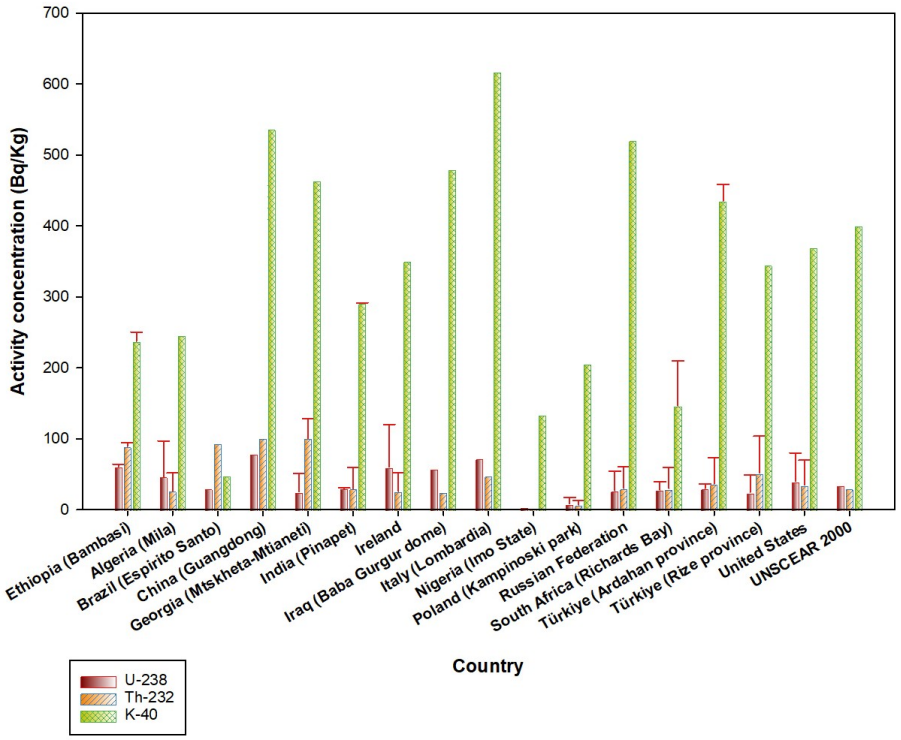

Figure 4.7: Comparison of mean radioactivity concentration in soil samples from districts of different countries with Bambasi district soil

Table 4.9: Values of the radiological doses

No	Sample Code	Ra_{eq}	$D(nGy\,h^{-1})$	$E(mSv/y)_{Outdoor}$	$E(mSv/y)_{Indoor}$
1	Bambasi-S1	289.9 ± 8.8	7129.3 ± 8.6	0.94 ± 0.05	3.74 ± 0.24
2	Bambasi-S2	190.09 ± 0.75	84.2 ± 4.6	0.61 ± 0.63	2.44 ± 0.13
3	Bambasi-S3	205.38 ± 11.02	90.5 ± 4.8	0.66 ± 0.03	2.62 ± 0.13
4	Bambasi-S4	190.7 ± 10.37	84.58 ± 4.4	0.61 ± 0.032	2.45 ± 0.127
5	Bambasi-S5	196.5 ± 11.28	86.9 ± 4.8	0.63 ± 0.034	2.52 ± 0.13
6	Bambasi-S6	200.6 ± 11.17	89 ± 4.9	0.64 ± 0.035	2.58 ± 0.14
7	Bambasi-S7	164.6 ± 15	72.7 ± 3.7	0.53 ± 0.026	2.10 ± 0.10
8	Bambasi-S8	102.39 ± 11.86	96.2 ± 5.22	0.70 ± 0.037	2.78 ± 0.15
9	**Mean Value**	192.5 ± 11.2	91.6 ± 5.1	0.66 ± 0.1	2.65 ± 0.14

Table 4.10: Values of the radiation hazard indexes

No	Sample Code	I_γ	H_{ex}	H_{in}	$ELCR(10^{-3})$
1	Bambasi-S1	1.02 ± 0.04	0.78 ± 0.03	1.022 ± 0.045	3.29 ± 0.175
2	Bambasi-S2	0.67 ± 0.02	0.51 ± 0.02	0.66 ± 0.024	2.13 ± 2.2
3	Bambasi-S3	0.71 ± 0.02	0.55 ± 0.02	0.72 ± 0.026	2.31 ± 0.105
4	Bambasi-S4	0.67 ± 0.025	0.51 ± 0.019	0.66 ± 0.23	2.13 ± 2.2
5	Bambasi-S5	0.69 ± 0.028	0.53 ± 0.02	0.68 ± 0.025	2.205 ± 0.119
6	Bambasi-S6	0.70 ± 0.027	0.54 ± 0.02	0.70 ± 0.025	2.24 ± 0.12
7	Bambasi-S7	0.57 ± 0.022	0.44 ± 0.017	0.56 ± 0.02	1.85 ± 0.09
8	Bambasi-S8	0.76 ± 0.029	0.58 ± 0.02	0.76 ± 0.027	2.45 ± 0.12
9	**Mean value**	0.72 ± 0.02	0.55 ± 0.02	0.72 ± 0.05	2.3 ± 0.6

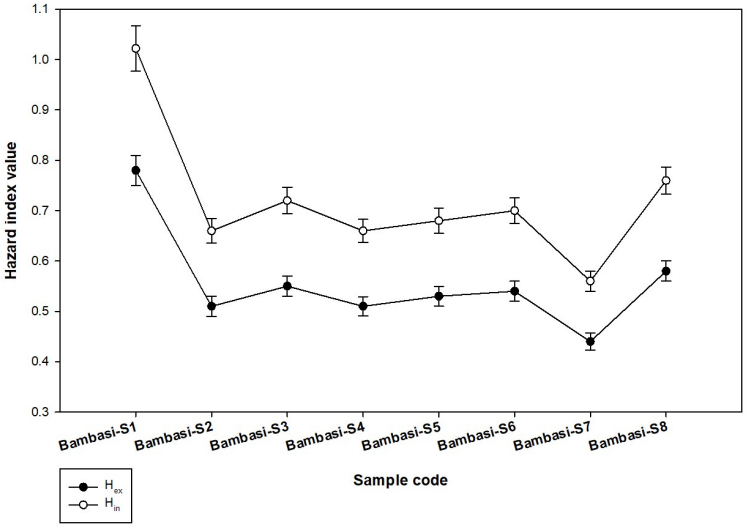

Figure 4.8: Plot for external and internal hazard indexes

Discussion

The radium equivalent activity Ra_{eq} values for the investigated soils varied from 102.39 ± 11.86 to $289.9 \pm 8.8\,Bq\,kg^{-1}$ with a mean of $192.5 \pm 11.2\,Bq\,kg^{-1}$ it is less than the safe value of $370\,Bq\,kg^{-1}$, is a standard values. As shown in Table 4.9, the absorbed dose rate values are varied from 72.7 ± 3.7 to $129.3 \pm 8.6\,nGy\,h^{-1}$ with an average of $91.6 \pm 5.1\,nGy\,h^{-1}$ and which is above the recommended safe value of $59\,nGy\,h^{-1}$. The annual effective dose rate for indoors is varied in the range of 2.10 ± 0.10 to $3.74 \pm 0.24\,mSv\,y^{-1}$ with an average of $2.65 \pm 0.14\,mSv\,y^{-1}$ and for the outdoors is 0.53 ± 0.026 to 0.94 ± 0.05 $mSv\,y^{-1}$ with an average of 0.66 ± 0.1 $mSv\,y^{-1}$. The mean value of indoor annual effective dose rate exceeds the world average annual effective dose rate value of $1\,mSv\,y^{-1}$ [2].

As shown in Figure 4.8, the external hazard indexes (H_{ex}) and internal hazard indexes (H_{in}) for all soil samples. Except the Bambasi-S1 soil sample the indexes are < 1, and their values varied from 0.44 ± 0.017 to 0.78 ± 0.03 with an average value of 0.55 ± 0.02 for H_{ex} and H_{in} takes value from 0.56 ± 0.02 to 1.022 ± 0.045 with an average of 0.72 ± 0.05, respectively. The average values of the external and internal hazard index are less than the recommended safe value of one (see Table 4.10). Values of the gamma index I_γ varied in the range of 0.57 ± 0.022 to 1.02 ± 0.04 with an average of 0.72 ± 0.02, which is less than one the recommended safe value. The values for I_γ, H_{in}, and H_{ex} of all soil samples are below the safe value of one, and so the soils have the safest hazard indexes.

As shown in Table 4.10, the value of excess lifetime cancer risk (ELCR) is in the range of $(1.85 \pm 0.09) \times 10^{-3}$ to $(3.29 \pm 0.175) \times 10^{-3}$, with a mean of $(2.3 \pm 0.6) \times 10^{-3}$ and it exceeds the standard safe index of 0.29×10^{-3}. The long time exposure to γ ray that comes from naturally occurred radionuclides found in Bambasi soil may cause serious health effects so that precaution are to be exercised.

4.1.3 Radioactivity in Soil Samples: Menge-Sherkole District

Study Area and Sample Collection

Radioactivity concentrations of soil samples, from Menge district, Gizen town, Benishangul Gumuz regional State are presented in Figure 4.9.

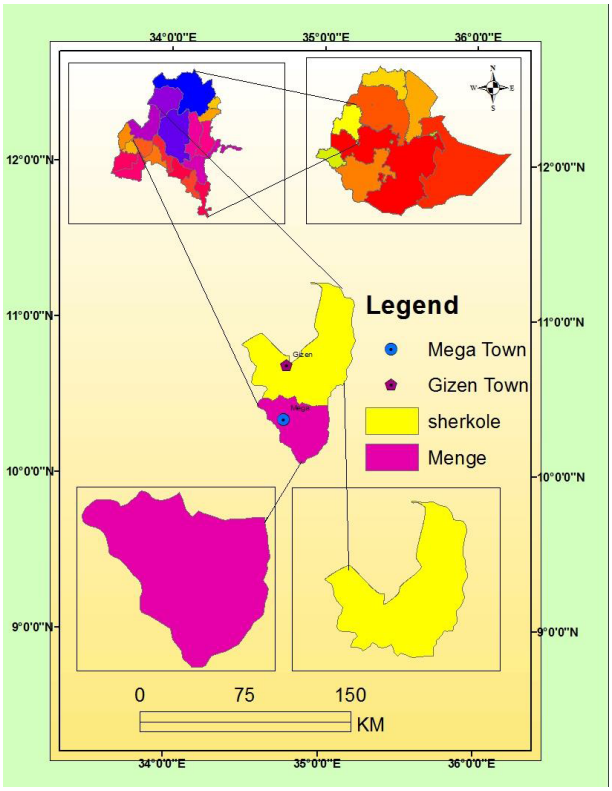

Figure 4.9: Map of Menge Sherkole district in Benishangul Gumuz region

Table 4.11: The GPS location of the collected soil samples

No	Sample Code	Location (GPS)North	Location (GPS)East
1	Menge-S1	10.353886°	34.764964°
2	Menge-S2	10.355164°	34.763861°
3	Menge-S3	10.356211°	34.765125°
4	Menge-S4	10.355869°	34.762133°
5	Menge-S5	10.359533°	34.761256°
6	Menge-S6	10.352289°	34.763953°
7	Sherkole-S1	10.583733°	34.781964°
8	Sherkole-S2	10.596681°	34.781633°
9	Sherkole-S3	10.600397°	34.767483°
10	Sherkole-S4	10.621086°	34.560456°
11	Sherkole-S5	10.600397°	34.777739°
12	Sherkole-S6	10.600358°	34.780119°
13	Sherkole-S7	10.6004°	34.777689°
14	Sherkole-S8	10.610394°	34.768131°

Presentation of Measured Radioactivity: Menge-Sherkole District

The average radioactivity concentration of ^{238}U, ^{232}Th, and ^{40}K for a total of 14 soil samples is $30.3 \pm 1.5\,\mathrm{Bq\,kg^{-1}}$, $42.5 \pm 2.45\,\mathrm{Bq\,kg^{-1}}$, and $201.5 \pm 9.8\,\mathrm{Bq\,kg^{-1}}$, respectively (see Table 4.12). The average activity concentrations of ^{238}U, ^{232}Th, and ^{40}K for each district's soils are, for the Menge district $24 \pm 1.2\,\mathrm{Bq\,kg^{-1}}$, $36.15 \pm 2\,\mathrm{Bq\,kg^{-1}}$, and $275.5 \pm 13.3\,\mathrm{Bq\,kg^{-1}}$, respectively, and Sherkole district $35.14 \pm 1.77\,\mathrm{Bq/kg^{-1}}$, $47.3 \pm 2.7\,\mathrm{Bq\,kg^{-1}}$, and $146 \pm 7.2\,\mathrm{Bq\,kg^{-1}}$, respectively. Specific activity concentration of radionuclides within the Menge and Sherkole soil samples have been depicted in bar graph Figure 4.10.

Table 4.12: Specific activity concentration of radionuclides in soil samples

No	Sample Code	A_U (Bq kg^{-1})	A_{Th} (Bq kg^{-1})	A_K (Bq kg^{-1})
1	Menge-S1	14.57 ± 0.81	24.8 ± 1.48	294.74 ± 14.35
2	Menge-S2	20.52 ± 1.08	32.7 ± 1.90	308.23 ± 14.87
3	Menge-S3	23.44 ± 1.21	35.35 ± 2.05	342.08 ± 16.55
4	Menge-S4	48.67 ± 2.41	69.1 ± 3.9	215.34 ± 10.42
5	Menge-S5	21.39 ± 1.11	32.35 ± 1.9	242.56 ± 11.68
6	Menge-S6	15.07 ± 0.80	22.6 ± 1.32	250.34 ± 12.09
7	**Mean value**	24 ± 1.2	36.15 ± 2	275.5 ± 13.3
8	Sherkole-S1	47.92 ± 2.57	70.4 ± 4.01	191.75 ± 9.39
9	Sherkole-S2	21.94 ± 1.09	32.05 ± 1.84	123.72 ± 6.10
10	Sherkole-S3	17.87 ± 0.95	28 ± 1.63	112.53 ± 5.70
11	Sherkole-S4	45.11 ± 2.24	57.8 ± 3.38	145.9 ± 7.41
12	Sherkole-S5	30.10 ± 1.48	36.5 ± 2.14	120.4 ± 5.99
13	Sherkole-S6	49.52 ± 2.44	65.55 ± 3.76	180.99 ± 8.94
14	Sherkole-S7	38.67 ± 1.96	50.5 ± 2.92	159.08 ± 8.03
15	Sherkole-S8	30.05 ± 1.47	37.9 ± 2.17	133.85 ± 6.63
16	**Mean value**	35.14 ± 1.77	47.3 ± 2.7	146 ± 7.2
17	**Total Mean value**	30.3 ± 1.5	42.5 ± 2.45	201.5 ± 9.8

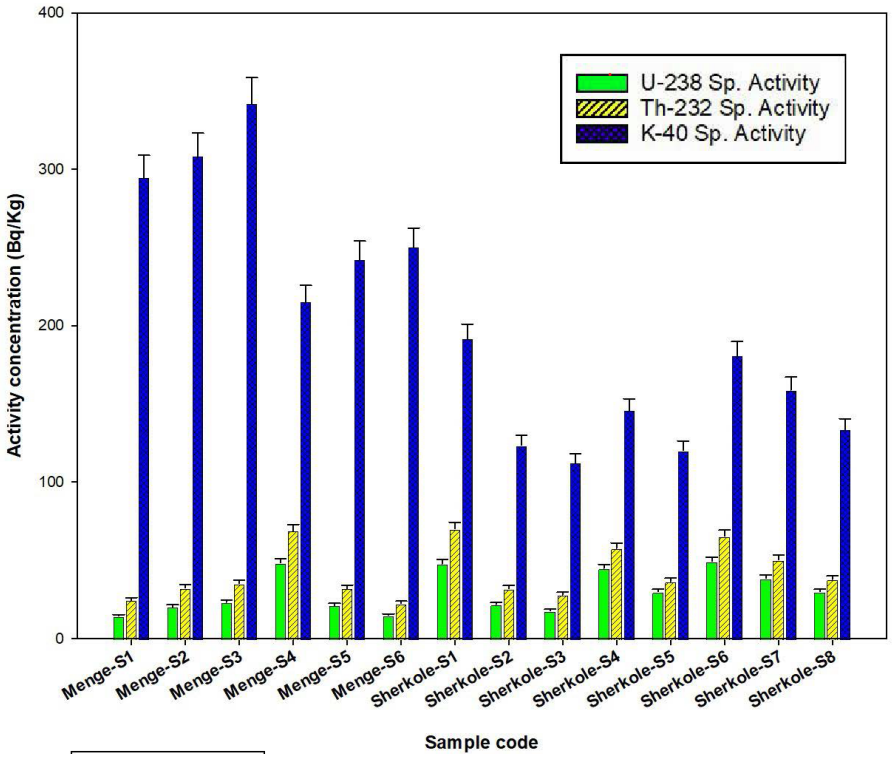

Figure 4.10: Specific activity concentration of radionuclides within the Menge and Sherkole soil samples

Comparison of radioactivity concentrations

The measured activity concentration of ^{238}U, ^{232}Th, and ^{40}K for Menge and Sherkole soil samples are in the range of 14.57±0.81 Bq/kg^{-1} to 49.52±2.44 Bq kg^{-1}, 22.6±1.32 Bq kg^{-1} to 70.4±4.01 Bq kg^{-1}, and 112.53 ± 5.70 Bq kg^{-1} to 342.08 ± 16.55 Bq kg^{-1}, respectively. The comparison of the mean radioactivity concentration of Menge and Sherkole districts with other countries gives relatively similar results as shown in Table 4.13. The soil samples from Menge and Sherkole districts have higher activity concentrations of ^{238}U, ^{232}Th, and ^{40}K than soils from Espirito Santo State of Brazil [42], Mtskheta

Mtianeti region of Georgia [43], Kampinoski National Park of Poland [45], Imo state of Nigeria [37], and Richards Bay of South Africa [38] (see Figure 4.11).

Table 4.13: Comparison of mean activity concentration of ^{238}U, ^{232}Th and ^{40}K found in Menge and Sherkole soil with selected of the world

No	Country	$A_{U/Ra}$(Bq kg^{-1})	A_{Th}(Bq kg^{-1})	A_K(Bq kg^{-1})	Reference
1	Ethiopia (Menge)	24 ± 1.2	36.15 ± 2	275.5 ± 13.3	This study
2	Ethiopia (Sherkole)	35.14 ± 1.77	47.3 ± 2.7	146 ± 7.2	-
3	Algeria (Mila)	46.7	26.7	246.5	[32]
4	Brazil (Espirito Santo)	30	94	48	[42]
5	China (Guangdong)	79.3	101	535.8	[33]
6	Georgia (Mtskheta)	25.4	26.9	464	[43]
7	India (Panipat)	30.2 ± 0.5	29.89 ± 0.6	291.06 ± 0.5	[35]
8	Italy (Lombardia)	72	48	617	[36]
9	Poland (Kampinoski)	8.54	6.65	206	[45]
10	Nigeria (Imo State)	4.15	1.64	134.13	[37]
11	South Africa (Richards)	28.2 ± 11.4	29.6 ± 11.5	146.7 ± 63.3	[38]
12	Turkiye (Ardahan)	29.9 ± 6.2	36.7 ± 6.8	435.1 ± 24	[39]
13	Russia Federation	19	30	520	[2]
14	United States	40	35	370	[2]
15	UNSCEAR2000	35	30	400	[2]

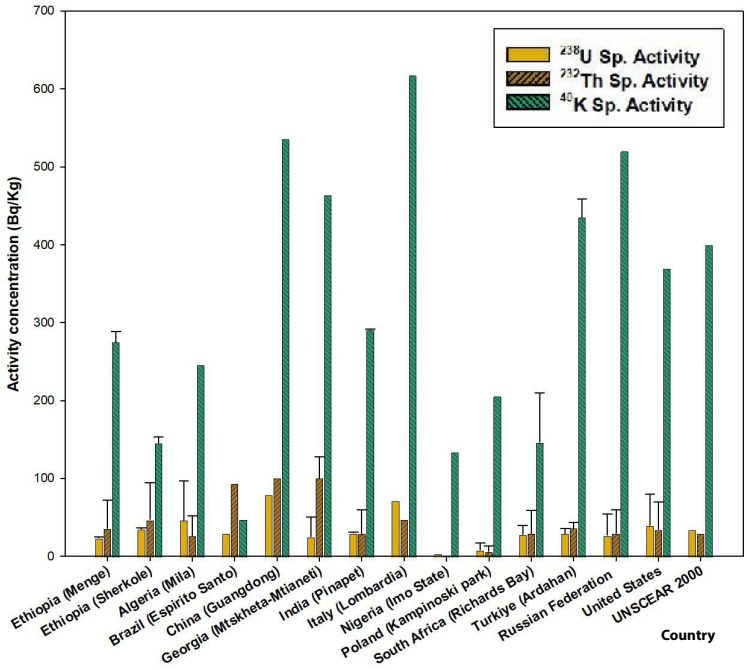

Figure 4.11: Comparison of radioactivity concentration in Menge-Sherkole soil samples with soil samples across the globe

Summarily, Menge and Sherkole districts soils have lower radioactivity concentrations of ^{238}U, ^{232}Th, and ^{40}K than soils from the Guangdong region of China [33], Ireland [2], Lombardia region of Italy [36], Ardahan province of Türkiye [39]. From comparison as shown in Figure 4.11, Menge and Sherkole soils have the safest concentrations of radionuclides, as this are less than the recommended world safe values of 35, 30, and 400 Bq kg^{-1} for Uranium ^{238}U, ^{232}Th, and ^{40}K respectively.

Table 4.14: Values of the radiological doses

No	Sample Code	Ra_{eq}	D(nGy h^{-1})	E(mSv/y)$_{Outdoor}$	E(mSv/y)$_{Indoor}$
1	Menge-S1	72.57 ± 4.02	33.8 ± 1.69	0.24 ± 0.01	0.98 ± 0.049
2	Menge-S2	90.92 ± 4.92	41.8 ± 2.19	0.30 ± 0.015	1.21 ± 0.06
3	Menge-S3	100.24 ± 5.4	46.2 ± 2.35	0.33 ± 0.016	1.33 ± 0.06
4	Menge-S4	164.05 ± 8.7	72.8 ± 3.8	0.53 ± 0.027	2.11 ± 0.11
5	Menge-S5	86.19 ± 4.7	39.3 ± 2.08	0.28 ± 0.014	1.13 ± 0.055
6	Menge-S6	66.64 ± 3.58	30.9 ± 1.5	0.22 ± 0.01	0.89 ± 0.04
7	Sherkole-S1	163.28 ± 8.9	72.3 ± 3.8	0.52 ± 0.027	2.09 ± 0.1
8	Sherkole-S2	77.26 ± 4.17	34.4 ± 1.85	0.25 ± 0.013	0.99 ± 0.053
9	Sherkole-S3	66.5 ± 3.7	29.7 ± 1.53	0.21 ± 0.01	0.86 ± 0.04
10	Sherkole-S4	138.9 ± 7.63	61.58 ± 3.3	0.44 ± 0.023	1.78 ± 0.09
11	Sherkole-S5	91.4 ± 4.98	40.82 ± 2.12	0.29 ± 0.015	1.18 ± 0.06
12	Sherkole-S6	157.12 ± 8.42	69.7 ± 3.67	0.50 ± 0.026	2.02 ± 0.10
13	Sherkole-S7	123.07 ± 6.67	54.8 ± 2.9	0.4 ± 0.02	1.58 ± 0.08
14	Sherkole-S8	94.54 ± 5.08	42.18 ± 2.17	0.3 ± 0.015	1.22 ± 0.062
15	**Total Mean value**	106.62 ± 5.7	47.8 ± 2.4	0.34 ± 0.01	1.3 ± 0.06

The radium equivalent (Ra_{eq}) for all soil samples varied from 66.64 ± 3.58 Bq kg^{-1} to 164.05 ± 8.7 Bq kg^{-1} with a mean value of 106.62 ± 5.7 Bq kg^{-1} (Table 4.14). These values are lower than recommended maximum level of radium equivalent i.e. 370 Bq kg^{-1} . The activity concentration of ^{238}U and ^{232}Th in Menge-S4, Sherkole-S1, Sherkole-S4, Sherkole-S6, and Sherkole-S7 samples are higher than the remaining samples which exceed the recommended safe values of 35, 30 Bq kg^{-1} for ^{238}U and ^{232}Th, respectively. The absorbed dose rate for all soil samples is in the range of 29.7 ± 1.53 nGy h^{-1} to 72.8 ± 3.8 nGy h^{-1} with an average value of 47.8 ± 2.4 nGy h^{-1} and which is less than the recommended safe value of 59 nGy h^{-1}. The absorbed dose rate for samples Menge-S4, Sherkole-S1, Sherkole-S4, and Sherkole-S6 are above the recommended safe value of 59 nGy h^{-1} [2] as depicted in Table 4.14.

Table 4.15: Values of the radiation hazard indexes

No	Sample Code	I_γ	H_{ex}	H_{in}	ELCR(10^{-3})
1	Menge-S1	0.27 ± 0.009	0.19 ± 0.006	0.23 ± 0.007	0.84 ± 0.035
2	Menge-S2	0.33 ± 0.01	0.24 ± 0.008	0.3 ± 0.009	1.05 ± 0.05
3	Menge-S3	0.36 ± 0.012	0.27 ± 0.009	0.33 ± 0.01	1.15 ± 0.056
4	Menge-S4	0.57 ± 0.021	0.443 ± 0.01	0.57 ± 0.02	1.85 ± 0.09
5	Menge-S5	0.31 ± 0.01	0.23 ± 0.008	0.29 ± 0.009	0.98 ± 0.049
6	Menge-S6	0.24 ± 0.008	0.18 ± 0.006	0.22 ± 0.007	0.77 ± 0.035
7	Sherkole-S1	0.57 ± 0.022	0.44 ± 0.017	0.57 ± 0.02	1.82 ± 0.09
8	Sherkole-S2	0.27 ± 0.01	0.20 ± 0.007	0.26 ± 0.009	0.87 ± 0.04
9	Sherkole-S3	0.23 ± 0.008	0.17 ± 0.006	0.22 ± 0.008	0.73 ± 0.035
10	Sherkole-S4	0.48 ± 0.0186	0.37 ± 0.014	0.49 ± 0.017	1.54 ± 0.08
11	Sherkole-S5	0.32 ± 0.01	0.24 ± 0.009	0.32 ± 0.011	1.01 ± 0.052
12	Sherkole-S6	0.55 ± 0.02	0.42 ± 0.016	0.55 ± 0.01	1.75 ± 0.09
13	Sherkole-S7	0.43 ± 0.016	0.33 ± 0.012	0.43 ± 0.015	1.4 ± 0.07
14	Sherkole-S8	0.33 ± 0.012	0.25 ± 0.009	0.33 ± 0.01	1.05 ± 0.05
15	**Total Mean value**	0.37 ± 0.01	0.28 ± 0.01	0.36 ± 0.01	1.2 ± 0.05

Discussion

The higher radioactivity concentration of ^{238}U is found in Sherkole-S6 soil and the lowest amount is found in Menge-S1 soil. A higher concentration of ^{232}Th is found in Sherkole-S1 soil and the lowest one in Menge-S6 soil. A higher concentration of ^{40}K is found in Menge-S3 and the lowest one is found in Sherkole-S3 soil. a look at the average values of radioactivity concentrations in Figure 4.10 shows that the Sherkole district has a higher concentration of uranium (^{238}U) and thorium (^{232}Th). While

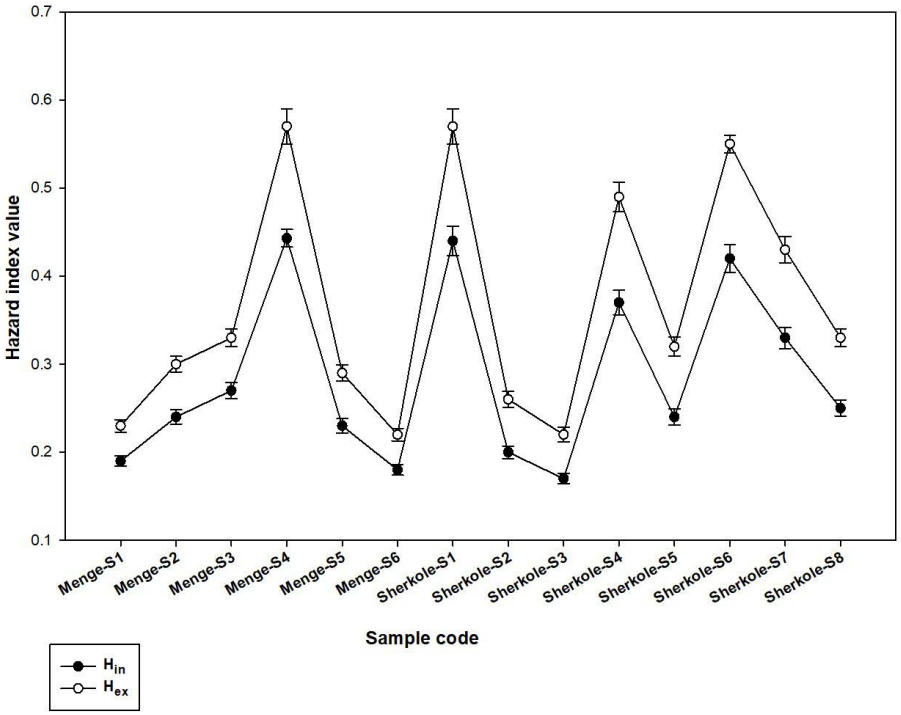

Figure 4.12: Plot for external and internal hazard index

Menge district has a high concentration of potassium (^{40}K) than the Sherkole district.

For all soil samples, the annual effective indoor dose rate varies from $0.86 \pm 0.04\,\mathrm{mSv\,y^{-1}}$ to $2.11 \pm 0.11\,\mathrm{mSv\,y^{-1}}$ with an average of $1.3 \pm 0.06\,\mathrm{mSv\,y^{-1}}$ and for the outdoor the variation is $0.21 \pm 0.01\,\mathrm{mSv\,y^{-1}}$ to $0.53 \pm 0.027\,\mathrm{mSv\,y^{-1}}$ with an average of $0.34 \pm 0.01\,\mathrm{mSv\,y^{-1}}$ 4.14. We note that average indoor annual effective dose rate of all soil samples is above the world mean value of 1 $mSv\ y^{-1}$. The indoor annual effective dose equivalent is greater than the outdoor annual effective dose equivalent. However, the average outdoor annual effective dose rate was less than the world annual safety value of 1 $mSv\ y^{-1}$.

Values of the gamma index varied in the range of 0.23 ± 0.008 to 0.57 ± 0.021 with an average value of 0.37 ± 0.013, which is less than the recommended safe value of one (see Table 4.15). The external and internal hazard index values vary on the range 0.17 ± 0.006 to 0.44 ± 0.017 with an average of 0.28 ± 0.01 and 0.22 ± 0.007 to 0.57 ± 0.02 with an average of 0.36 ± 0.01, respectively (as shown in Table 4.15). The values for the H_{in} and H_{ex} of all soil samples are below the safe value of one (Figure 4.12). From the gamma index, external and internal hazard indexes of the soil samples have the safest values. Thus indicates that the levels of radon and its short-lived daughters that occur on the soils do not have significant effects on the respiratory organs of individuals living in those areas. The mean value of excessive lifetime cancer risk (ELCR) for all soil samples is $(1.2 \pm 0.05) \times 10^{-3}$ (see Table 4.15). The values of excessive lifetime cancer risk of all soil samples exceed the threshold value of 0.29×10^{-3}. The long time exposure to γ ray that comes from naturally occurred radionuclides found in Menge and Sherkole soils can make a significant health effects.

4.1.4 Radioactivity in Soil Samples: Mekele City

Study Area and Sample Collection

Soil samples were collected from selected sites in Mekelle City, focusing on densely populated areas such as universities, residential neighborhoods, and transportation terminals. The samples were air-dried at room temperature, these after these were grounded until fully homogenized. Seven districts within Mekelle City, each approximately 3 kilometers apart, were chosen for sampling, as listed in Table 4.16. Mekelle City, the capital of the Tigray regional state, is one of the eleven regions in Ethiopia, as illustrated in Figure 4.13. Mekelle is located approximately 780 kilometers by road north of Addis Ababa. Specifically, the city lies between coordinates ($13°25'24''$ to $13°33'44''$) N and ($39°25'26''$ to $39°33'14''$) E, with an altitude ranging from 1930 to 2353 meters above mean sea level [47]. All samples were carefully collected from a depth of 5 to 15 cm below the soil surface, and each weighing approximately 1 g. The samples were labeled as $Y-S1, Y-S2, \cdots, Y-S7$.

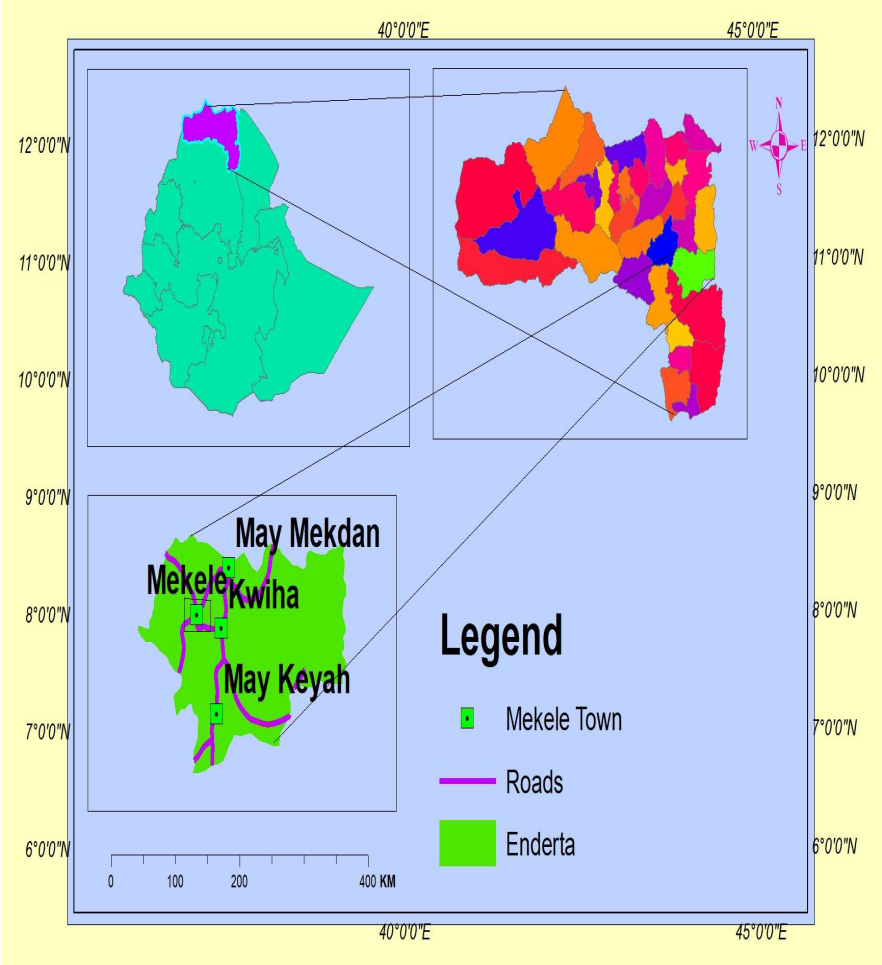

Figure 4.13: Map of Mekelle City in Tigray region, Ethiopia

Table 4.16: The GPS location of the collected samples

No	Sample Code	Sample Place	Location (GPS)North	Location (GPS)East
1	Y-S1	Elala	$13°31'2.856''$	$39°29'36.445''$
2	Y-S2	Mai Woini	$13°28'25.51411''$	$39°27'42.098''$
3	Y-S3	Arid	$13°28'46.3836''$	$39°29'4.0272''$
4	Y-S4	Romanat	$13°29'26.3228''$	$39°28'26.01''$
5	Y-S5	Lache	$13°32'20.774''$	$39°30'20.5848''$
6	Y-S6	Medre Genet1	$13°27'18.7488''$	$39°27'18.7488''$
7	Y-S7	Meder Genet2	$13°27'18.7488''$	$39°27'18.7488''$

Presentation of Measured Radioactivity Results

Table 4.17: The specific activity concentration of radionuclides in soil samples

No	Sample Code	Site name	A_{Ra}(Bq kg^{-1})	A_{Th}(Bq kg^{-1})	A_K(Bq kg^{-1})
1	Y-S1	Elala	22.9 ± 1.025	43.25 ± 2.25	321.7 ± 14.2
2	Y-S2	Mai Woini	24.35 ± 1.185	57.15 ± 3.15	613.7 ± 28.1
3	Y-S3	Arid	27.855 ± 5.66	64.65 ± 12.95	410.5
4	Y-S4	Romanat	13.7 ± 0.58	25.4 ± 1.4	206 ± 9.8
5	Y-S5	Lache	20.95 ± 1.035	37 ± 2.07	321.1 ± 14.95
6	Y-S6	Medre Genet1	32.14 ± 1.485	58.9 ± 3.19	355.18 ± 16
7	Y-S7	Meder Genet2	33.35 ± 1.55	85.29 ± 4.57	371.2 ± 16.8
8	**Mean value**		25.035 ± 1.788	53.091 ± 4.22	371.34 ± 14.26

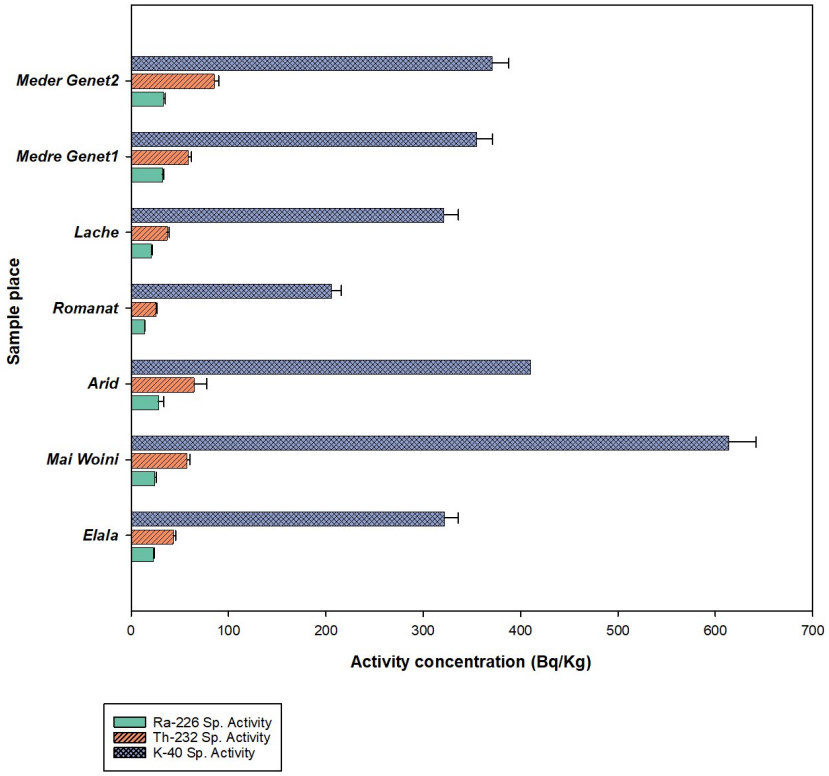

Figure 4.14: Specific activity concentration of radionuclides within the soil samples

Comparison with Global Average and Safety Thresholds

The mean radioactivity concentration of Radium (^{226}Ra), Thorium (^{232}Th), and Potassium (^{40}K) of Mekelle City soil samples have smaller variations as compared to other countries as shown in Figure 4.15. In Georgia from the Kvemo Kartli region, Kharami Massif area the mean specific activity concentrations for soil samples are 38.57, 53.18, and 879.76 Bq kg^{-1} for ^{226}Ra, ^{232}Th, and ^{40}K, respectively [34]. The radioactivity concentration of Mekelle soil samples is also compared to soil samples of Sijua Dhanbad City in Jharkhand State of India. In India Dhanbad City the mean radioactivity concentration values for ^{226}Ra, ^{232}Th, and ^{40}K are 60.29 Bq kg^{-1}, 64.50 Bq kg^{-1}, and 481.0 Bq kg^{-1}, respectively [48]. Whereas the mean radioactivity concentrations of ^{226}Ra, ^{232}Th, and ^{40}K for Mekelle soil samples are 25.035±1.788 Bq kg^{-1}, 53.091±4.22 Bq kg^{-1}, and 371.34±14.26 Bq kg^{-1}, respectively. Also, the average radioactivity concentration of ^{238}U, ^{232}Th, and ^{40}K for soil samples from Nigeria in Orlu, Imo State is 4.15, 1.64, and 134.13 Bq kg^{-1}, respectively [37] as shown in Table 4.18.

Table 4.18: Comparison activity concentrations in Mekelle soil with other countries' soil

No	Country	A_{Ra} (Bq kg^{-1})	A_{Th} (Bq kg^{-1})	A_K (Bq kg^{-1})	Reference
1	Ethiopia (Mekelle City)	25.03 ± 1.7	53.09 ± 4.2	371.3 ± 14	Present study
2	Algeria	30	25	370	[2]
3	Belgium	26	27	380	-
4	China	33	41	440	-
5	Croatia	54	45	490	-
6	Georgia (Kharami)	38.57	53.18	879.76	[34]
7	India (Dhanbad City)	60.29	64.50	481	[48]
8	Ireland	60	26	350	[2]
9	Japan	29	28	310	-
10	Nigeria (Imo State)	4.15	1.64	134.13	[37]
11	Switzerland	40	25	370	[2]
12	Turkiye (Ardahan)	29.9 ± 6.2	36.7 ± 6.8	435.1 ± 24	[39]
13	Russia Federation	19	30	520	[2]
14	United States	40	35	370	[2]

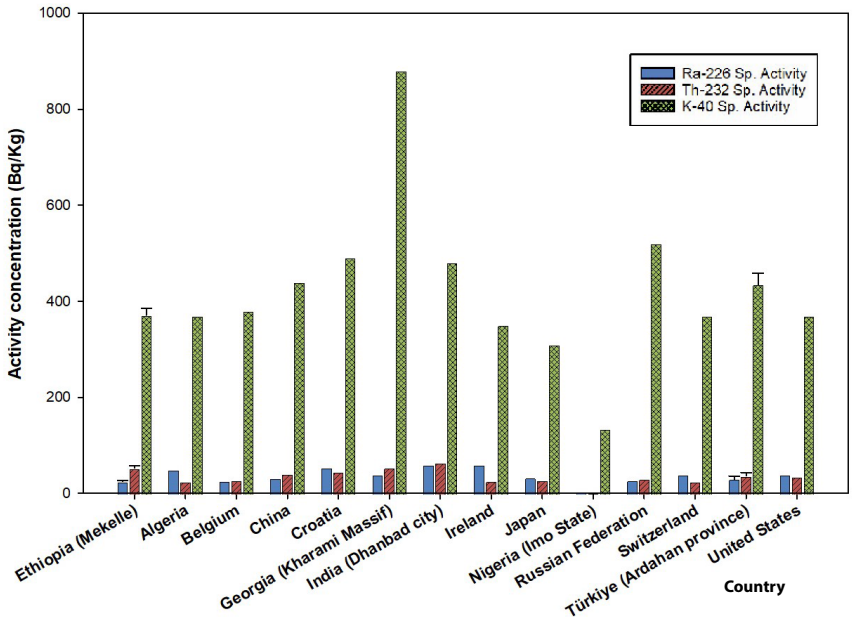

Figure 4.15: Comparison of Activity concentrations in Mekelle soil with other countries'

In Ardahan province of Turkiye, the mean specific activity concentrations of the soil are 29.9 ± 6.2, 36.7 ± 6.8, and $435.1 \pm 23.9\,Bq/kg^{-1}$ for ^{226}Ra, ^{232}Th, and ^{40}K, respectively [39]. A comparison of activity concentartion shows that, Mekelle City soils have lower radionuclide concentrations than soils from Dhanbad City of India, Ardahan province of Türkiye, and Kvemo Kartli region of Georgia, but higher than Orlu, Imo state of Nigeria. The mean radioactivity concentration of Mekelle soil is less than the recommended world means values of 35, 30, and $400\,Bq\,kg^{-1}$ for Radium ^{226}Ra, ^{232}Th, and ^{40}K, respectively, exception are found for ^{232}Th .

Discussion

In the Mekelle soil studies, the selected sites cover different geographical features, mostly Mai Woini and Romanat have dry soil characters so these can be grouped into sandy soil. Arid districts soil also has dry soil type and categorized as silt soil. Medre Genet1, Elala, and Lache districts have wet soil characters and grouped into clay soil type. Medre Genet2 soil samples have been categorized as chalk soil . The collected soils geographical location is varying. Dry soil samples have been found mostly in lowland areas whereas the wet soil types were found in highland area.

Figure 4.14 shows there is a high concentration of ^{226}Ra found in Medre genet 2, but it is below the recommended safe value of $35\,Bq\,kg^{-1}$, the high radioactivity concentration of ^{232}Th is observed from the result within Medre Genet districts (Y-S6 and Y-S7), which means these can have significant radiation hazard risks for the population around those areas. Also, there is a high radioactivity concentration of ^{40}K which is found in the Mai Woini (Y-S2) district, so safety measures have to be placed around those areas. From the data shown in Table 4.17, the mean radioactivity concentrations of ^{226}Ra, ^{232}Th, and ^{40}K for Mekelle soil samples are $25.035 \pm 1.788 Bq\,kg^{-1}$, $53.091 \pm 4.22\,Bq\,kg^{-1}$, and $371.34 \pm 14.26\,Bq\,kg^{-1}$, respectively.

The radium equivalent activity Ra_{eq} values for all soil samples are vary from 60.85 ± 2.983 to $153.32 \pm 7.845\,Bq\,kg^{-1}$. These values are much less than the safe value of $370\,Bq\,kg^{-1}$. As shown in Table 4.19, the average absorbed dose rate is $67.9 \pm 4\,nGy\,h^{-1}$ which is below the recommended safe value $59 nGy\ h^{-1}$. The calculated values of outdoor annual effective dose equivalent obtained in present study vary from $0.061 \pm 0.001\,mSv\,y^{-1}$ to $0.155 \pm 0.0065\,mSv\,y^{-1}$ with an average of $0.08 \pm 0.01\,mSv\,y^{-1}$ and indoor annual effective dose rate ranged from $0.148 \pm 0.0073\,mSv\,y^{-1}$ to $0.621 \pm 0.026\,mSv\,y^{-1}$ with an average of $0.3 \pm 0.01\,mSv\,y^{-1}$. The mean value of annual effective dose rate are less than the world average annual effective dose rate of $1\,mSv\,y^{-1}$ [2].

Table 4.19: Values of the radiological doses

No	Sample Code	Ra_{eq}	$D(nGy\,h^{-1})$	$E(mSv/y)_{Outdoor}$	$E(mSv/y)_{Indoor}$
1	Y-S1	109.5 ± 5.208	50.103 ± 1.094	0.061 ± 0.001	0.245 ± 0.0053
2	Y-S2	153.32 ± 7.845	71.25 ± 3.609	0.087 ± 0.004	0.349 ± 0.017
3	Y-S3	151.90 ± 19.17	69 ± 10.433	0.084 ± 0.012	0.338 ± 0.0511
4	Y-S4	65.78 ± 3.334	30.25 ± 1.508	0.037 ± 0.01	0.148 ± 0.0073
5	Y-S5	98.58 ± 6.826	45.406 ± 2.342	0.0556 ± 0.002	0.2227 ± 0.0114
6	Y-S6	143.7 ± 7.275	82.9 ± 4.086	0.101 ± 0.0497	0.406 ± 0.02
7	Y-S7	144.62 ± 6.245	126.6 ± 5.37	0.155 ± 0.0065	0.621 ± 0.026
8	**Mean value**	123.9 ± 7.9	67.9 ± 4	0.08 ± 0.01	0.3 ± 0.01

The high value of AEDR is obtained in Meder Genet district. The calculated values of the external

hazard index obtained in the present study ranged from 0.1008 ± 0.0069 to 0.412 ± 0.0209 with a mean of 0.3 ± 0.013 and the internal hazard index ranged from 0.231 ± 0.0116 to 0.487 ± 0.0206 with a mean of 0.4 ± 0.02, respectively (see Table 4.20). The external and internal hazard index values are less than the recommended safe value of one (see Figure 4.16). The mean excessive lifetime cancer risk (ELCR) for the given soil samples is $(1.23 \pm 0.04) \times 10^{-3}$ and it exceeds the standard safe values 0.29×10^{-3}. The highest values of ELCR is found mainly in Elala, Medre Genet1, and Medre Genet2 districts as shown in Table 4.20. From the values of ELCR it can be noticed that, long time exposure to indoor radioactivity may cause serious health effects so that sufficient precautions are addressed for the population of those districts.

Table 4.20: Values of the radiation hazard indexes

No	Sample Code	I_γ	H_{ex}	H_{in}	ELCR($\times 10^{-3}$)
1	Y-S1	0.39 ± 0.05	0.29 ± 0.013	0.35 ± 0.05	0.85 ± 0.01
2	Y-S2	0.5 ± 0.02	0.41 ± 0.02	0.47 ± 0.02	1.2 ± 0.05
3	Y-S3	0.55 ± 0.082	0.4 ± 0.006	0.48 ± 0.02	1.6 ± 0.02
4	Y-S4	0.23 ± 0.008	0.17 ± 0.008	0.2 ± 0.01	0.5 ± 0.02
5	Y-S5	0.36 ± 0.01	0.26 ± 0.012	0.32 ± 0.015	0.7 ± 0.04
6	Y-S6	0.5 ± 0.02	0.38 ± 0.018	0.4 ± 0.02	1.4 ± 0.06
7	Y-S7	0.5 ± 0.02	0.39 ± 0.01	0.4 ± 0.02	2.17 ± 0.09
8	**Mean value**	0.43 ± 0.03	0.3 ± 0.01	0.4 ± 0.02	1.23 ± 0.04

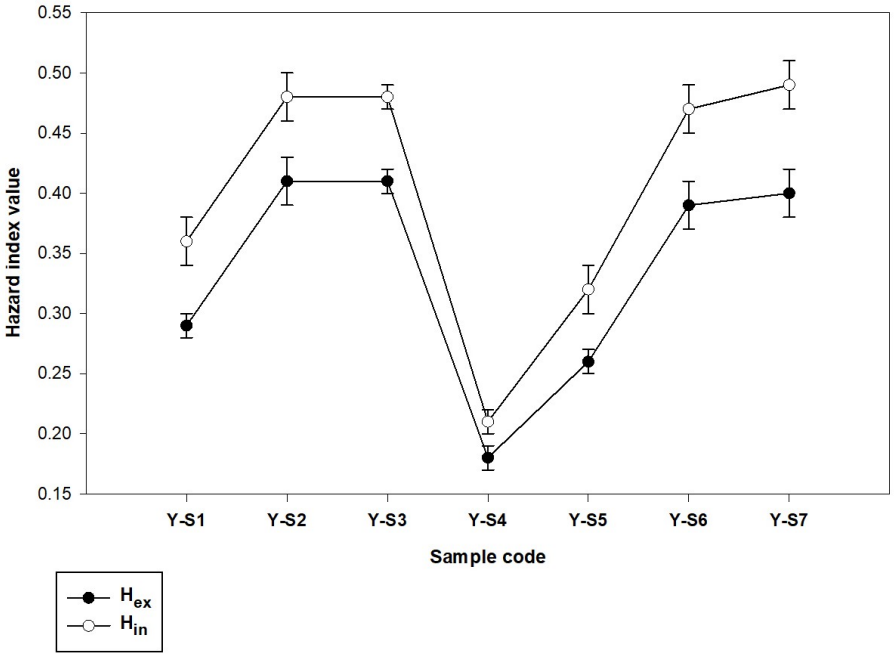

Figure 4.16: Internal and external hazard index values for Mekelle soil samples

4.2 Radioactivity in Medicinal and Food Plants

The objective of this study is to investigate the natural radioactivity concentration of different Medicinal and food plants collected from Assosa town.

4.2.1 Radioactivity in Medicinal Plants

Sample collection and Preparation

Assosa city is found in the western part of Ethiopia at a distance of 687 km from the capital City of Ethiopia, Addis Ababa, and located 90 km away from the Ethio-Sudanese border [49].

The collected plants grow in many different areas of the region. Roselle or Karkade (Hibiscus sabdariffa) is taken mainly as a tea and widely taken to fight colds, known as a blood pressure moderator and also used to treat malaria. Whereas Okra (Abelmoschus esculentus) can be used as a food source and a good source of minerals, vitamins, antioxidants, and fiber. Moringa oleifera which belongs to the family Moringaceae [50], is mostly taken for antioxidant, anemia, arthritis, and other joint pain, also used for asthma, stomach pain, headache, and used for many types of health benefits. All the plants types have important elemental contents that use for human health. Many studies were undertaken to find out what type of element these contain, and it is estimated that these elements are important for health.

Three types of plants that are used for medicinal and food sources were collected from farmers and traditional marketplaces in the Asossa zone mainly from Assosa town in Benishangul Gumuz Region (see Figure 4.1). The collected plant samples were Okra (Abelmoschus esculentus), Moringa oleifera, and Karkade (Hibiscus Flower or Roselle) (see Figure 4.17). Special codes were assigned to each of the samples before storage. In sample classification, Y-M is used for sample code. After collecting the samples and washing these with water, and by air-dried the leaves in a drying chamber at $100^{\circ}C$ in a heated oven. The leaves were crushed into powder by agate mortar then filtered by a 0.25 mm-mesh sieve. About 500 g of each sample was sealed in a polyethylene capsule, the sample was stored for 28 days before gamma-ray analysis, as it allows ^{226}Ra and its daughters to achieve secular equilibrium.

Presentation of Measured Radioactivity Results

Table 4.21: Mean activity concentration of natural radionuclides and annual committed effective dose

No	Code	Plants	A_U(Bq kg^{-1})	A_{Th}(Bq kg^{-1})	A_K(Bq kg^{-1})	AACED(mSv/y)
1	Y-M1	Okra	4.65	14.2 ± 0.1	191 ± 11.1	0.025 ± 0.0011
2	Y-M2	Moringa	18.8 ± 0.07	64.45 ± 7.9	1487.2 ± 83	0.03 ± 0.0033
3	Y-M3	Roselle	3.74 ± 0.06	7.37 ± 0.01	60 ± 4.1	0.003 ± 0.00004
4	Mean value		9.06 ± 0.06	28.6 ± 2.6	579 ± 32.8	0.019 ± 0.001

Comparison with Global Average and Safety Thresholds

The threshold value of E_{ave} due to ingestion of naturally occurring radionuclides is 0.3 mSv y^{-1}. For each natural radionuclide ingestion to the body for adults the committed effective dose values are 45 for Uranium-238, 230 for Thorium-232 and 6.2 $nSvBq^{-1}$ for Potassium-40.

Discussion

Radionuclides can be found on the surface of the earth. It is known that medicinal plants deposited organic and inorganic constituents. Several types of research have been done on organic constituents. In the present study the activity concentration of radionuclides of Uranium(^{238}U), Thorium (^{232}Th),

Figure 4.17: Preparation of the collected medicinal plants

and Potassium(^{40}K) have been recorded using an HPGe detector. Naturally occurring radionuclides concentration in foods can depend on climate and agricultural conditions. The chemical constituents found in the plants are the main cause for their medicinal properties including bases comprising alkaloids, amines, and glycosides [51]. Specific parts are studied for different plants such as leaves, fruits, bark, stem, and roots. Mostly these are used as medicines [52]. One way of contamination of plant products for some radionuclides is direct deposition, those known by their low root uptake and short-lived radionuclides and these can transfer rapidly through the food chain.

From releases of radionuclides, medicinal plants exposure to contamination of radioactivity can happen. Most vegetation for food may be subjected to this contamination. Contamination on terrestrial vegetation which is the accumulation of radionuclides from the atmosphere on the plant is above the ground parts. Different types of elements of varying concentrations are found in different parts of the plants. Mainly these are found in seeds, roots, and leaves. which are taken as a food item and also as an ingredient for the ayurvedic preparation [53].

The plant leaves are used in some countries for example in India, Malaysia, and Greece mainly for therapeutic effects. From the consumption of foods, ^{40}K is uniformly distributed in the body. Its concentration found in the body is within homeostatic control. Other than inhalation into the internal body system, also the ingestion exposure occurs from the consumption of food sources exposes to radionuclides. Contamination of plants happens in two ways, by transfer from the source into plants directly through the atmosphere and by depositing radionuclides in the ground. For the body of adults and children, the amount content of ^{40}K is about 0.18% and 0.2%, respectively. Continuous exposure

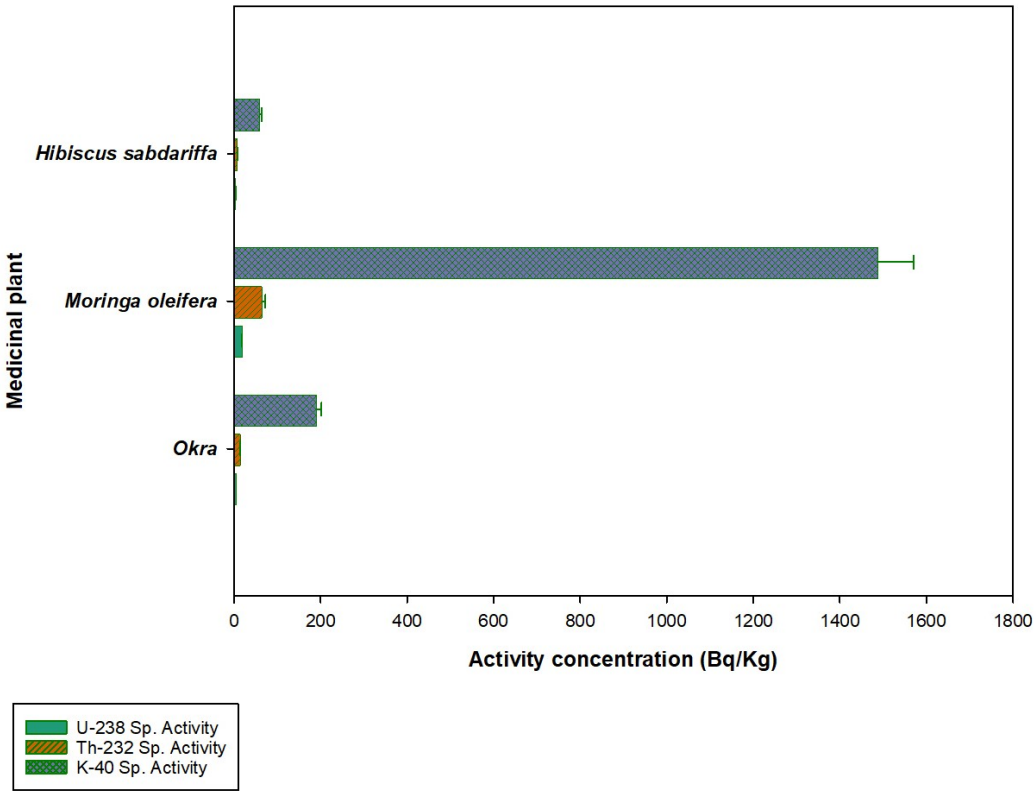

Figure 4.18: Mean radioactivity concentration of U-238, Th-232, and K-40 in Medicinal plants

to radiation is a causes for diseases like lung cancer, melanoma, cancer of the kidney, skin cancer, and breast cancer [2].

From the result as shown in Table 4.21, high activity concentration of ^{40}K of 1487.2 ± 83.4Bq kg^{-1}, is found in the Moringa oleifera plant, so safety measures are needed. Over high activity concentration of ^{232}Th is observed in Moringa oleifera plant as shown in Figure 4.18. Okra (Abelmoschus esculentus) and Roselle (Hibiscus sabdariffa) samples have radioactivity concentration below the limit 35, 30, and 400 Bq/Kg for Uranium-238, Thorium-232, and K-40, respectively. From the result the average annual committed effective doses varied from $0.003 \pm 0.00004 mSv\ y^{-1}$ to 0.03 ± 0.0033 mSv y^{-1} with a mean value of 0.019 ± 0.0015 mSv y^{-1} (see Table 4.21).

4.3 Radioactivity in Industrial Product

4.3.1 Radioactivity in Cement Raw Materials

Study Area and Sample Collection

The materials from Messebo cement factory collected are used as raw samples in the production of Ordinary Portland Cement (OPC) and Pozzolana Portland Cement (PPC) which are the major products. In this factory, other cement products produced are used for the construction of irrigation and electric power dams. The raw materials are collected in the Tigray region. Gypsum and pozzolana deposits are in wajirat province, Iron and silica from Wukro province, limestone and shale from Messebo Mountain, where the Messebo factory is located.

A total of 6 raw material samples and (OPC and PPC) products in amounts, weighting upto 1 kg were mainly collected from the Messebo cement factory, located at 13.5697721 (latitude) and 39.4741283 (longitude). In Messebo cement factory, the production of OPC uses 85% of Limestone and Shale, 10% Iron and Silica, and 5% is gypsum. In the case PPC, the factory uses 20% Pozzolana as raw material. This data can give us amount of different radioactivity concentration found in the raw material. The samples were collected from the sampling sites listed in Table 4.22, and the samples are air-dried at room temperature. The dried samples were grinded until homogenize, and taken to the research laboratory using polyethylene capsules or vials and processed in such a way to make these suitable for gamma-ray detector.

Table 4.22: List of the collected samples

No	Sample code	Sample type	Sample source place
1	Y-C1	Sandstone (Silica)	Wukro
2	Y-C2	Limestone	Messebo Mountain
3	Y-C3	Shale	Messebo Mountain
4	Y-C4	Iron	Wukro
5	Y-C5	Gypsum	Hintalo Wajirat
6	Y-C6	Pozzolana	Hintalo Wajirat
7	Y-C7	OPC	Messebo Factory
8	Y-C8	PPC	Messebo Factory

Presentation of Measured Radioactivity Results

The average radioactivity concentration of ^{226}Ra, ^{232}Th, and ^{40}K in cement raw material and product samples are $22.7 \pm 0.8\,\mathrm{Bq\,kg^{-1}}$, $30.5 \pm 1.7\,\mathrm{Bq\,kg^{-1}}$, and $183.5 \pm 8.8\,\mathrm{Bq\,kg^{-1}}$, respectively listed in Table 4.23. Regarding the results obtained in this study, the limestone, gypsum, pozzolana, and iron have not or have minimum radioactivity concentrations of ^{226}Ra, ^{232}Th, and ^{40}K as shown in Figure 4.19. PPC from the Messebo cement factory has 30.7 ± 1.5, 28.65 ± 1.65, and $143 \pm 7.3\,\mathrm{Bq\,kg^{-1}}$ for ^{226}Ra, ^{232}Th, and ^{40}K, respectively, which are below the recommended safe values. Although, the thorium activity concentration in sandstone and shale raw materials, collected from Wukro and Messebo mountain provinces are above the threshold, but their radiation hazard index values are below the recommended safe values.

Table 4.23: Specific activity concentration of ^{226}Ra, ^{232}Th and ^{40}K of the Samples

No	Sample Code	A_{Ra}(Bq kg^{-1})	A_{Th}(Bq kg^{-1})	A_K(Bq kg^{-1})	Ra_{eq}
1	Y-C1	21.2 ± 0.99	53.2 ± 2.9	304 ± 13.8	120.676 ± 6.202
2	Y-C3	18.6 ± 0.9	36.15 ± 2	273.2 ± 12.5	91.32 ± 4.729
3	Y-C4	20.61 ± 0.05	4.04 ± 0.35	14 ± 1.73	27.458 ± 0.673
4	Y-C8	30.7 ± 1.5	28.65 ± 1.65	143 ± 7.3	82.67 ± 4.412
5	**Mean value**	22.7 ± 0.8	30.5 ± 1.7	183.5 ± 8.8	80.5 ± 4

From the result the Messebo cement factory products OPC and PPC are compatible with standards of UNSCEAR reports on activity concentration of naturally occurring radionuclides, so it can be used for commercial purpose. The values of radium equivalent ranged from $27.458 \pm 0.673\,\mathrm{Bq\,kg^{-1}}$ to $120.676 \pm 6.202\,\mathrm{Bq\,kg^{-1}}$ with an average value of $80.5 \pm 4\,\mathrm{Bq\,kg^{-1}}$, this value is below the recommended safe value of 370Bq kg^{-1} [2]. The average absorbed dose rate for all studied samples is 36.5 ± 1.7 nGy h^{-1}, which is less than the recommended safe value of $59 nGy\, h^{-1}$. The average outdoor and indoor annual effective

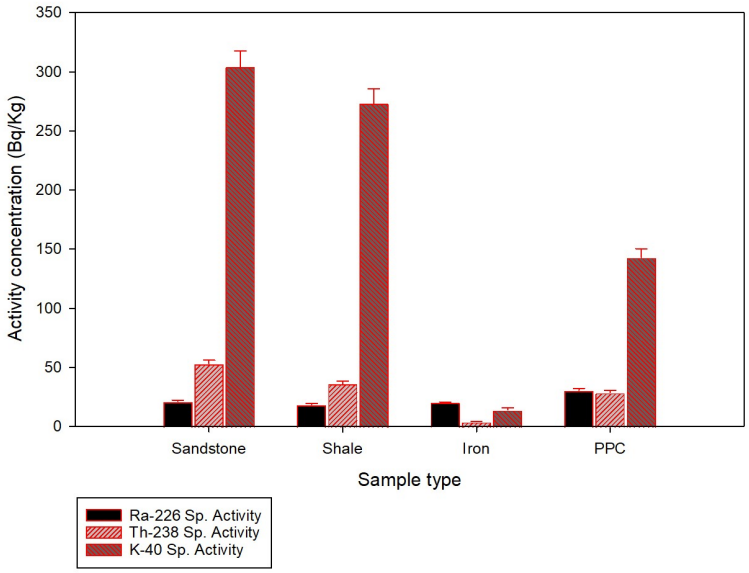

Figure 4.19: Specific radioactivity concentration in raw materials and cement product samples

dose equivalent values for all cement raw materials and products are $0.04 \pm 0.001\,\text{mSv}\,\text{y}^{-1}$ and $0.16 \pm 0.008\,\text{mSv}\,\text{y}^{-1}$, respectively which are less than the average worldwide safety value $1\,\text{mSv}\,\text{y}^{-1}$ see Table 4.24.

Table 4.24: Values of radiological doses

No	Sample Code	D(nGy h^{-1})	E(mSv/y)$_{\text{Outdoor}}$	E(mSv/y)$_{\text{Indoor}}$
1	Y-C1	54.48 ± 2.765	0.066 ± 0.003	0.2 ± 0.013
2	Y-C3	41.74 ± 2.134	0.051 ± 0.002	0.204 ± 0.01
3	Y-C4	12.53 ± 0.3016	0.015 ± 0.00035	0.061 ± 0.001
4	Y-C8	37.38 ± 1.984	0.045 ± 0.0023	0.18 ± 0.0097
5	**Mean value**	36.5 ± 1.7	0.04 ± 0.001	0.16 ± 0.008

Table 4.25: Values of radiation hazard indexes

No	Sample Code	I_γ	H_{ex}	H_{in}	ELCR(10^{-3})
1	Y-C1	0.437 ± 0.0215	0.341 ± 0.0164	0.382 ± 0.018	0.7 ± 0.04
2	Y-C3	0.33 ± 0.044	0.245 ± 0.0121	0.295 ± 0.0149	0.7 ± 0.03
3	Y-C4	0.092 ± 0.00235	0.0734 ± 0.00182	0.1294 ± 0.00195	0.2 ± 0.003
4	Y-C8	0.292 ± 0.0145	0.212 ± 0.0114	0.304 ± 0.0154	0.6 ± 0.03
5	**Mean value**	0.28 ± 0.02	0.22 ± 0.01	0.28 ± 0.01	0.54 ± 0.02

As shown in Table 4.25, the average values for external hazard index, internal hazard index, gamma index, and alpha index are 0.22 ± 0.01, 0.28 ± 0.01, 0.28 ± 0.02, and 0.11 ± 0.003, respectively which are less than the recommended safe value of one. This result indicates that the cement raw material and products have negligible radiation risks on the human from emitted radiation. The average values of excessive lifetime cancer risk for sample Sandstone (Y-C1), Shale (Y-C3), Iron (Y-C4), and Pozzolana (Y-C8) is $(0.546 \pm 0.028 \times 10^{-3})$. The excessive lifetime cancer risk for sample Iron (Y-C4) is below the threshold values of 0.29×10^{-3}. For samples Y-C1, Y-C3, and Y-C8 the value of ELCR is above the threshold limits.

Comparison with Global Average and Safety Thresholds

For the purpose of comparison of the radioactivity concentration of the samples included in the present study with those from other countries, is shown in data Table 4.26. Radioactivity concentration of ^{226}Ra is high in Tanzania Pozzolana [54] and Macedonia Pozzolana 2 [55], but lower in Macedonia Gypsum. Similarly, radioactivity concentration of Thorium-232 is higher in Tanzania Pozzolana and Macedonia Pozzolana 2, but lower in Tanzania Sandstone. As for Potassium-40, its concentration is higher in Tanzania Pozzolana and lower in Macedonia Gypsum. The Messebo PPC exhibits a lower minimum radioactive concentration when compared to Poland cement which utilizes fewer additives. Additionally, as shown in Figure 4.20, the specific activity concentrations of ^{226}Ra, ^{232}Th, and ^{40}K found in the raw materials of Messebo cement are lower than those found in Ghana, India, and Poland cements [56], [22], and [57], respectively. It is important to note that these activity concentrations are below the safe limits of 35, 30, and 400 Bq kg^{-1} for ^{226}Ra, ^{232}Th, and ^{40}K, respectively.

Table 4.26: Comparison of radioactivity concentration of Messebo cement with other countries

No	Country	Sample	A_U (Bq kg^{-1})	A_{Th} (Bq kg^{-1})	A_K (Bq kg^{-1})	Ref.
1	Ethiopia (Messebo)	PPC	30.7 ± 1.5	28.65 ± 1.65	143 ± 7.3	Studied
2	Ethiopia (Messebo)	Sandstone	21.2 ± 0.99	53.2 ± 2.9	304 ± 13.8	-
3	Ethiopia (Messebo)	Shale	18.6 ± 0.9	36.15 ± 2	273.2 ± 12	-
4	Ghana	Cement	35.94	25.44	233	[56]
5	India	Cement	54 ± 15.06	66 ± 12.1	490.6 ± 105	[22]
6	Macedonia	Cement	42 ± 10	28 ± 6	264 ± 50	[55]
7	Macedonia	Pozzolana1	64 ± 12	69 ± 15	105 ± 43	-
8	Macedonia	Pozzolana2	80 ± 20	171 ± 48	349 ± 168	-
9	Macedonia	Gypsum	5.9 ± 1.1	1.44 ± 0.44	11.0 ± 5.2	-
10	Poland	Cement	29	48	283	[57]
11	Tanzania (Songwe)	Pozzolana	93.2 ± 2.8	172.8 ± 5.2	997 ± 29	[54]
12	Tanzania (Songwe)	Sandstone	18.3 ± 0.5	30.3 ± 0.9	501 ± 15	-
13	Tanzania (Wazo)	Sandstone	7.7 ± 0.2	12.8 ± 0.4	180.4 ± 5.4	-

Discussion

Building materials are containing radionuclides are a significant potential source of indoor radioactivity. Cement is a fundamentally main material used in construction activities. Buildings are often constructed using cement blocks and concrete, and cement is also utilized for plastering structures. Various brands of cement are available in the market, each with its own trademark. The primary raw materials used in cement production include limestone ($CaCO_3$), shale ash, and iron oxide, along with additional elements such as gypsum, which contains silicates and aluminates known for their ionization tendency. The production process of cement involves several stages, starting with the assessment of potential limestone deposits through geophysical methods, followed by quarrying, grinding, and blending of the clinker. Finally, the finished products are packed and transported for sale. Earlier research [58] has indicated that quarrying and mining activities can elevate the activity concentration of radionuclides in the surrounding environment.

Portland cement has resulted from the grinding of clinker. The clinker is produced by burning a mixture of limestone, clay, and gypsum at high temperatures (1450-1600^oC for the materials, and approximately 2000°C for the combustion fumes). Portland cement dust is a gray powder with an

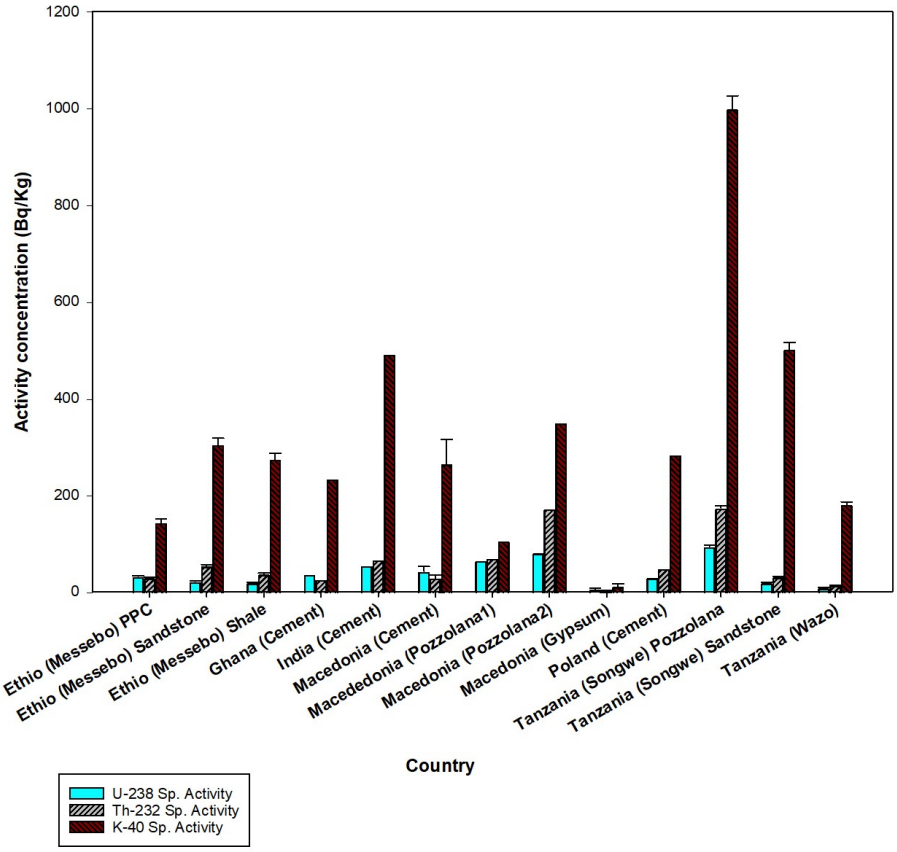

Figure 4.20: Comparison of radioactivity concentration with other countries

aerodynamic diameter ranging from 0.05 to 5.0 m [55]. From this study, the activities of natural radionuclides ^{226}Ra, ^{232}Th, ^{40}K, and also the radiological parameters are measured. The radiological indices parameters are such as the radium equivalent, indoor absorbed dose rate, annual effective dose rate, gamma index, external, and internal hazard indices were determined. The radiation risk associated with the cement and its composites produce different clinical and occupational exposures had been reported, which pose various health effects to human beings. The radioactive dust causes respiratory health problems where lung is the most affected organ as has been observed in the occupational workers exposed to the dust. The use of cement in the construction of residential and commercial buildings results in external and internal radiation exposure to the population.

Limestone which is the main constituent in cement is largely abundant in the earth's crust, and earth crust is known for the residence of primordial radionuclides. This material is used in the dwelling units. The quarry is the main process in cement production, and this required energy inputs and heat. Coalfly ash slag or pozzolans may be blended with the raw material, as the addition of these optional materials result in lower emissions. Mostly, a typical kiln size is around 3000 tonnes clinker per day. The clinker burning is the most important part of the process in terms of the key environmental issues for cement manufacture in terms of its energy use and air pollution [11].

Messebo cement factory is one of the biggest cement factories in Ethiopia located in Mekelle City. The factory is founded in 2000 G.C with a production capacity of more than 2000 tons of clinker per day. According to one of the recent studies, indicated that the dust emitted from the Messebo cement factory is affecting the physicochemical properties of the soils in the surrounding area [59].

Moreover, the surrounding communities have been complaining about the health and environmental impacts of the factory [60]. From the radiological point of view most important exposure with regards to health is from radon (^{222}Rn, ^{220}Rn) and its short-lived decay products. This becomes the major source of internal exposure when inhaled. The radiation exposure by gamma rays emitted from the radionuclides in the building materials is the reason for external dose.

The knowledge of natural radioactivity in building materials is important for the determination of the indoor population exposure to radiation since people spend about 80% of their time in dwellings [2]. Control of building materials by applying a reference level for indoor external exposure to gamma radiation emitted by building materials of 1 mSv y^{-1}, in addition to exposure. The contents of ^{226}Ra, ^{232}Th, and ^{40}K in cement materials can vary considerably depending on their chemical composition to geological source and geochemical characteristics [61]. The present work aims to determine the radiation levels for natural radioactivities in cement raw materials and products by determining the Absorbed Dose Rate(D), Annual Effective Dose Rate (AEDR), Radium Equivalent (Ra_{eq}), External Hazard Index(H_{ex}), and Internal Hazard Index (H_{in}) for individuals living in the dwelling and the workplace.

CHAPTER 5

CONCLUSIONS AND RECOMMENDATIONS

5.1 Conclusions

In present study was conducted to assess the natural radioactivity levels in soil samples collected from different regions, including Assosa City, Bambasi District, Menge-Sherkole District, and Mekelle City of Ethiopia. The concentrations of radionuclides ^{238}U, ^{232}Th, and ^{40}K were measured and compared with global averages and safety standards. The findings of our work provide essential data regarding the potential radiological hazards associated with naturally occurring radioactive materials (NORM) in the aforesaid selected regions. The following key conclusions are drawn:

- The average activity concentrations of ^{238}U, ^{232}Th, and ^{40}K in Assosa City soil samples were found to exceed the global recommended safety limits for ^{238}U (35 Bq/kg) and ^{232}Th (30 Bq/kg), indicating a potential radiological health risk in the region. The concentrations of ^{40}K is found below the global average of 400 Bq/kg.
- In Bambasi District, the concentrations of ^{238}U and ^{232}Th were also found to exceed the global safety limits, with the highest values observed in soil samples from Bambasi-S1. This suggests that the region may pose a risk to public health due to elevated radiation levels.
- The radioactivity levels in Menge and Sherkole districts were found to be lower than in Assosa and Bambasi, with mean concentrations of ^{238}U, ^{232}Th, and ^{40}K below the global recommended levels. However, certain soil samples from Sherkole exhibited elevated concentrations of ^{232}Th, which warrants further investigation.
- The results from Mekelle City show that the average concentrations of ^{238}U, ^{232}Th, and ^{40}K are within acceptable limits as per international safety standards. Therefore, Mekelle soil poses minimal radiological risk.
- The assessment of radiological hazard indices such as the radium equivalent activity (Ra_{eq}), absorbed dose rate (D), and the annual effective dose (E) revealed that most soil samples from Assosa and Bambasi exceed recommended safety values. In contrast, the samples from Menge-Sherkole and Mekelle generally fall within safe levels.
- The calculated values for the external hazard index (H_{ex}) and internal hazard index (H_{in}) were below the recommended limit of one for all soil samples except those from Bambasi-S1 and Sherkole-S1, which crossed the safety limit. This suggests that prolonged exposure to soil from these regions may pose health risks, particularly through inhalation of radon gas and its decay products.
- The Excess Lifetime Cancer Risk (ELCR) values for Assosa and Bambasi exceeded the recommended safe value of 0.29×10^{-3}, indicating a higher likelihood of cancer risk in these regions from exposure over a lifetime.

Allmost all the regions exhibit natural radioactivity levels within acceptable limits. However, the elevated concentrations of ^{238}U and ^{232}Th in Assosa and Bambasi soils suggest a potential health hazard, warranting further investigation and suggesting possible mitigation efforts.

5.2 Recommendations

Based on the findings in the present work, the following recommendations are made:

- **Public Awareness:** The elevated levels of radioactivity in Assosa and Bambasi districts should be communicated to the local population and public health authorities. Educational campaigns on minimizing exposure to radioactive materials in these regions should be implemented, particularly for people involved in agricultural and construction activities.
- **Soil Management:** In regions where radionuclide concentrations exceed global safety standards, such as Assosa and Bambasi, measures should be taken to avoid the use of these soils for agricultural purposes, especially where food crops are grown. Alternatives such as soil amendments or relocation of agricultural activities may help in reducing the risk of radiation exposure.
- **Regular Monitoring:** A systematic monitoring program should be formulated to regularly assess the levels of natural radioactivity in high-risk areas such as Assosa and Bambasi. This would help to track changes in radionuclide concentrations and ensure that any increase is detected early for prompt mitigation measures.
- **Radiological Protection Standards:** Local authorities should adopt and enforce radiological protection standards based on the guidelines provided by international organizations such as UNSCEAR and the IAEA. This includes setting up regulatory thresholds for radionuclide concentrations in soil and construction materials.
- **Further Research:** Further research is recommended to investigate the specific geological and anthropogenic factors contributing to the elevated levels of ^{238}U and ^{232}Th in Assosa and Bambasi. Studies focusing on soil remediation techniques and the mobility of radionuclides in these regions are crucial for developing effective mitigation strategies.
- **Health Risk Assessment:** A comprehensive health risk assessment should be conducted in regions where radiological hazard indices and cancer risk exceed safe limits. This assessment should include studies on the potential impact of long-term exposure to radionuclides on local populations, particularly those working in mining and agriculture.
- **Policy and Regulation:** National policies on radiation protection should be strengthened, and radiation safety standards should be incorporated into environmental and health policies, particularly in regions with elevated levels of natural radioactivity. Regulatory bodies should enforce guidelines that ensure public safety and environmental protection.

In conclusion, while most of the regions studied exhibit safe levels of natural radioactivity, but attention needs to be focused on Assosa and Bambasi, where elevated levels of ^{238}U and ^{232}Th present potential health risks. By implementing public awareness campaigns, soil management practices, and regulatory frameworks, the risks associated with natural radioactivity can be mitigated to certain extent.

BIBLIOGRAPHY

[1] Knoll, G. F., *Radiation Detector And Measurment*, John Willey and Sons, Inc, 3rd ed., 2000.

[2] UNSCEAR, *Sources and Effects of Ionizing Radiation*, United Nations, New York, 2000.

[3] Protection, R., "ICRP publication 103," *Ann ICRP*, Vol. 37, No. 2.4, 2007, pp. 2.

[4] Liu, Q., Feng, G., Lu, Z., Tang, C., Wu, B., Mao, P., and Cai, C., "Assessment of TENORM and potential radiological hazards from the main brand glazed tiles produced in China with statistical analysis," *International Journal of Environmental Analytical Chemistry*, Vol. 102, No. 2, 2022, pp. 602–613.

[5] Salerno, S., Nardi, C., Pace, M., Rabiolo, L., Flammia, F., Loverre, F., Matranga, D., Granata, C., Tomà, P., and Colagrande, S., "Communicating radiation dose in medical imaging: How to best inform our patients?" *Acta Radiologica Open*, Vol. 12, No. 4, 2023, pp. 20584601231168967.

[6] ICRU, *Methods for Initial Phase Assessment of Individual Doses Following Acute Exposures to Ionizing Radiation*, International Commission on Radiation Units and Measurements, 1994.

[7] Merril Eisenbud, T. G., *EnviromentalRadioactivity*, 1997.

[8] UNSCEAR, *Reports on Sources and Effects of Ionizing Radiation*, United Nations, New York, 1993.

[9] ICRP, *Recommendations On Radiological Protection*, International commission on radiological Protection, 200.

[10] IAEA, *Measurement of Radionuclides in Food and The Environment*, 295, International Atomic Energy Againcy, 1989.

[11] Miroslav Stajanca, A. E., "Environmental Impact of Cement production," 2012.

[12] Markovic, J. and Stevovic, S., "Radioactive Isotopes in Soils and Their Impact on Plant Growth," *Health Physics*, 2018.

[13] EML, *Environmental Measurements Laboratory*, Vol. 1, U.S. Department of Energy, 28th ed., 1997.

[14] C.C. Arwui, G. E.-R. and , E. D., "Natural Radioactivity and its Associated Radiological Hazards in Ghanaian Cement," 2011.

[15] Ghazwa Alzubaidi, F. B. S. H. and Rahman, I. A., "Assessment of Natural Radioactivity Levels and Radiation Hazards in Agricultural and Virgin Soil in the State of Kedah, North of Malaysia," *Scientific World Journal*, , No. 9, 2016.

[16] Jong, D., "Exposure to natural radioactivity in the Netherlands: the impact of building materials.Groningen: s.n," 2010.

[17] V., G. C. and M, M. K., *New Developments in Field Gamma-ray Spectrometry*, Department of Energy, Environmental Measurements Lab, New York, United States, December 1977.

[18] IAEA, *Guidelines For Radio Element Mapping Using Gamma-ray Spectrometry Data*, IAEA TECDOC-1363, International Atomic Energy Againcy, 2003.

[19] J.Beretka and Mathew, P. J., "Natural radioactivity of Australian building materials, industrial wastes and by-products," *Health Physics*, 1985.

[20] IAEA, *Nuclear Medicine Physics: A handbook for students and teachers*, International Atomic Energy Againcy, Vienna, 2014.

[21] OECD, N. o. E. o. t. N. E. A., *Exposure to Radiation from Natural Radioactivity in Building Materials*, 1979.

[22] Christa E, Pereira Vaidyan V K., S. A. B. B. S. R. M. J. and J, J. P., "Radiological assessment of cement and clay based building materials from southern coastal region of Kerala," *Indian journal of pure and applied physics*, Vol. 49, No. 6, 2011, pp. 372.

[23] EC, *Radiological Protection Principles Concerning the Natural Radioactivity of Building Materials*, Europian Commision, Radiation Protection 112, 1999.

[24] Avwiri G. O., Olatubosun S. A., O., "Evaluation of Radiation Hazard Indices for Selected Dump sites in Port Harcourt, Rivers State, Nigeria," *International Journal of Science and Technology*, Vol. 3, No. 10, 2015.

[25] Taskin H. M., Karavus P., A. A. T. S. H. and G, K., "Radionuclide concentration in soil and lifetime cancer risk due to gamma radioactivity in Kirklareli, Turkey," *Journal of Environmental Radioactivity*, , No. 100, 2009, pp. 49–53.

[26] Lordford Tettey Larbi, Emmanuel Ofori Daroko, C. S. A. A. A., "Natural radioactivity levels of some medicinal plants commonly used in Ghana," *Springer plus*, Vol. 2, 2013.

[27] Raymond L. Njinga, S.A. Jonah, M., "Preliminary investigation of naturally occurring radionuclides in some traditional medicinal plants used in Nigeria," *Journal of Radiation Research and Applied Science*, Jan 2015.

[28] Abdu Hamoud Al-Khawlany, A. R. Khan, J. M. P. D. B., "Determination of Natural Radioactivity Levels and Radiation Hazards for Soil Samples from Aurangabad Maharashtra-India," *Department of Physics, Maulana Azad College*, 2018.

[29] Matiur M Rahman, Aleya Begum, M. J. F. and Islam, M. A., "Determination of Radionuclide in soil from Barendra region in Rajshahi and mining region in Dinajpur," *Malaysian Journal of Science*, Vol. 32, No. 2, 2013, pp. 67–75.

[30] Feroz A Mir, S. A. R., "Measurement of radioactive nuclides present in soil samples of district Ganderbal of Kashmir Province for radiation safety purposes." *Journal of Radiation Research and Applied Science*, Vol. 8, 2014, pp. 155=159.

[31] ATAMP, *Municipality of Asosa Town Asosa*, Asosa town asset management plan, Assosa, 2014.

[32] Amina Bramki, Mourad Ramdhane, F. B., "Natural radioelement concentrations in fertilizers and the soil of the Mila region of Algeria," *Journal of Radiation Research and Applied Sciences*, Vol. 11, 2018, pp. 49.

[33] Jianzhou Yang, Y. S., "Natural radioactivity and dose assessment in surface soil from Guangdong, a high background radiation province in China," *Journal of Radiation Research and Applied Sciences*, Vol. 15, 2022, pp. 145–151.

[34] Kakhaber Kapanadze, Archil Magalashvili, P. I., "Distribution of natural radionuclides in the soils and assessment of radiation hazards in the Khrami Late Variscan crystal massif (Georgia)," *Heliyon 5*, 2019.

[35] Amanjeet, Ajay Kumar, S. K. J. S. P. S. B. B., "Assessment of natural radioactivity levels and associated dose rates in soil samples from historical city Panipat, India," *Journal of Radiation Research and Applied Sciences*, Vol. 10, 2017, pp. 283–288.

[36] Laura Guidotti, Franca Carini, R. R. M. G. R. M. C. G. M. B., "Gamma-spectrometric measurement of radioactivity in agricultural soils of the Lombardia region, northern Italy," *Journal of Environmental Radioactivity*, Vol. 142, 2015, pp. 36–44.

[37] Charles Chisom Mbonu, U. C. B., "Assessment of radiation hazard indices due to natural radioactivity in soil samples from Orlu, Imo State, Nigeria," *Helyon 7*, 2021.

[38] Masok F.B, Masiteng P.L, M. R. M. P. W. H., "Measurement of radioactivity concentration in soil samples around phosphate rock storage facility in Richards Bay, South Africa," *Journal of Radiation Research and Applied Sciences*, Vol. 11, 2018, pp. 29–36.

[39] Cengiz, G. B., "Natural radioactivity analysis in soil samples of Ardahan province, Turkey for the assessment of the average effective dose," *Sakarya Universities*, Vol. 2, No. 6, 2017, pp. 1583–1590.

[40] Reda Elsaman, Mohammed Ahmed, A. O. E.-M. M. S. and El-Taher, A., "Natural Radioactivity Levels and Radiological Hazards in Soil Samples Around Abu Karqas Sugar Factory," *Journal of Environmental Science and Technology*, Vol. 11, 2018, pp. 28–38.

[41] Shimels Tikuye Yalew, B. F., "Prevalence of bovine trypanosomosis and its associated risk factors in Bambasi woreda, Western Ethiopia," *J Dairy Vet Anim Res*, Vol. 5, No. 2, 2017, pp. 44–49.

[42] Ricardo Washington Dutra GarcÃłz, JosÃĺ Marques Lopes, S. S. P. D. C. L. E. P. V. F. G. d. C. F. C. A. R. A. X. d. S., "Activity concentration and mapping of radionuclides in EspÃŋrito Santo State soils, Brazil," *Radiation Physics and Chemistry*, Vol. 167, 2020.

[43] Nodar Kekelidze, Teimuraz Jakhutashvili, B. T. E. T. M. A. L. M., "Radioactivity of soils in Mtskheta-Mtianeti region (Georgia)," *Annals of Agrarian Science*, Vol. 15, 2017, pp. 304–311.

[44] H, T. A. and F, N. B., "Radioactivity distribution in soil samples of the Baba Gurgur dome of Kirkuk oil feld in Iraq," *International Journal of Environmental Analytical Chemistry*, 2022, pp. 1–9.

[45] Aneta ÅĄukaszek Chmielewska, Martin Girard, O. S. B. P. K. W. and Isajenko, K., "Measurements of natural radioactivity in soil samples collected in the Kampinoski National Park," *E3S Web of Conferences*, Vol. 100, 2019, pp. 52.

[46] Ayse Durusoy, M. Y., "Determination of radioactivity concentrations in soil samples and dose assessment for Rize Province, Turkey," *Journal of Radiation Research and Applied Sciences*, Vol. 10, 2017, pp. 348–352.

[47] Ayele A. Fenta, Hiroshi Yasuda, N. H. A. S. B., "The dynamics of urban expansion and land use/land cover changes using remote sensing and spatial metrics: the case of Mekelle City of northern Ethiopia," *International Journal of Remote Sensing*, Vol. 38, 2017, pp. 4107–4129.

[48] Zubair M, S., "Measurement of natural radioactivity in several sandy-loamy soil samples from Sijua, Dhanbad, India," *Heliyon 6*, 2020.

[49] Asmelash Tassew, A. A. and Legesse, K., "Isolation, Identification and Antimicrobial Resistance Profile of Staphylococcus aureus and Occurrence of Methicillin Resistant S. Aureus Isolated from Mastitic Lactating Cows in and around Assosa Town, Benishangul Gumuz Region, Ethiopia," Dec 2017.

[50] Eva Tabuaa Gyamfi, Yeboah, M. S.-A. and Fletcher, J. J., "Assessment of essential elements in Moringa oleifera," Jun 2011.

[51] Dinesh Kumer Ray, PK Nayak, T. R. V. V. S. J., "Elemental analysis of anti-diabetic medicinal plants using energy dispersive X-ray fluorescence technique," *Indian J. Phys*, Vol. 78, No. 1, 2004, pp. 103–105.

[52] Vivek Singh, A. N. G., "Availability of essential trace elements in ayurvedic Indian medicinal herbs using instrumental neutron activation analysis," *Applied Radiation Isotopes*, Vol. 48, 2016, pp. 97–101.

[53] Ram Lokhande, Pravin Singare, M. A. R. A., "Study of some Indian medicinal plants by application of INAA and AAS techniques," Jan 2010.

[54] Aloyce Isaya Amasi, Kelvin Mark Mtei, I. J. N. P. J. o. and Dinh, C. N., "Natural Radioactivity in Tanzania Cements and their Raw Materials," *Research Journal of Environmental and Earth Sciences*, Vol. 6, No. 10, 2014, pp. 15–24.

[55] Kpeglo D.O, Lawluvi H, F. A. A. A. D. P. W. S. A. C. E.-R. G. a. D. E., "Natural Radioactivity and its Associated Radiological Hazards in Ghanaian Cement," *Research Journal of Environmental and Earth Sciences*, Vol. 3, No. 2, 2012, pp. 160–166.

[56] Usikalu Mojisola R, Oderinde Ajibola, A. T. A. and A, A., "Radioactivity concentration and dose assessment of soil samples in cement factory and environs in Ogun State Nigeria," *International Journal of Civil Engineering and Technology*, Vol. 9, No. 9, 2018, pp. 1047–1059.

[57] Sylwia Lewicka, Barbara Piotrowska, A. Å.-C. and DrzymaÅĆa, T., "Natural Radioactivity and Hazards Assessment in Medicinal Plants in Bangladesh," *Int J Environ Res Public Health*, Vol. 19, No. 18, 2022, pp. 11695.

[58] Usikalu M.R., Akinyemi M.L, A. J., "Investigation of Radiation Levels in Soil Samples Collected from Selected Locations in Ogun State, Nigeria," *IERI Procedia*, 2014, pp. 156–161.

[59] Estifanos, S. and Degefa, A., "Assessing the Effect of Cement Dust Emission on the Physicochemical Nature of Soil around Messebo Area, Tigray, North Ethiopia," *International Journal of Economic and Environmental Geology*, Vol. 3, No. 2, 2012, pp. 12–20.

[60] Assefa Berhe, Tesfahun Alemayehu, K. K. F., "Environmental Impact Study of Cement Factory using a Multi-Criteria Analysis:Evidence from Messebo Cement Factory, Ethiopia," 2014.

[61] Bello I.A., Zakari Y.I., G. N. V. A. K. N., "Radioactivity level in water around a cement factory in North Central Nigeria." *Science World Journal*, 2018.

APPENDIX A

GAMMA SPECTRA FOR SOIL SAMPLES

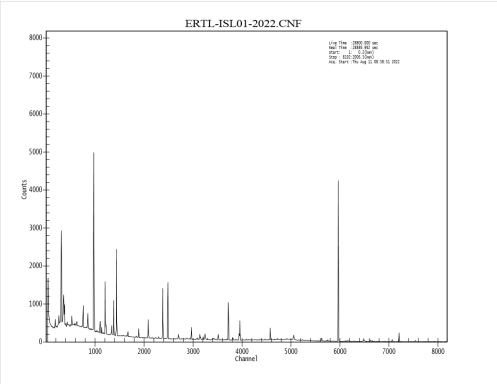

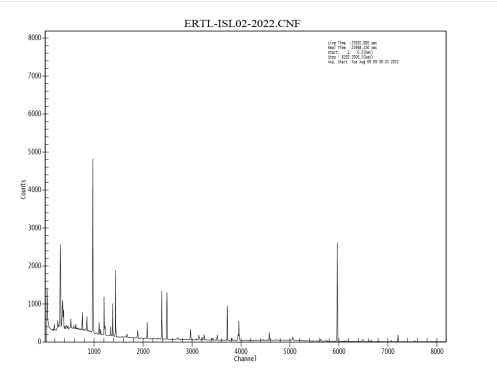

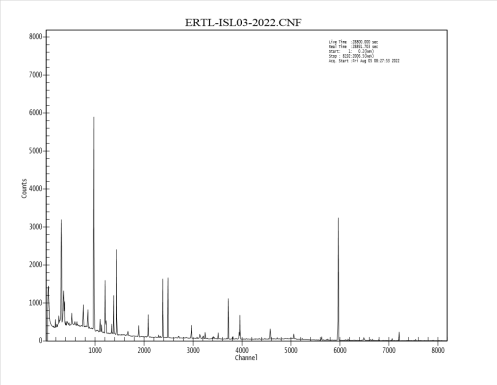

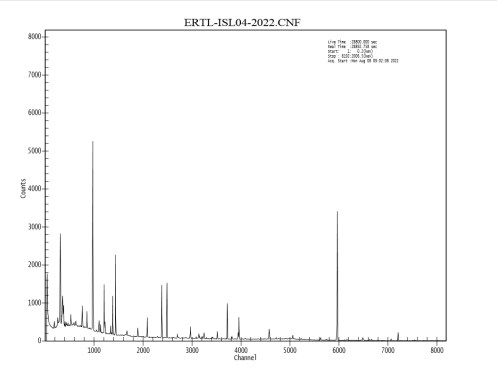

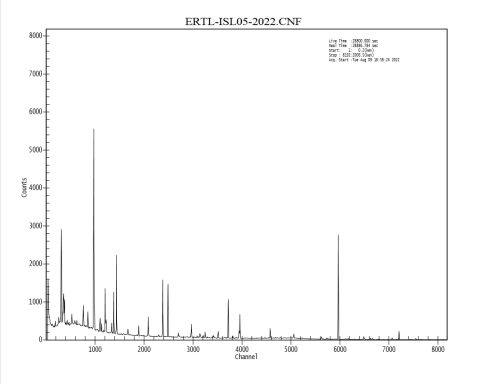

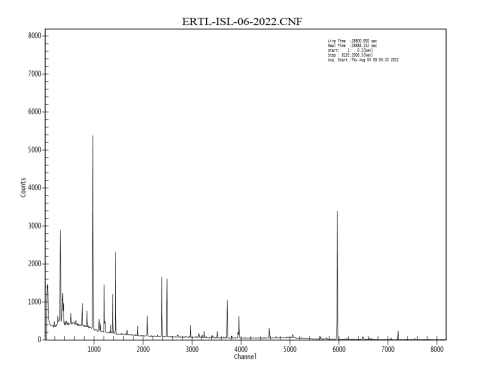

APPENDIX B

PUBLICATIONS

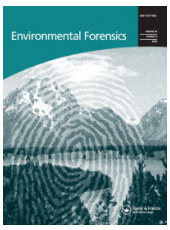

Environmental Forensics

ISSN: (Print) (Online) Journal homepage: www.tandfonline.com/journals/uenf20

Evaluation of Radioactivity Levels in Soil Samples from Assosa City in Benishangul Gumuz Region, Ethiopia

Yared Birhane Kidane, Tilahun Tesfaye Deressu & Guadie Degu Belete

To cite this article: Yared Birhane Kidane, Tilahun Tesfaye Deressu & Guadie Degu Belete (21 Mar 2024): Evaluation of Radioactivity Levels in Soil Samples from Assosa City in Benishangul Gumuz Region, Ethiopia, Environmental Forensics, DOI: 10.1080/15275922.2024.2330025

To link to this article: https://doi.org/10.1080/15275922.2024.2330025

Published online: 21 Mar 2024.

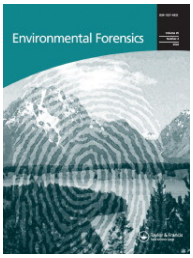

Environmental Forensics

ISSN: (Print) (Online) Journal homepage: www.tandfonline.com/journals/uenf20

Evaluation of Radioactivity Levels in Soil Samples from Assosa City in Benishangul Gumuz Region, Ethiopia

Yared Birhane Kidane, Tilahun Tesfaye Deressu & Guadie Degu Belete

To cite this article: Yared Birhane Kidane, Tilahun Tesfaye Deressu & Guadie Degu Belete (21 Mar 2024): Evaluation of Radioactivity Levels in Soil Samples from Assosa City in Benishangul Gumuz Region, Ethiopia, Environmental Forensics, DOI: 10.1080/15275922.2024.2330025

To link to this article: https://doi.org/10.1080/15275922.2024.2330025

ENVIRONMENTAL FORENSICS
https://doi.org/10.1080/15275922.2024.2330025

Evaluation of Radioactivity Levels in Soil Samples from Assosa City in Benishangul Gumuz Region, Ethiopia

Yared Birhane Kidane[a,b], Tilahun Tesfaye Deressu[a], and Guadie Degu Belete[b]

[a]Department of Physics, Natural and Computational Science College, Addis Ababa University, Addis Ababa, Ethiopia; [b]Department of Physics, Natural and Computational Science College, Assosa University, Assosa, Ethiopia

ABSTRACT

The specific activity concentrations of naturally occurring radionuclides in soil samples collected from suburban areas of Assosa City was measured using a High purity Germanium (HPGe) detector. The average specific activity concentrations of ^{238}U and ^{232}Th exceed the recommended safe value of 35.0 and 30.0 Bq kg^{-1}, respectively. For ^{40}K, the average activity concentration is below the recommended safe value of 400.0 Bq kg^{-1}. The calculated mean value of the absorbed dose rate is 72.8 ± 3.72 nGy h^{-1} which exceed the recommended safe value of 59 nGy h^{-1}. The calculated mean annual effective dose equivalent values for indoor and outdoor are 2.11 ± 0.1 mSv y^{-1} and 0.52 ± 0.02 mSv y^{-1}, respectively. The calculated mean values of the internal hazard index, external hazard index, and gamma index are 0.43 ± 0.013, 0.56 ± 0.01, and 0.5 ± 0.01, respectively, and those values are below the recommended safe value of one. The mean value of excessive lifetime cancer risk is above the threshold value of 0.29 × 10^{-3}. From this study, it is recommended that Assosa soil needs further investigations.

KEYWORDS

Assosa; detector; health; gamma-ray; radionuclide; soil

Introduction

Human beings are exposed to natural terrestrial radiations predominantly originating from the upper 30 cm of the soil. The most notable radionuclides with half-lives comparable to the age of the earth or their associated decay products existing in terrestrial material are ^{238}U, ^{232}Th, and ^{40}K (Senthilkumar et al. 2010). The background radiation, originating from soil, consists of two main components: natural and technologically enhanced radioactivity. The natural component originates from radioelements that are existing in the bedrock as well as in the soil. The composition and distribution of these radioelements vary from place to place (Kekelidze et al. 2017; Ntsohi et al. 2021).

The intensity and distribution of the natural background radiation can be altered due to human activities such as mining, long use of coal fired power plants, and waste disposal. External or internal exposure to these background radiations can lead to various health concerns among the population (Shahbazi-Gahrouei, Gholami, and Setayandeh 2013). External exposure occurs due to irradiation, there are different pathways to internal exposure. For example inhalation of Radon (^{222}Rn) and Radon daughter products from air and ingestion of contaminated dairy products or vegetable products that possess high uptake of these radionuclides are possible path ways to internal exposure. When rocks are fractured by natural processes, radionuclides are transported to the soil by rain and runoff. Radionuclides also naturally occur in rock and soil, which can easily be transported to the environment through plants and water (Ibraheem, El-Taher, and Alruwaili 2018).

The level of exposure depends on climate factors, fertilizer usage, local geology, and drainage patterns, which vary in each region of the world. Terrestrial radionuclides encompass the radioactive series of uranium-radium, thorium, and potassium in the earth's crust. Prolonged exposure to ^{238}U and ^{232}Th can affect human health. Some health effects include acute leucopenia, anemia, chronic lung diseases, and necrosis of the mouth from ^{238}U exposure; radium exposure can cause bone, cranial, and nasal tumors; while health effects such as lung, pancreas, hepatic, bone, and kidney cancers can result from ^{232}Th exposure (Uosif and El-Taher 2008). Communities residing in environments with high radionuclide concentrations must take precautions.

CONTACT Yared Birhane Kidane yaredbirhanek@gmail.com Department of Physics, Assosa University, Assosa, Ethiopia

Measurement of radioactive concentration has been applied to geological, environmental, medicinal, and industrial samples. Thorium and Uranium may be redistributed during igneous, sedimentary, and metamorphic cycles of geological evolution, eventually forming small deposits under steady geological processes (Elsaman et al. 2018). Natural sources of ionizing gamma radiation in the environment can be classified into terrestrial and cosmogenic radiation sources. The interaction of atmospheric gases with cosmic rays induces cosmogenic radioactivity such as ^{14}C radionuclides. Terrestrial radionuclides contribute to both external and internal exposures. External exposure to these radionuclides is mostly due to their emitted γ-rays, while internal exposure is due to their deposition in the human body and their emitted α, β, and γ radiation. Radioactivity levels can be used to assess public dose rates and radioactive contamination, and to detect variations in environmental radioactivity caused by nuclear accidents, industrial activities, and other human activities (UNSCEAR 2000).

Agricultural soils' radioactivity primarily stems from the extensive use of fertilizers rich in phosphates, leading to increased concentrations of uranium and thorium in the environment. Fertilizers are one of the technologically enhanced sources of natural radiation. Studying the radioactive components in soil enhances understanding of radioactivity behaviors in ecosystems, as these materials emit radiation through the disintegration of natural radionuclides, contributing to the total absorbed dose through ingestion, inhalation, and external irradiation (Abbady et al. 2006; IAEA 1989). Radiation studies are of major concern worldwide, as significant concentrations accumulated in soils, buildings, homes, workplaces, and groundwater can result in several health problems.

In this study, our main objective is to determine the concentrations of naturally occurring radionuclides in diverse soil samples collected from Assosa City in the Benishangul Gumuz region, Ethiopia. The outcomes of this investigation are evaluated for safety or potential hazard through comparison with recommended safety values established by international organizations, including those provided by UNSCEAR (2000) report. In Ethiopia, majority of the population depends on agriculture, both in rural and urban areas, and soils are commonly used for constructing houses. Therefore, understanding the radioactivity levels in the soil is crucial for ensuring the safety of these environments.

Materials and Methods

Description of the Study Area

This study aims to investigate the natural radioactivity levels in various soil samples collected from Assosa town, the administrative center of the Benishangul Gumuz Regional State. Benishangul Gumuz is one of the eleven regional states within the Ethiopian federal structure (Figure 1). Geographically, Assosa town is positioned approximately 662 km southwest of the capital, Addis Ababa, along the main highway. It is situated around 90 km from the Ethio-Sudanese border, with an average altitude of 1550 m on a flat terrain. Assosa City's geographical coordinates are between 10°00 □ and 10°07′ north and between 34°30′ to 34°35′ east, covering an area of about 2000 hectares (Kebede, Alene, and Endalemaw 2021). Assosa City is situated in the Assosa zone, one of the three zones in the Benishangul Gumuz region, alongside Kamashi and Metekel. Assosa zone is recognized for its potentially lucrative gold deposits (Bullock and Morgan 2018).

Sample Collection and Preparation

Assosa district is well known for extensive gold mining activities and rapid urbanization is undergoing in the regional capital. The selection of soil samples in this area is justified by the fact that the highly populated environ is mining site and subject to natural and enhanced natural exposure to radiation. Soil samples were collected from 10 selected mutually more than 3 km apart locations of Assosa City. Samples were carefully dug out of the surface soil from a depth of 5–30 cm using hand tools.

Originally, collected soil samples were separated from stones. Approximately 1 kg soil samples were sealed in a polyethylene bag and identification code was given to each bag, as Assosa-S1 to Assosa-S10; locations are listed as shown in Table 1. The sealed soil samples were transferred to the laboratory of the Ethiopian Conformity Assessment Enterprise for sample preparation as per the Environmental Measurments Labratory (EML) procedures manual 3.1. The samples were air-dried for a few days and put in an oven at 100 °C for 10–24 h depending on the moisture of the soils. The dried soil samples were crushed into powder size using a crushing material. The powdered soil samples were sieved using 0.25 mm mesh. About 500 g of the homogeneous soil samples were sealed in an airtight cylindrical Marinelli beaker and stored for 28 days to achieve secular equilibrium. Finally, the prepared samples were transferred to

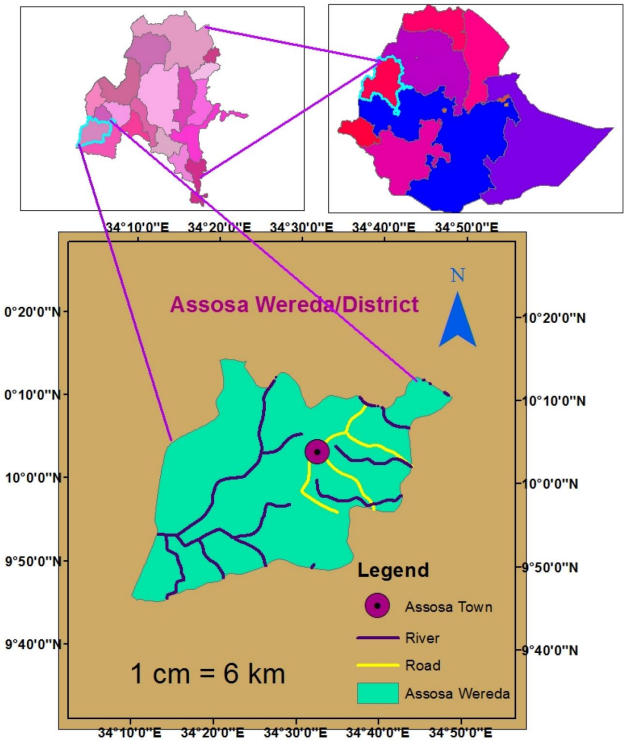

Figure 1. Map of Assosa Town in Benishangul Gumuz region of Ethiopia.

Table 1. Locations of the collected soil samples in Assosa City using global positioning system (GPS).

Locations			
№	Sample code	Latitude (north)	Longitude (east)
1	Assosa-S1	10.066981°	34.556967°
2	Assosa-S2	10.071328°	34.559092°
3	Assosa-S3	10.077333°	34.558828°
4	Assosa-S4	10.084292°	34.569458°
5	Assosa-S5	10.058986°	34.553344°
6	Assosa-S6	10.054631°	34.5558°
7	Assosa-S7	10.072486°	34.548783°
8	Assosa-S8	10.075719°	34.544672°
9	Assosa-S9	10.071539°	34.539628°
10	Assosa-S10	10.088636°	34.560456°

Ethiopian Radiation Protection Authority for radiation measurement using an HPGe detector.

Experimental Setups

The gamma-ray emitting radionuclides concentrations in the soil samples were measured by using HPGe detector coupled with a multichannel analyzer. Recognized for its suitability as a semiconductor radiation detector, the HPGe detector boasts high-resolution capabilities for photo peaks. The Marinelli beakers sample geometry was 538 G-E. The HPGe detector has 77% relative photopeak efficiency. The detector has 1.8 keV energy resolutions. Multichannel analyzer of 8192 channel performance is connected to a computer equipped with Genie 2000 software. The voltage of 3499 V was used for the detector. The calibrate radionuclides for the detector were ^{60}Co and ^{137}Cs, which are the quality standard sources according to ISO 9001. The quality standard used for calibrating the detector was ISO/IEC 17025. To prevent background radiation from the surroundings, the detector was enclosed in a lead shield (100 mm thickness), cadmium (2 mm thickness), and copper (2.5 mm thickness). The calibration of the experiment was done using International Atomic Energy Agency-certified standard reference sources. The counting time of the gamma-ray spectrum was 28,800 s.

The minimum detection limits of the detector according to ISO 11929, were reported as 1.12, 0.79,

and 4.10 Bq kg^{-1} for ^{238}U, ^{232}Th, and ^{40}K, respectively. The specific energy spectrum for each radionuclide were obtained by photopeak area analysis. The specific activity of ^{238}U was derived from gamma-ray lines of ^{214}Pb at 351 keV and ^{214}Bi at 609.3 and 1764.5 keV, while the activity concentration of ^{232}Th was determined from gamma-ray lines of ^{228}Ac at 338.4, 911.1, and 968.9 keV, ^{212}Pb at 238.63 keV, and ^{208}Tl at 583.19 keV. The specific activity of ^{40}K was directly determined from its gamma-ray line at 1460.8 keV (Alzubaidi, Hamid, and Abdul Rahman 2016).

Measurements of Activity Concentration

The specific activity concentrations (A_c) in Bq kg^{-1} of the soil samples were calculated using the equation from Beretka and Matthew (1985).

$$A_c = \frac{N_c}{I\varepsilon M T_s} \tag{1}$$

A_c : Radioactivity concentration of the samples (Bq kg^{-1}), N_c : It is the net count for packed sample (N_s) minus count for the background (N_b), ε: Efficiency of the detector for the gamma-ray energy of interest, I: Probability of gamma-ray absolute intensity, and M: Mass of the packed sample (kg). T_s : It is the actual sample counting time. The uncertainty on the activity concentration (ΔA), was obtained by the following equation (Djeufack et al. 2022).

$$\frac{\Delta A}{A} = \sqrt{\left(\frac{\Delta N_c}{N_c}\right)^2 + \left(\frac{\Delta I}{I}\right)^2 + \left(\frac{\Delta \varepsilon}{\varepsilon}\right)^2 + \left(\frac{\Delta M}{M}\right)^2} \tag{2}$$

Where, ΔN_c, ΔI, Δε, and ΔM represent the uncertainty in net count, probability in gamma-ray intensity, efficiency, and mass of the sample, respectively.

Estimation of Radiological Dose and Hazardous Indices

Absorbed Dose Rate (D)

The absorbed dose rates in the air due to radionuclides were calculated using the formula from UNSCEAR (2000).

$$D(\text{nGy/h}) = 0.462A_U + 0.602A_{Th} + 0.0417A_K \tag{3}$$

The result was comparable to the world average of 59 nGy h^{-1} outdoors and 84 nGy h^{-1} indoors.

Annual Effective Dose Equivalent (AEDE)

The absorbed dose rate values serve as the basis for estimating the annual effective dose equivalent (AEDE) in mSv y^{-1}. This estimation involves applying a conversion coefficient of 0.7 Sv Gy^{-1} for absorbed doses in the air to the effective dose received. The calculation considers an indoor occupancy factor of 0.8, reflecting that the population typically spends 80% of their time indoors, and an outdoor occupancy factor of 0.2, implying that 20% of their time is spent outdoors. It is known that, globally, the average annual total effective dose equivalent due to external radiation is reported as 0.48 mSv y^{-1} (UNSCEAR 2000).

It is known that, the world's annual effective dose rate due to external radiation is 0.41 mSv y^{-1} indoors and 0.07 mSv y^{-1} outdoors. The worldwide annual total effective dose rate safety limit is 1 mSv y^{-1} (UNSCEAR 2000). For people living in a certain area, the annual effective dose equivalent values for outdoor and indoor could be calculated using equations from UNSCEAR (2000) which are expressed as follows.

$$\text{AEDE}(\text{mSv/y})_{\text{outdoor}} = D(\text{nGy/h}) \times 24\text{h} \times 365.2\text{d} \times 0.2 \times 0.7\ \text{Sv Gy}^{-1} \tag{4}$$

Where 0.7 is the absorbed/ambient dose conversion factor and 0.2 is the outdoor occupancy.

$$\text{AEDE}(\text{mSv/y})_{\text{Indoor}} = D(\text{nGy/h}) \times 24\text{h} \times 365.2\text{d} \times 0.8 \times 0.7\ \text{Sv Gy}^{-1} \tag{5}$$

Which is an indoor occupant

$$\text{AEDE}(\text{mSv/y})_{\text{Indoor}} = D(\text{nGy/h}) \times 7010\text{hy}^{-1} \times 0.7\ \text{Sv Gy}^{-1}$$

Where D is the calculated dose rate in (nGy/h), T is the indoor occupancy time

$0.8 \times 24\,\text{h} \times 365.25\,\text{d} \cong 7010\text{hy}^{-1}$,

and F is the conversion factor$(0.7 \times 10^{-6}\text{SvGy}^{-1})$

Radium Equivalent (Ra_{eq})

The radium equivalent has been calculated by using a standard value of 370 Bq kg^{-1} per a sum of the value of, for ^{238}U a value of 370 Bq kg^{-1}, for ^{232}Th 259 Bq kg^{-1}, and ^{40}K 4810 Bq kg^{-1}. From Beretka and Matthew (1985), the equation for radium equivalent activity (Ra_{eq}) can be calculated as follows.

$$Ra_{eq} = A_U + 1.43A_{Th} + 0.077A_K \tag{6}$$

For environmental, soil, and building materials its value should be less than 370 Bq kg^{-1}, and for industries, it can be 370–740 Bq kg^{-1} (IAEA 1989; OECD and NEA 1979; UNSCEAR 2000).

Gamma Index (I_γ)

It is one of the measurements of a radiation hazard that comes from gamma radiation and the recommended maximum value must be less than one. The gamma index I_γ is calculated using the following formula obtained from EC (1999).

$$I_\gamma = \frac{A_U}{300} + \frac{A_{Th}}{200} + \frac{A_K}{3000} \leq 1 \quad (7)$$

A value of 0.5 or less for I_γ related to a dose rate (0.3 mSv y^{-1}), while a value of 1 or less for I_γ related to a dose rate of 1.0 mSv y^{-1}.

External Hazard Index (H_{ex})

The external hazard index is an expression of external exposure that comes from radioactive nuclides. The external hazard index (H_{ex}) is calculated using the formula (Beretka and Matthew 1985; Rafique et al. 2013).

$$H_{ex} = \frac{A_U}{370} + \frac{A_{Th}}{259} + \frac{A_K}{4810} \leq 1 \quad (8)$$

Internal Hazard Index (H_{in})

The internal hazard index is an expression of internal exposure that comes from radon and its short-lived progeny. The internal hazard index (H_{in}) is also calculated as follows (Beretka and Matthew 1985; Rafique et al. 2013).

$$H_{in} = \frac{A_U}{185} + \frac{A_{Th}}{259} + \frac{A_K}{4810} \leq 1 \quad (9)$$

The expressions, A_U, A_{Th}, and A_K found in the above equations represent the activity concentrations of uranium (^{238}U), thorium (^{232}Th), and potassium (^{40}K) in Bq kg^{-1}, respectively. The external hazard indexes and internal hazard index values should be below unity, which is to provide the safest environment to the population.

Excessive Lifetime Cancer Risk (ELCR)

ELCR or excessive lifetime cancer risk, serves as an expression for the probability of developing cancer over a lifetime from a specific amount of radiation exposure. An elevation in *ELCR* correlates with an increased probability of developing various types of cancer, including but not limited to blood cancer, breast cancer, and prostate cancer (Avwiri, Olatubosun, and Ononugbu 2014). ELCR is calculated using the equation from Taskin et al. (2009).

$$ELCR = AEDE \times DL \times RF \quad (10)$$

AEDE stands for (annual effective dose equivalent), and DL for average life expectancy which is an average of 70 years. RF factor which is cancer risk per Sievert (Sv^{-1}) from the ICRP (Taskin et al. 2009), its value is 0.05 Sv^{-1} and is used for the public given by ICRP (2007). It is also associated with a value that shows the expected number of cancers in each person on exposure to a carcinogen at a given dose. Moreover, the safest value of ELCR is below 0.29×10^{-3}.

Results and Discussion

Radioactivity Concentrations and Radiological Hazard Indices

As shown in Figure 2, the soil sample from Assosa-S9 exhibits the highest concentration of ^{238}U radioactivity, while the lowest concentration is observed in Assosa-S6 soil. Also, Figure 3 shown that Assosa-S2 soil has the highest concentration of ^{232}Th, whereas the lowest concentration is found in Assosa-S6 soil. Figure 4 shown that, Assosa-S10 soil possesses the highest concentration of ^{40}K, while the lowest concentration is recorded in Assosa-S6 soil. The average radioactivity concentration across the ten soil samples is 45.2 ± 2.3 Bq kg^{-1} for ^{238}U, 70 ± 3.8 Bq kg^{-1} for ^{232}Th, and 238.8 ± 11.6 Bq kg^{-1} for ^{40}K (Table 2). The mean activity concentration of ^{238}U and ^{232}Th in the soil samples from Assosa town exceeds the recommended safe values of 35 and 30 Bq kg^{-1}, respectively.

The result values of radium equivalent (Ra_{eq}) for all soil samples ranged from 78.16 ± 4.24 to

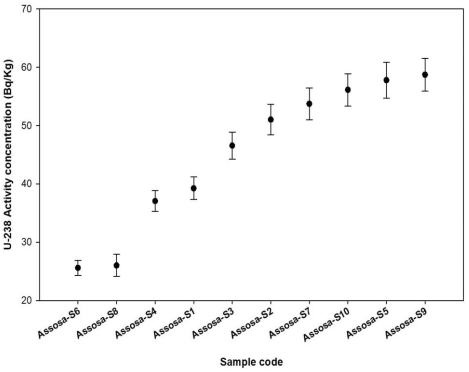

Figure 2. Specific activity concentration of ^{238}U radionuclide within the soil samples.

235.35 ± 10.62 Bq kg^{-1} with a mean value of 163.6 ± 8.6 Bq kg^{-1} (Table 2). This value is lower than the recommended safe value of 370 Bq kg^{-1}.

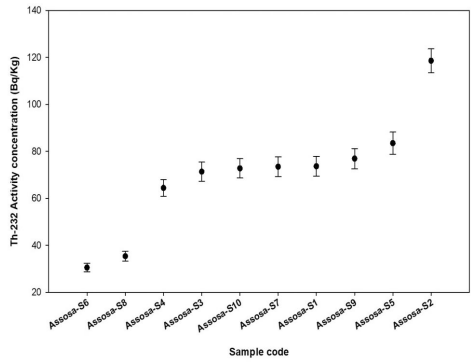

Figure 3. Specific activity concentration of ^{232}Th radionuclide within the soil samples.

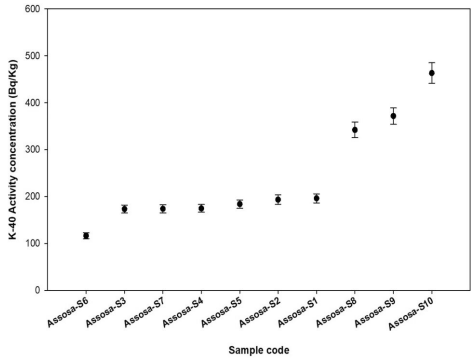

Figure 4. Specific activity concentration of ^{40}K radionuclide within the soil samples.

As shown in Table 2, the absorbed dose rate values for all soil samples are in the range of 34.9 ± 1.74 to 102.8 ± 4.6 nGy h^{-1}, with a mean value of 72.865 ± 3.72 nGy h^{-1}. This mean value exceed the recommended safe value of 59 nGy h^{-1} (Figure 5). The annual effective dose rate values for indoor exposure ranged from 1.01 ± 0.05 to 2.98 ± 0.13 mSv y^{-1}, with a mean value of 2.11 ± 0.1 mSv y^{-1}. For outdoor exposure, this values ranged from 0.254 ± 0.01 to 0.75 ± 0.0003 mSv y^{-1}, with a mean value of 0.52 ± 0.02 mSv y^{-1}. As shown in Table 3, the annual effective dose rate results for all soil samples surpass the global mean external exposure value of 0.48 mSv y^{-1}.

However, the mean annual effective dose rate remains below the worldwide annual safe limit of 1 mSv y^{-1}. The indoor annual effective dose rate values are greater than the outdoor annual effective dose rate values. From the result, as shown in Figure 6, both external hazard index and internal hazard index values are below 1. They range from 0.21 ± 0.007 to

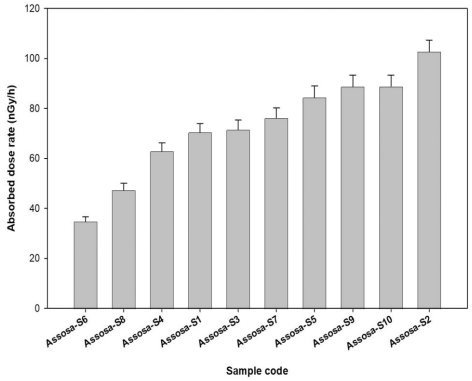

Figure 5. The absorbed dose rate values of the soil samples.

Table 2. Activity concentrations of radionuclides in the collected soil samples.

Sample code	A_U (Bq kg^{-1})	A_{Th} (Bq kg^{-1})	A_K (Bq kg^{-1})	Ra_{eq} (Bq kg^{-1})	D(nGy h^{-1})
Assosa-S1	39.25 ± 1.93	73.65 ± 4.13	196.01 ± 9.45	159.55 ± 8.55	70.5 ± 3.58
Assosa-S2	51.05 ± 2.65	118.55 ± 5.05	193.36 ± 10.07	235.35 ± 10.6	102.8 ± 4.6
Assosa-S3	46.58 ± 2.32	71.34 ± 4.07	173.27 ± 8.65	161.89 ± 8.78	71.6 ± 3.75
Assosa-S4	37.06 ± 1.78	64.405 ± 3.57	174.66 ± 8.35	142.46 ± 7.52	63 ± 3.24
Assosa-S5	57.80 ± 3.09	83.48 ± 4.71	183.88 ± 9	191.2 ± 10.5	84.5 ± 4.5
Assosa-S6	25.61 ± 1.29	30.52 ± 1.8	116.30 ± 5.96	78.16 ± 4.24	34.9 ± 1.74
Assosa-S7	53.75 ± 2.7	73.45 ± 4.23	173.72 ± 8.76	172.12 ± 9.41	76.24 ± 4.1
Assosa-S8	26.02 ± 1.9	35.35 ± 2.05	342 ± 16.55	102.8 ± 6.09	47.42 ± 2.63
Assosa-S9	58.74 ± 2.83	76.9 ± 4.32	371.64 ± 17.42	197.25 ± 10.34	88.79 ± 4.62
Assosa-S10	56.15 ± 2.76	72.75 ± 4.14	463.32 ± 22.03	195.78 ± 10.35	88.9 ± 4.51
Min.	25.61 ± 1.29	30.52 ± 1.8	116.30 ± 5.96	78.16 ± 4.24	34.9 ± 1.74
Max.	58.74 ± 2.83	118.55 ± 5.05	463.32 ± 22.03	235.35 ± 10.6	102.8 ± 4.6
Mean value	45.2 ± 2.3	70 ± 3.8	238.8 ± 11.6	163.6 ± 8.6	72.865 ± 3.72

Table 3. Annual effective dose rates and hazard indexes values for the collected soil samples.

Sample code	AEDE $_{(Indoor)}$	AEDE $_{(outdoor)}$	I_γ	H_{ex}	H_{in}	ELCR (10^{-3})
Assosa-S1	2.07 ± 0.1	0.519 ± 0.02	0.56 ± 0.02	0.42 ± 0.016	0.53 ± 0.01	1.81 ± 0.07
Assosa-S2	2.98 ± 0.13	0.75 ± 0.0003	0.82 ± 0.026	0.63 ± 0.02	0.77 ± 0.024	2.625 ± 0.001
Assosa-S3	2.07 ± 0.1	0.52 ± 0.027	0.56 ± 0.02	0.43 ± 0.01	0.56 ± 0.02	1.82 ± 0.09
Assosa-S4	1.82 ± 0.09	0.45 ± 0.023	0.50 ± 0.019	0.38 ± 0.014	0.48 ± 0.016	1.57 ± 0.08
Assosa-S5	2.45 ± 0.13	0.61 ± 0.032	0.67 ± 0.02	0.51 ± 0.02	0.67 ± 0.024	2.135 ± 0.1
Assosa-S6	1.01 ± 0.05	0.254 ± 0.01	0.27 ± 0.01	0.21 ± 0.007	0.28 ± 0.009	0.88 ± 0.035
Assosa-S7	2.21 ± 0.11	0.55 ± 0.029	0.60 ± 0.023	0.46 ± 0.01	0.61 ± 0.02	1.92 ± 0.1
Assosa-S8	1.37 ± 0.076	0.3 ± 0.01	0.37 ± 0.01	0.27 ± 0.01	0.34 ± 0.013	1.05 ± 0.035
Assosa-S9	2.57 ± 0.133	0.648 ± 0.033	0.7 ± 0.024	0.53 ± 0.01	0.69 ± 0.022	2.26 ± 0.11
Assosa-S10	2.57 ± 0.13	0.64 ± 0.03	0.7 ± 0.023	0.52 ± 0.018	0.68 ± 0.022	2.24 ± 0.105
Mean value	2.11 ± 0.1	0.52 ± 0.02	0.5 ± 0.01	0.43 ± 0.013	0.56 ± 0.01	1.8 ± 0.07

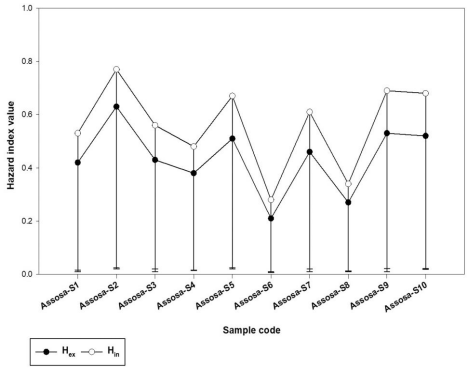

Figure 6. The comparison of internal and external hazard indexes values of the soil samples.

0.63 ± 0.02, with a mean value of 0.43 ± 0.013 for the external hazard index, and from 0.28 ± 0.009 to 0.77 ± 0.024, with a mean value of 0.56 ± 0.01 for the internal hazard index. The values of the external and internal hazard index are less than the recommended safe value of one (UNSCEAR 2000).

The gamma index values varied from 0.27 ± 0.01 to 0.82 ± 0.026 with a mean value of 0.5 ± 0.01, which is less than the recommended safe value of one. The ELCR values varied from 0.88 ± 0.035 to 2.625 ± 0.001, with a mean value of (1.8 ± 0.07) × 10^{-3}. This mean value exceed the threshold value of 0.29 × 10^{-3} (Table 3). The result values of gamma index (I_γ), internal hazard index (H_{in}), and external hazard index (H_{ex}) for all soil samples indicates that, the levels of radon and its short-lived daughters that occur in the soil do not have significant health effects on the respiratory organs of individuals living in those areas.

Measurement of background radiation is important in any measurement of radioactivity concentrations. This is true for forensic elemental analysis methods, such as neutron activation and X-ray fluorescence (XRF). Therefore, this study results will be relevant and usable for forensic applications.

Comparison of Activity Concentration with Similar Studies

The radioactivity concentrations of Assosa City soils were compared with soils from various districts or provinces see in Table 4. According to the result, Assosa City soil exhibit an average activity concentrations of 45.2 ± 2.3, 70 ± 3.8, and 238.8 ± 11.6 Bq kg^{-1} for ^{238}U, ^{232}Th, and ^{40}K, respectively.

The mean activity concentrations of ^{238}U, ^{232}Th, and ^{40}K in Assosa City soils are lower than those in soils from the Guangdong province of China (Yang and Sun 2022), Pinapet region of India (Amanjeet et al. 2017), Lombardia region of Italy (Dutra Garcèz et al. 2020), and Kedah region of Malaysia (Alzubaidi, Hamid, and Abdul Rahman 2016). However, when compared with similar studies, as shown in Figure 7, the measured mean activity concentrations of ^{238}U, ^{232}Th, and ^{40}K in Assosa City soils are higher than soils from the Mila region of Algeria (Bramki, Ramdhane, and Benrachi 2018), Imo state of Nigeria (Mbonu and Ben 2021), Kampinoski park of Poland (Łukaszek-Chmielewska et al. 2019), and Richard Bay of South Africa (Masok et al. 2018).

Statistical Analysis for Data

In this study, the analysis of the statistical data was performed using an Excel workbook sheet. The statistical analyses carried out are the Pearson correlation coefficient (PCC), Quantile-Quantile (Q-Q) plot, and the Frequency distribution for ^{238}U, ^{232}Th, and ^{40}K.

Pearson Correlation Coefficient (PCC)

One of the statistical analysis methods that measure the strength and direction of a linear relationship between two variables is the PCC. By using this method, the degree of association that exists between the measured radiological parameters were obtained (Table 5). From the Pearson correlation matrix, the correlation of ^{238}U with ^{232}Th; ^{238}U with ^{40}K;

Table 4. Comparison of mean activity concentration of ^{238}U, ^{232}Th, and ^{40}K within Assosa soil in Ethiopia with other countries' province soils.

№	Country	Average radioactivity concentrations			References
		A_u (Bq kg^{-1})	A_{Th} (Bq kg^{-1})	A_k (Bq kg^{-1})	
1	Ethiopia (Assosa City)	45.2 ± 2.3	70 ± 3.8	238.8 ± 11.6	Present study
2	Algeria (Mila)	46.7	26.7	246.5	Bramki, Ramdhane, and Benrachi (2018)
3	Brazil (Espirito Santo)	30	94	48	Dutra Garcèz et al. (2020)
4	China (Guangdong)	79.3	101	535.8	Yang and Sun (2022)
5	Georgia (Mtskheta-Mtianeti)	25.4	26.9	464	Kekelidze et al. (2017)
6	India (Pinapet)	30.24 ± 0.53	29.89 ± 0.61	291.06 ± 0.57	Amanjeet et al. (2017)
7	Ireland	60	26	350	UNSCEAR (2000)
8	Italy (Lombardia)	72	48	617	Guidotti et al. (2015)
9	Malaysia (Kedah)	102.08 ± 3.9	133.9 ± 2.9	325.8 ± 9.8	Alzubaidi, Hamid, and Abdul Rahman (2016)
10	Nigeria (Imo State)	4.15	1.64	134.13	Mbonu and Ben (2021)
11	Poland (Kampinoski park)	8.54	6.65	206	Łukaszek-Chmielewska et al. (2019)
12	Russian Federation	27	30	520	UNSCEAR (2000)
13	South Africa (Richards Bay)	28.26 ± 11.40	29.64 ± 11.50	146.77 ± 63.3	Masok et al. (2018)
14	Türkiye (Rize province)	24.5	51.8	344.9	Durusoy and Yildirim (2017)
15	United States	40	35	370	UNSCEAR (2000)
16	UNSCEAR standard value	35	30	400	UNSCEAR (2000)

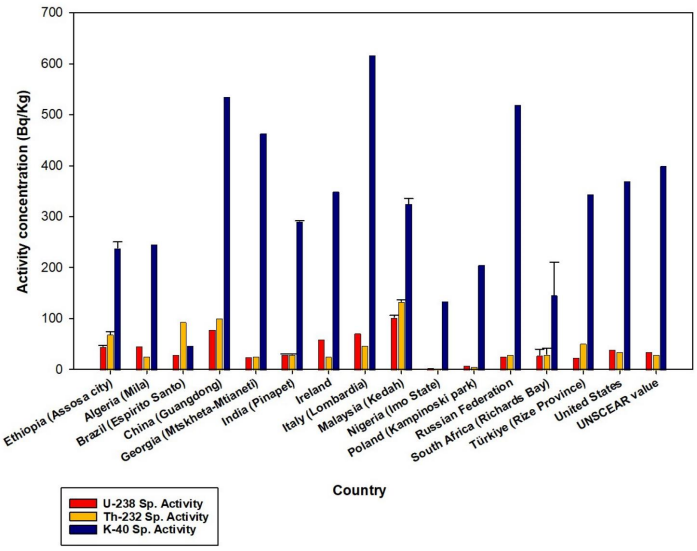

Figure 7. The comparison of radioactivity concentrations in soil samples with different countries.

Table 5. Pearson correlation values between ^{238}U, ^{232}Th, ^{40}K, radium equivalent, absorbed dose rate, and annual effective dose equivalent.

	^{238}U	^{232}Th	^{40}K	Ra_{eq}	D	AEDE
^{238}U	1	0.745	0.303	0.885	0.894	0.892
^{232}Th		1	−0.01	0.94	0.93	0.93
^{40}K			1	0.25	0.307	0.302
Ra_{eq}				1	0.99	0.99
D					1	0.99
AEDE						1

^{226}Th with ^{40}K, and also the correlation between ^{238}U, ^{232}Th, and ^{40}K with hazard indexes (Ra_{eq}, D, and AEDE) were determined. It is known that, the Pearson correlation values r varied in between $-1 < 0 < 1$ (Turney 2023).

The Pearson correlation results reveal a strong positive correlation ($r = 0.745$) between ^{238}U and ^{232}Th radioactive nuclides, as shown in Figure 8(a). This indicates that the activity concentrations of both ^{238}U and ^{232}Th increase or decrease proportionally with nearly equal ranges of values (Table 2). For ^{238}U and ^{40}K, the Pearson correlation value is 0.303, which indicate a moderate positive correlation (Figure 8(b)). As shown in Figure 8(c), the correlated value for ^{226}Th with ^{40}K is $r = -0.01$, and which indicate a weak negative correlation. In

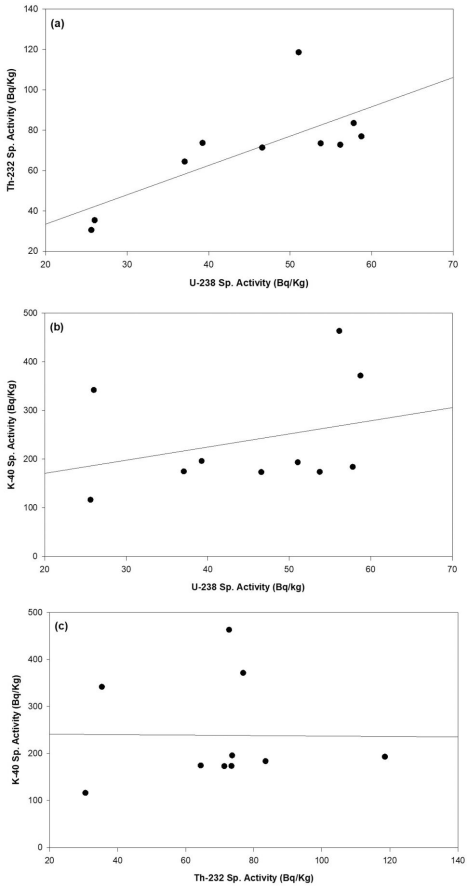

Figure 8. The Pearson correlation between (a) for ^{238}U and ^{232}Th, (b) for ^{238}U and ^{40}K, and (c) for ^{232}Th and ^{40}K.

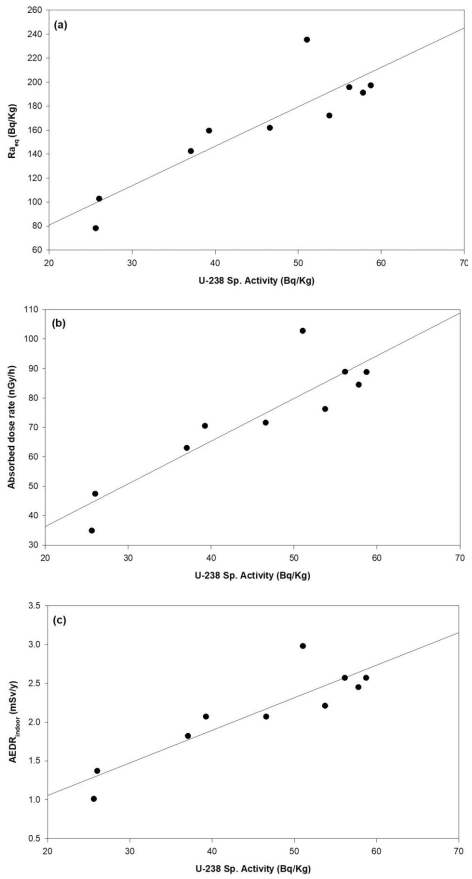

Figure 9. The Pearson correlation between (a) for ^{238}U and radium equivalent (Ra_{eq}), (b) for ^{238}U and absorbed dose rate (D), and (c) for ^{238}U and indoor annual effective dose equivalent (AEDE).

summary, the decay series of the radionuclides of ^{238}U and ^{232}Th have a positive direct proportional correlation per given decay time. Moreover, the correlation values between uranium (^{238}U) with radium equivalent (Ra_{eq}), absorbed dose rate (D), and AEDE are 0.885, 0.894, and 0.892, respectively, indicating the strong positive direction as shown in Figure 9(a–c).

Q-Q Plot and Frequency Distribution

Q-Q plot shows whether the linearity of the points or data points lie on the axis related to normally distributed, and points follow nonlinear suggesting, the data are not normally distributed. Frequency distribution shows the number of times each possible value occurs in a data set. As shown in Figures 10(a), 11(a), and 12(a), the Q-Q plots indicates that the concentrations follow normal distributed. As shown in Figure 10(b), Frequency distribution for ^{238}U activity concentration is multi-modal, which signifying multiple peak values. For ^{232}Th activity concentration, as shown in Figure 11(b), the frequency distribution is normal, characterized by a single peak value at the mid of the distribution mode or a Gaussian distribution. As shown in Figure 12(b), a unimodal frequency distribution for ^{40}K, with a single peak value to the left of the distribution mode.

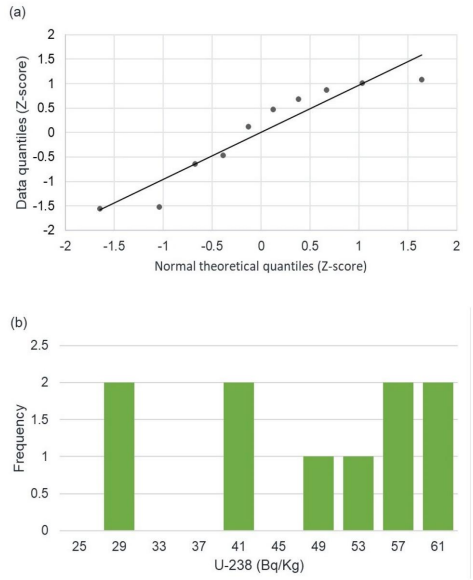

Figure 10. Statistical plot for ^{238}U: (a) quantile-quantile and (b) frequency distribution.

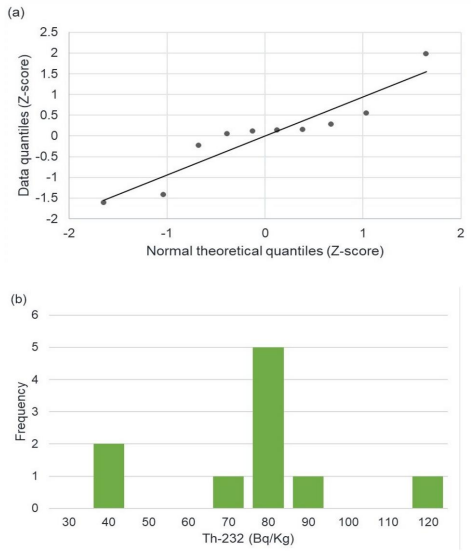

Figure 11. Statistical plot for ^{232}Th: (a) quantile-quantile and (b) frequency distribution.

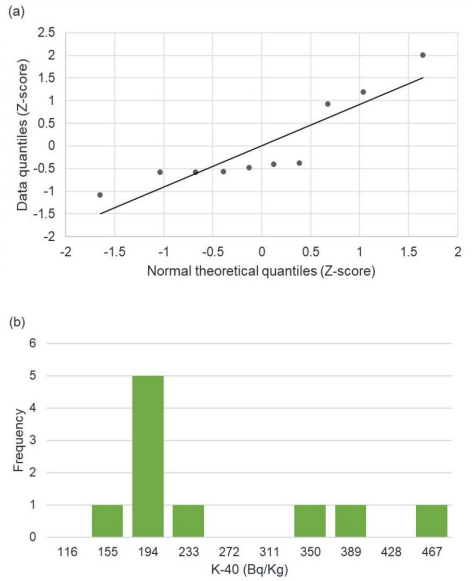

Figure 12. Statistical plot for ^{40}K: (a) quantile-quantile and (b) frequency distribution.

Conclusions

The average specific activity concentration of ^{238}U and ^{232}Th in the soil of Assosa City surpasses the recommended safe thresholds of 35 Bq kg^{-1} for ^{238}U and 30 Bq kg^{-1} for ^{232}Th. In this study, particularly, soil samples of Assosa-S2, Assosa-S5, Assosa-S7, Assosa-S9, and Assosa-S10 exhibit elevated concentrations of ^{238}U and ^{232}Th, which surpassed the established safety limits. Overall, Assosa City soil exhibits a higher mean radioactivity concentration of ^{238}U and ^{232}Th, which exceeds the recommended safe values, therefore, Precautions are advisable, as such elevated concentrations may pose significant health risks to the community. From this study, the measured radioactivity concentrations underscore, the necessity for continuous monitoring of Assosa City soil.

Acknowledgments

I would like to thank, Assosa University and Addis Ababa University for supporting my research, Ethiopian Conformity Assessment Enterprise staff members, and Ethiopia Radiation Protection Authority for the experimental work using HPGe detector.

Author Contributions

Yared Birhane has done sample preparation, data analysis, data interpretation, and manuscript writing. Yared Birhane and Dr. Tilahun Tesfaye have contributed to the study's conception and design. Both Yared Birhane and Guadie Degu have contributed to the selection of the study area and sample collection.

Disclosure Statement

No potential conflict of interest was reported by the author(s).

Data Availability Statement

There will be data available upon reasonable request to the corresponding author.

References

Abbady, A., A. M. El-Arabi, A. E. Abbady, and S. Taha. 2006. "Gamma Ray Measurements of Natural Radioactivity in Cultivated and Reclaimed Soil Upper Egypt." Paper presented at *VIII Radiation Physics & Protection Conference,* November 2006. Beni Sueif-Fayoum, Egypt.

Alzubaidi, Ghazwa, Fauziah B. S. Hamid, and I. Abdul Rahman. 2016. "Assessment of Natural Radioactivity Levels and Radiation Hazards in Agricultural and Virgin Soil in the State of Kedah, North of Malaysia." *TheScientificWorldJournal* 2016 (9): 6178103–6178109. https://doi.org/10.1155/2016/6178103

Amanjeet, Ajay Kumar, Suneel Kumar, Joga Singh, Parminder Singh, and B. S. Bajwa,. 2017. "Assessment of Natural Radioactivity Levels and Associated Dose Rates in Soil Samples from Historical City Panipat, India." *Journal of Radiation Research and Applied Sciences* 10 (3): 283–288. https://doi.org/10.1016/j.jrras.2017.05.006

Avwiri, G. O., S. A. Olatubosun, and C. P. Ononugbu. 2014. "Evaluation of Radiation Hazard Indices for Selected Dumpsites in Port Harcourt, Rivers State, Nigeria." *International Journal of Science and Technology* 3 (10): 663–673.

Beretka, J., and P. J. Matthew. 1985. "Natural Radioactivity of Australian Building Materials, Industrial Wastes and by-Products." *Health Physics* 48 (1): 87–95. https://doi.org/10.1097/00004032-198501000-00007

Bramki, Amina, Mourad Ramdhane, and Fatima Benrachi. 2018. "Natural Radioelement Concentrations in Fertilizers and the Soil of the Mila Region of Algeria." *Journal of Radiation Research and Applied Sciences* 11 (1): 49–55. https://doi.org/10.1016/j.jrras.2017.08.002

Bullock, Liam A., and Owen Morgan. 2018. "The Asosa Region of Western Ethiopia: A Golden Exploration Opportunity." *Geology Today* 34 (1): 31–34. https://doi.org/10.1111/gto.12217

Djeufack, Léonard Boris, Guillaume Samuel Bineng, Oumar Bobbo Modibo, and Joseph Emmanuel Ndjana Nkoulou II, and Saïdou. 2022. "Correlation between Ground ^{222}Rn and ^{226}Ra and Long-Term Risk Assessment at the at the Bauxite Bearing Area of Fongo-Tongo, Western Cameroon." *Radiation* 2 (4): 387–404. https://doi.org/10.3390/radiation2040029

Durusoy, Ayşe, and Meryem Yildirim. 2017. "Determination of Radioactivity Concentrations in Soil Samples and Dose Assessment for Rize Province, Turkey." *Journal of Radiation Research and Applied Sciences* 10 (4): 348–352. https://doi.org/10.1016/j.jrras.2017.09.005

Dutra Garcêz, Ricardo Washington, José Marques Lopes, Sueli da Silva Perez, Dejanira da Costa Lauria, Eduardo Paim Viglio, Fernanda Gonçalves da Cunha, Fernando Carlos Araújo Ribeiro, and Ademir Xavier da Silva. 2020. "Activity Concentration and Mapping of Radionuclides in Espírito Santo State Soils, Brazil." *Radiation Physics and Chemistry* 167: 108209. https://doi.org/10.1016/j.radphyschem.2019.03.013

EC (European Commission). 1999. *Radiological Protection Principles Concerning the Natural Radioactivity of Building Materials. Radiation Protection Report—RP-112.* Luxembourg: European Commission.

Elsaman, Reda, Mohammed Ahmed Ali, El-Montaser Mahmoud Se, and Atef El-Taher. 2018. "Natural Radioactivity Levels and Radiological Hazards in Soil Samples around Abu Karqas Sugar Factory." *Journal of Environmental Science and Technology* 11 (1): 28–38. https://doi.org/10.3923/jest.2018.28.38

Guidotti, Laura, Franca Carini, Riccardo Rossi, Marina Gatti, Roberto M. Cenci, and Gian Maria Beone. 2015. "Gamma-Spectrometric Measurement of Radioactivity in Agricultural Soils of the Lombardia Region, Northern Italy." *Journal of Environmental Radioactivity* 142: 36–44. https://doi.org/10.1016/j.jenvrad.2015.01.010

IAEA (International Atomic Energy Agency). 1989. *Measurement of Radionuclides in Food and the Environment.* Vienna, Austria: IAEA.

Ibraheem, Awad A., Atef El-Taher, and May H. M. Alruwaili. 2018. "Assessment of Natural Radioactivity Levels and Radiation Hazard Indices for Soil Samples from Abha, Saudi Arabia." *Results in Physics* 11: 325–330. https://doi.org/10.1016/j.rinp.2018.09.013

ICRP (International Cooperation for Radiation Protection). 2007. "International Commission on Radiological Protection." *Annals of the ICRP* 37: 2–4. https://www.icrp.org/page.asp.

Kebede, Yadeta S., Mulgeta M. Alene, and Nega T. Endalemaw. 2021. "Urban Landfill Investigation for Managing the Negative Impact of Solid Waste on Environment Using Geospatial Technique. A Case Study of Assosa Town, Ethiopia." *Enviromental Challenges* 4: 100103. https://doi.org/10.1016/j.envc.2021.100103

Kekelidze, Nodar, Teimuraz Jakhutashvili, Bezhan Tutberidze, Eremia Tulashvili, Mariam Akhalkatsishvili, and Lela Mtsariashvili. 2017. "Radioactivity of Soils in Mtskheta-Mtianeti Region (Georgia)." *Annals of Agrarian Science* 15 (3): 304–311. https://doi.org/10.1016/j.aasci.2017.07.003

Łukaszek-Chmielewska, Aneta, Martin Girard, Olga Stawarz, Barbara Piotrowska, Karol Wojtkowski, and Krzysztof Isajenko. 2019. "Measurements of Natural Radioactivity in Soil Samples Collected in the Kampinoski National Park." *E3S Web of Conferences* 100: 00052. https://doi.org/10.1051/e3sconf/201910000052

Masok, F. B., P. L. Masiteng, R. D. Mavunda, P. P. Maleka, and H. Winkler. 2018. "Measurement of Radioactivity Concentration in Soil Samples around Phosphate Rock Storage Facility in Richards Bay, South Africa." *Journal of Radiation Research and Applied Sciences* 11 (1): 29–36. https://doi.org/10.1016/j.jrras.2017.10.006

Mbonu, Charles Chisom, and Ubong Camilus Ben. 2021. "Assessment of Radiation Hazard Indices Due to Natural Radioactivity in Soil Samples from Orlu, Imo State, Nigeria." *Heliyon* 7 (8): e07812. https://doi.org/10.1016/j.heliyon.2021.e07812

Ntsohi, L., I. Usman, R. Mavunda, and O. Kureba. 2021. "Characterization of Uranium in Soil Samples from a Prospective Uranium Mining in Serule, Botswana for Nuclear Forensic Application." *Journal of Radiation Research and Applied Sciences* 14 (1): 23–33.

OECD (Organization for Economic Cooperation and Development) and NEA (Nuclear Energy Agency. 1979. *Exposure to Radiation from Natural Radioactivity in Building Materials*. Reports by Group of experts of NEA, NEA (6711), Paris, France.

Rafique, Muhammad, Abdul Jabbar, Abdul Razzaq Khan, Saeed Ur Rahman, Muhammad Basharat, Azhar Mehmood, and Matiullah. 2013. "Radiometric Analysis of Rock and Soil Samples of Leepa Valley; Azad Kashmir, Pakistan." *Journal of Radioanalytical and Nuclear Chemistry* 298 (3): 2049–2056. https://doi.org/10.1007/s10967-013-2681-x

Senthilkumar, B., V. Dhavamani, S. Ramkumar, and P. Philominathan. 2010. "Measurement of Gamma Radiation Levels in Soil Samples from Thanjavur Using γ-Ray Spectrometry and Estimation of Population Exposure." *Journal of Medical Physics* 35 (1): 48–53. https://doi.org/10.4103/0971-6203.55966

Shahbazi-Gahrouei, Daryoush, Mehrdad Gholami, and Samaneh Setayandeh. 2013. "A Review on Natural Background Radiation." *Advanced Biomedical Research* 2 (1): 65. https://doi.org/10.4103/2277.115821

Taskin, H., M. Karavus, P. Ay, A. Topuzoglu, S. Hidiroglu, and G. Karahan. 2009. "Radionuclide Concentration in Soil and Lifetime Cancer Risk Due to Gamma Radioactivity in Kirklareli, Turkey." *Journal of Environmental Radioactivity* 100 (1): 49–53. https://doi.org/10.1016/j.jenvrad.2008.10.012

Turney, S. 2023. "Pearson Correlation Coefficient (r) Guide & Examples." *Scribbr*. https://www.scribbr.com/statistics/pearson-correlation-coefficient/

UNSCEAR (United Nations Scientific Committee on the Effects of Atomic Radiations). 2000. *Sources and Effects of Ionizing Radiation. Report to General Assembly, with Scientific Annexes*. New York, NY: United Nations.

Uosif, M. A. M., and A. El-Taher. 2008. "Radiological Assessment of Abo-Tartur Phosphate, Western Desert, Egypt." *Radiation Protection Dosimetry* 130 (2): 228–235. https://doi.org/10.1093/rpd/ncm502

Yang, Jianzhou, and Yanling Sun. 2022. "Natural Radioactivity and Dose Assessment in Surface Soil from Guangdong, a High Background Radiation Province in China." *Journal of Radiation Research and Applied Sciences* 15 (1): 145–151. https://doi.org/10.1016/j.jrras.2022.01.019

Wiley
Journal of Analytical Methods in Chemistry
Volume 2024, Article ID 6633673, 14 pages
https://doi.org/10.1155/2024/6633673

WILEY

Research Article

Evaluation of Natural Radioactivity Level in Surface Soil from Bambasi District in Benishangul Gumuz Region, Ethiopia

Yared Birhane Kidane,[1,2] **Tilahun Tesfaye Deressu**,[1] **and Guadie Degu Belete**[2]

[1]*Department of Physics, Natural and Computational Science College, Addis Ababa University, Addis Ababa, Ethiopia*
[2]*Department of Physics, Natural and Computational Science College, Assosa University, Assosa, Ethiopia*

Correspondence should be addressed to Yared Birhane Kidane; yaredbirhanek@gmail.com

Received 18 March 2023; Revised 23 July 2024; Accepted 28 August 2024

Academic Editor: Cecilia Cagliero

The study assessed the concentration of natural radionuclides in soil samples from the Bambasi district in Ethiopia's Benishangul Gumuz region using a gamma-ray spectrometer equipped with a high-purity germanium (HPGe) detector. The measured activity concentrations of ^{238}U, ^{232}Th, and ^{40}K in soil samples varied from 46.2 ± 2.25 to 88.49 ± 5.73 Bq/kg, 73.4 ± 4.12 to 119.65 ± 8.45 Bq/kg, and 176.78 ± 8.63 to 396.71 ± 25.39 Bq/kg, respectively. The average concentration of ^{238}U and ^{232}Th exceeded the recommended worldwide population weighted average values of 32.0 and 45.0 Bq/kg, respectively, while the average concentration of ^{40}K was below the recommended value of 420.0 Bq/kg. The mean absorbed dose rate was calculated to be 91.6 ± 5.1 nGy/h, which is above the recommended safe value of 59 nGy/h. The average annual effective dose equivalents for indoor and outdoor exposure were determined to be 2.65 ± 0.14 mSv/y and 0.66 ± 0.1 mSv/y, respectively. The calculated mean values of the internal hazard index, external hazard index, and gamma index across all soil samples were 0.72 ± 0.05, 0.55 ± 0.02, and 0.72 ± 0.02, respectively, all below the recommended safe threshold of one. These findings suggest that the activity concentrations observed in the soil samples exceed safe levels, indicating the necessity for further investigation into radioactivity levels and epidemiological studies regarding potential hazards from high background radiation.

1. Introduction

The natural environment has long been imbued with radiation, originating from a myriad of natural and man-made sources. These sources collectively contribute to what we commonly refer to as background radiation, a ubiquitous presence of low-level ionizing radiation constantly surrounding us [1]. Human interaction with this radiation is inherent to our existence, as we ingest or inhale nuclides present in the air, food, and water. Exposure levels vary widely based on factors such as climate, local geology, and human activity patterns unique to each region [2].

One significant source of background radiation stems from radioactive elements naturally present in the Earth's crust, such as uranium, thorium, and their decay products. These elements emit radiation continuously, with radionuclides finding their way into rocks, soil, and building materials, particularly in regions with elevated concentrations of these elements. This study focuses on analyzing soil radioactivity in samples collected from the Bambasi area in western Ethiopia [2, 3].

Soil, being a complex matrix, hosts a diverse array of both naturally occurring and anthropogenic radionuclides. Monitoring soil radioactivity is of paramount environmental concern due to its potential impacts on human health and ecosystems. The concentration and distribution of radionuclides in surface soils are crucial factors in assessing environmental radioactivity levels, evaluating associated health risks, and formulating effective regulatory measures [2, 4]. Radionuclides present in soil emit gamma radiation, contributing to alterations in background radiation levels in the environment. The extent of this radiation depends on various geographical and geological factors. Radionuclides such as thorium and uranium may undergo redistribution

during geological evolution cycles, resulting in small concentration deposits under favourable geological processes [1, 5].

Zircon, a mineral found in nature, serves as a source of uranium and thorium and occurs in sedimentary, igneous, and metamorphic rocks. Commonly, zircon along with thorite is a source of Th, U, Y, and heavy rare earth elements (HREE) [6]. The mobilization of radionuclides from rock to soil is influenced by specific concentrations, indicating leaching of ^{238}U to rock rather than soil, lower mobility of thorium from rock to soil due to its stability, and a higher concentration of potassium (^{40}K) in soil compared to rocks, as potassium is a mobile element [7].

Everyone in the world is exposed to; in fact lives with these background radiation levels, with external exposure occurring through irradiation and internal exposure resulting from ingestion and inhalation. The predominant source of radiation exposure for humans is the natural environment, which contributes up to 85% of the annual exposure dose received globally [1, 8]. Soil, a foundational component of our environment, is comprised of a complex mixture of mineral particles, organic matter, air, and water. Its composition and structure vary significantly across different regions, influencing the types of vegetation it can support [9].

Understanding how radionuclides interact with soil and plants is crucial, as plants can absorb these radionuclides and transport them to edible parts. This absorption process depends on factors such as the radionuclide's chemical availability and its proximity to the root zone [10]. The primary aim of this study was to determine the concentration of naturally occurring radionuclides in various soil samples collected from the Bambasi district in the Benishangul Gumuz region, Ethiopia. This research aimed to categorize the radioactivity concentration of soil samples as either safe or hazardous by comparison of the results with the recommended safe values set by the United Nations Scientific Committee on the Effects of Atomic Radiation (UNSCEAR).

2. Materials and Methods

2.1. Description of the Study Area. Benishangul Gumuz region is one of the eleven regional states comprising the Ethiopian federal structure. Bambasi woreda is situated in Ethiopia, approximately 614 km away from the capital city, Addis Ababa (Figure 1). Its geographical coordinates are within latitude 9°–10°N and longitude 034°–035°E [11]. Bambasi district is located in the Assosa zone. Assosa zone is one of the three zones situated in the Benishangul Gumuz Regional State (BGRS). Assosa zone is mainly known for its potential gold deposits, holding promise for high-profit opportunities [12].

2.2. Sample Collection and Preparation. Samples were obtained from specific locations in Bambasi town. Bambasi district chosen in this study was based on, increasing of its population density, having a high agricultural demand, and there are gold mining activities. A total of eight sites in Bambasi town, as shown in Table 1, were selected for the collection of surface soil samples. Each sample was carefully dug out from a depth of 5–30 cm of the surface soil, with an approximate weight of 1 kg per sample. These samples were coded as Bambasi-S1 to Bambasi-S8, and their respective locations are outlined in Table 1.

After collection, the samples were securely packed in polyethylene bags and transported to the laboratory of the Ethiopian Conformity Assessment Enterprise (ECAE) for further processing. The gathered soil samples underwent air-drying at 100°C for 10–24 hours, depending on the soil moisture content. Subsequently, the dried samples were crushed to ensure homogeneity, with the crushing process continuing until the soil samples reached a powder-like consistency. A 0.25 mm mesh was employed for sieving the samples. Around 500 g of the homogenized soil samples were then packed and sealed in airtight cylindrical Marinelli beakers and stored for 28 days (four weeks) to achieve secular equilibrium. Finally, the processed samples were transported to the Ethiopian Technology Authority (ETA) for the use of HPGe detector.

2.3. Experimental Setups. The gamma-ray emitting radionuclides concentrations in the soil samples were measured by using an HPGe detector coupled with a multichannel analyzer (MCA). HPGe detector is a suitable semiconductor radiation detector, and it has a high-resolution capacity for photo peaks. The Marinelli beaker sample geometry was 538 G-E. The HPGe detector has 77% relative photopeak efficiency. The detector has a 1.8 keV energy resolution. Multichannel analyzer of 8192 channel performance is connected to computer software of Genie 2000. The voltage of 3499 V was used for the detector. The calibrated radionuclides for the detector were ^{60}Co and ^{137}Cs, which are the quality standard sources according to ISO 9001. The quality standard used for calibrating the detector was ISO/IEC 17025. The detector is enclosed with a lead shield (100 mm thickness), cadmium (2 mm thickness), and copper (2.5 mm thickness) to prevent the background radiation that comes from the surroundings. The calibration of the experiment was done using IAEA-certified standard reference sources. The counting time of the gamma-ray spectrum was 28,800 s. The soil samples were placed in their Marinelli beakers, directly on the front face of the detector.

The peak areas in the spectrum were calculated, and the background radiation counting was subtracted to obtain the net count rate. The minimum detection limits of the detector according to ISO 11929 reports were 1.33, 1.02, and 4.99 Bq/kg for ^{238}U, ^{232}Th, and ^{40}K, respectively. The specific energy spectrum for each radionuclide was obtained by photopeak area analysis. The specific activity of ^{238}U was assessed from gamma-ray lines of ^{214}Pb at 351 keV and ^{214}Bi at 609.3 and 1764.5 keV, while the activity of ^{232}Th was evaluated from gamma-ray lines of ^{228}Ac at 338.4, 911.1, and 968.9 keV, ^{212}Pb at 238.63 keV, and ^{208}Tl at 583.19 keV. The specific activity of ^{40}K was directly determined from its gamma-ray line at 1460.8 keV [13].

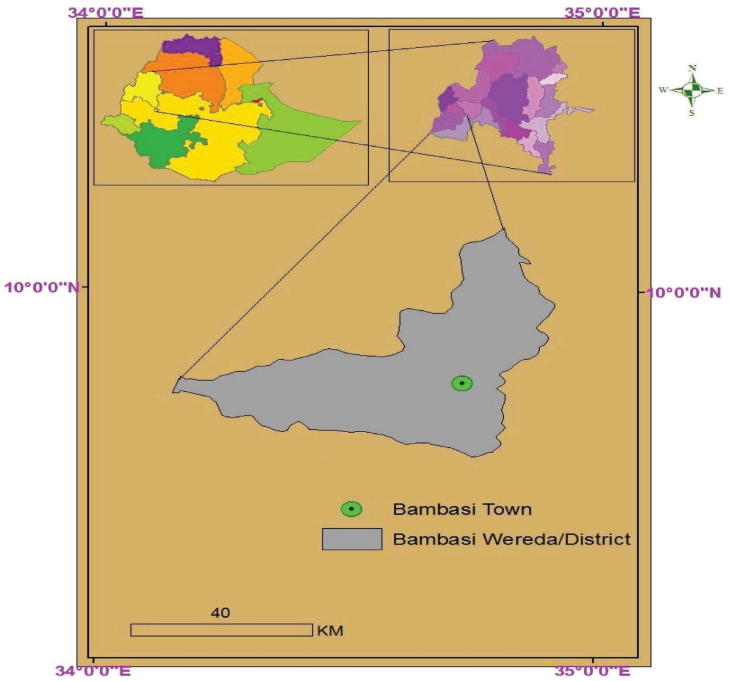

Figure 1: Location map of Bambasi district using ArcGIS 10.2.

Table 1: Sample collected locations in Bambasi town using global positioning system (GPS).

No.	Sample code	Latitude (North)	Longitude (East)
1	Bambasi-S1	9.751911°	34.726703°
2	Bambasi-S2	9.751736°	34.729544°
3	Bambasi-S3	9.753097°	34.73175°
4	Bambasi-S4	9.756256°	34.730528°
5	Bambasi-S5	9.757667°	34.728025°
6	Bambasi-S6	9.760117°	34.726661°
7	Bambasi-S7	9.761314°	34.728581°
8	Bambasi-S8	9.759558°	34.731228°

2.4. Measurements of Activity Concentration. The specific activity concentrations (A_c) in Bq/kg of the soil samples were calculated as follows [14]:

$$A_c = \frac{N_c}{I\varepsilon M T_s}. \tag{1}$$

where A_c is radioactivity concentration of the samples (Bq/kg), N_c is the net count for packed sample (N_s) minus count for the background (N_b), ε is efficiency of the detector for the gamma ray energy of interest, I is probability of gamma-ray absolute intensity, M is mass of the packed sample (kg), and T_s is the actual sample counting time. The error associated with each measured activity of the samples was calculated using standard deviation (σ_s) [15].

$$\text{Count rate} = \frac{N_c}{T_s} = \frac{N_s}{T_s} \pm \sigma_s,$$
$$\text{where } \sigma_s = \sqrt{\frac{N_t}{{T_t}^2} + \frac{N_b}{{T_b}^2}}, \tag{2}$$

where σ_s is the standard deviation of the measured sample, N_t is the total count, T_t is the total count time, and T_b is the background counts time.

2.5. Estimation of Radiological Dose and Hazardous Indices

2.5.1. Absorbed Dose Rate (D). This refers to the rate at which ionizing radiation is absorbed per unit of time. The absorbed dose rate in the air, resulting from the uniform distribution of ^{238}U, ^{232}Th, and ^{40}K radionuclides at a height of 1 meter above the ground surface, was calculated using the following formula [1]:

$$D\left(\frac{\text{nGy}}{\text{h}}\right) = 0.462A_U + 0.602A_{Th} + 0.0417A_K. \tag{3}$$

The world average absorbed dose rate thresholds are 59 nGy/h for outdoors and 84 nGy/h for indoors.

2.5.2. Annual Effective Dose Equivalent (AEDE). The annual effective dose equivalent denotes the biological effect equivalent to the deposition of one joule of radiation energy

per kilogram of the human body over the course of a year. To estimate the annual effective dose equivalent in mSv/y, the absorbed dose rate values are utilized, employing a conversion coefficient of 0.7 Sv/Gy for converting absorbed doses in the air to the received effective dose. The calculation also incorporates an indoor occupancy factor of 0.8, reflecting that, on average, the population spends 80% of their time indoors. Additionally, an outdoor occupancy factor of 0.2 is considered, implying that 20% of their time is spent outdoors [1].

It is known that the world's annual effective dose rate due to external radiation is 0.41 mSv/y indoors and 0.07 mSv/y outdoors. For people living in a certain area, the annual effective dose equivalent for outdoor and indoor could be calculated using the following equations [1]:

$$\mathrm{AEDE}\left(\frac{\mathrm{mSv}}{\mathrm{y}}\right)_{\mathrm{outdoor}} = D\left(\frac{\mathrm{nGy}}{\mathrm{h}}\right) \times 24\,\mathrm{h} \times 365.2\,\mathrm{d} \times 0.2 \times 0.7\,\frac{Sv}{Gy}, \tag{4}$$

where 0.7 is the absorbed dose conversion factor and 0.2 is the outdoor occupancy.

$$\mathrm{AEDE}\left(\frac{\mathrm{mSv}}{\mathrm{y}}\right)_{\mathrm{indoor}} = D\left(\frac{\mathrm{nGy}}{\mathrm{h}}\right) \times 24\,\mathrm{h} \times 365.2\,\mathrm{d} \times 0.8 \times 0.7\,\frac{Sv}{Gy}. \tag{5}$$

This is for an indoor occupant.

$$\mathrm{AEDE}\left(\frac{\mathrm{mSv}}{\mathrm{y}}\right)\mathrm{indoor} = D \times T \times F \times 0.8,$$

$$\mathrm{AEDE}\left(\frac{\mathrm{mSv}}{\mathrm{y}}\right)\mathrm{indoor} = D\left(\frac{\mathrm{nGy}}{\mathrm{h}}\right) \times 7010\,\mathrm{hy}^{-1} \times 0.7\,\frac{Sv}{Gy}, \tag{6}$$

$$T \times 0.8 = 24\,\mathrm{h} \times 365.25\,\mathrm{d} \times 0.8 \cong 7010\,\mathrm{hy}^{-1},$$

where D is the calculated dose rate in (nGy/h), T is the indoor occupancy time factor within a year (8760 h), and F is the conversion factor (0.7 Sv/Gy).

2.5.3. Radium Equivalent (Ra_{eq}). The radium equivalent has been calculated by using a standard value of 370 Bq/kg per a sum of the value of 370 Bq/kg, 259 Bq/kg, and 4810 Bq/kg for ^{238}U, ^{232}Th, and ^{40}K, respectively. The equation for radium equivalent activity ($\mathrm{Ra_{eq}}$) would be [14]

$$\mathrm{Ra_{eq}} = A_U + 1.43A_{\mathrm{Th}} + 0.077A_K. \tag{7}$$

For environmental, soil, and building materials, its value should be less than 370 Bq/kg, and for industries, it can be 370–740 Bq/kg [1, 4, 16].

2.5.4. Gamma Index (Iγ). It is one of the measurements of a radiation hazard that comes from gamma radiation, and the recommended maximum value must be less than one. The gamma index $I\gamma$ is calculated using the following equation [17]:

$$I_\gamma = \frac{A_U}{300} + \frac{A_{Th}}{200} + \frac{A_K}{3000}. \tag{8}$$

Its permissible limit is $I_\gamma = 1$ corresponds to an absorbed gamma dose rate of 0.3 mSv/y, implying that materials with $I_\gamma \geq 1$ should be avoided.

2.5.5. External Hazard Index (H_{ex}). The external hazard index is an expression of external exposure that comes from radioactive nuclides. The external hazard index (H_{ex}) is calculated using the following equation [14, 18]:

$$H_{ex} = \frac{A_U}{370} + \frac{A_{Th}}{259} + \frac{A_K}{4810} \leq 1. \tag{9}$$

2.5.6. Internal Hazard Index (H_{in}). The internal hazard index is an expression of internal exposure that comes from radon and its short-lived progeny. The internal hazard index (H_{in}) is also calculated as follows [14, 18]:

$$H_{in} = \frac{A_U}{185} + \frac{A_{Th}}{259} + \frac{A_K}{4810} \leq 1, \tag{10}$$

where the expression A_U, A_{Th}, and A_K found in the above expressions represent the activity concentrations of uranium (^{238}U), thorium (^{232}Th), and potassium (^{40}K) in Bq/kg, respectively.

2.5.7. Excessive Lifetime Cancer Risk (ELCR). This is associated with the probability of developing cancer over a lifetime at a given exposure level. An increase in the ELCR causes a proportionate increase in the rate at which an individual can get cancer of blood cancer, breast cancer, and prostate cancer [19]. The excessive lifetime cancer risk is calculated as follows [20]:

$$\mathrm{ELCR} = \mathrm{AEDE} \times \mathrm{DL} \times \mathrm{RF}. \tag{11}$$

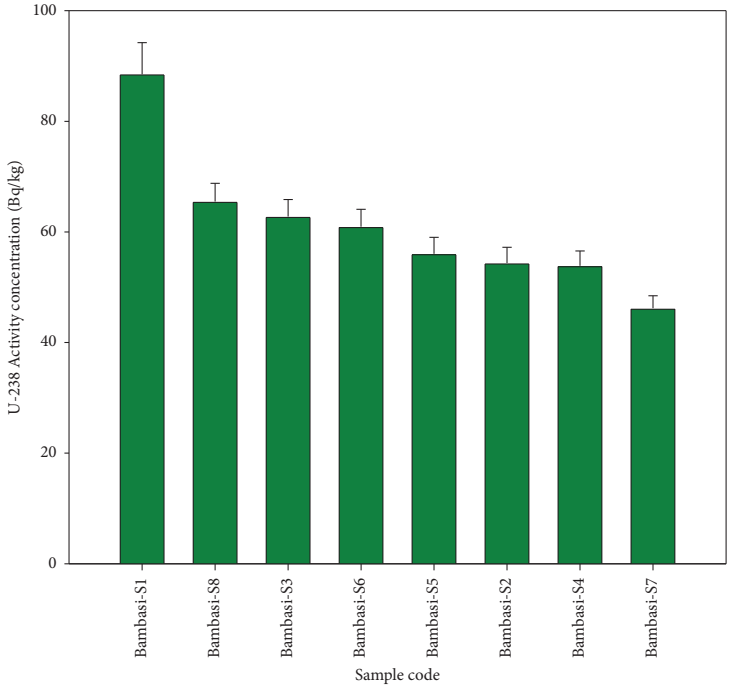

FIGURE 2: Specific activity concentration of ^{238}U radionuclide within the soil samples.

AEDE stands for annual effective dose equivalent, and DL for average life expectancy which is an average of 70 years. RF factor is cancer risk per sievert (Sv^{-1}) from the ICRP [21], and its value is 0.05 Sv^{-1} and is used for the public given by [20]. It is a value depicting the number of cancers expected in each number of people on exposure to a carcinogen at a given dose. The threshold value of ELCR is 0.29×10^{-3}.

3. Results and Discussion

3.1. Radioactivity Concentrations and Radiological Hazard Indices. The Bambasi-S1 soil exhibits the highest radioactivity concentration of ^{238}U, while the lowest concentration is observed in Bambasi-S7 soil (see Figure 2). Figure 3 shows that a higher concentration of ^{232}Th found in Bambasi-S1 soil, with the lowest concentration found in Bambasi-S7 soil. As shown in Figure 4, Bambasi-S1 soil registers the highest concentration of ^{40}K, while the lowest concentration is observed in Bambasi-S3 soil. The average radioactivity concentrations for all soil samples are 61 ± 3.2 Bq/kg for ^{238}U, 89.2 ± 5.3 Bq/kg for ^{232}Th, and 237.7 ± 12.7 Bq/kg for ^{40}K. From the result values, as shown in Table 2, the mean activity concentration of ^{238}U and ^{232}Th in the soil of the Bambasi district surpassed the recommended global population weighted average values of 32 and 45 Bq/kg, respectively. It is known that the recommended global population weighted average values of ^{238}U, ^{232}Th, and ^{40}K in soil are 32, 45, and 420 Bq/kg, respectively [1].

The values of radium equivalent (Ra_{eq}) for all soil samples varied from 102.39 ± 11.86 to 289.9 ± 8.8 Bq/kg, with a mean value of 192.5 ± 11.2 Bq/kg (Table 2). The mean value of Ra_{eq} is below 370 Bq/kg, which is the recommended safe value for radium equivalent.

Table 3 shows the absorbed dose rate for all soil samples ranged from 72.7 ± 3.7 to 129.3 ± 8.6 nGy/h, with an average value of 91.6 ± 5.1 nGy/h, surpassed the recommended safe value of 59 nGy/h (Figure 5). The annual effective dose rate values for indoor exposure ranged from 2.10 ± 0.10 to 3.74 ± 0.24 mSv/y, with average value of 2.65 ± 0.14 mSv/y, while for outdoor exposure, they varied from 0.53 ± 0.026 to 0.94 ± 0.05 mSv/y, with an average of 0.66 ± 0.1 mSv/y. According to Table 3, the annual effective dose rate for all soil samples exceeds the recommended mean external radiation safe value of 0.48 mSv/y. Values of the indoor annual effective dose rates are higher than those of outdoor rates, as shown in Figure 6. However, the mean annual effective dose rate remains below the global average annual effective safety threshold of 1 mSv/y.

In Table 4, the external hazard indexes (H_{ex}) and internal hazard index (H_{in}) for all soil samples, not include Bambasi-S1 sample, are less than 1. Their values ranged from 0.44 ± 0.017 to 0.78 ± 0.03 for H_{ex}, with an average of 0.55 ± 0.02, and from 0.56 ± 0.02 to 1.022 ± 0.045 for H_{in}, with an average of 0.72 ± 0.05. The mean values for both external and internal hazard indexes fall below the recommended safe limit of one (Figure 7).

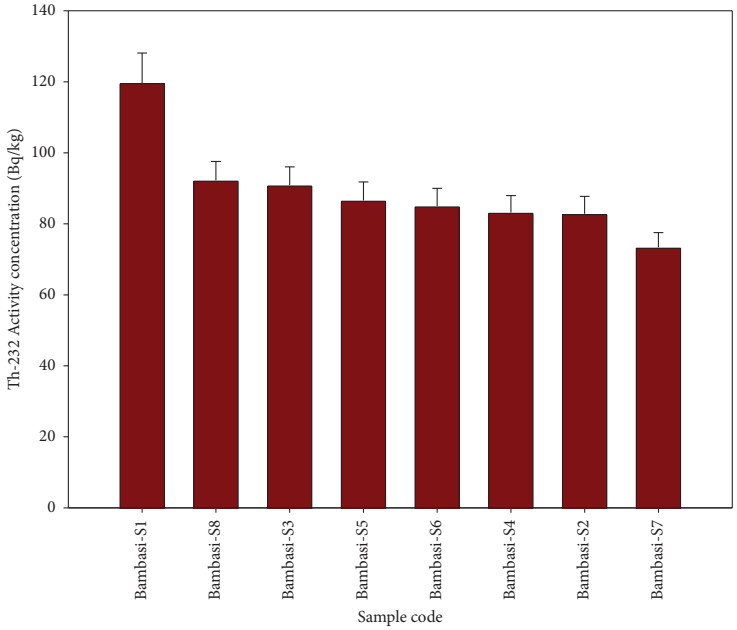

Figure 3: Specific activity concentration of ^{232}Th radionuclide within the soil samples.

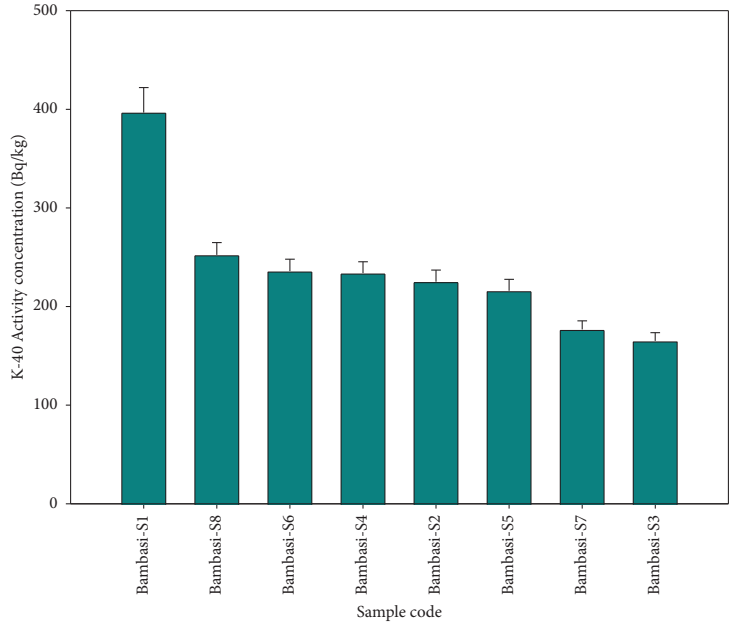

Figure 4: Specific activity concentration of ^{40}K radionuclide within the soil samples.

Table 2: Mean radioactivity concentrations in the collected soil samples.

No.	Sample code	A_U (Bq/kg)	A_{Th} (Bq/kg)	A_K (Bq/kg)	Ra_{eq} (Bq/kg)
1	Bambasi-S1	88.49 ± 5.73	119.65 ± 8.45	396.71 ± 25.39	289.9 ± 8.8
2	Bambasi-S2	54.39 ± 2.85	82.83 ± 4.91	225.27 ± 11.73	190.09 ± 0.75
3	Bambasi-S3	62.78 ± 3.09	90.87 ± 5.17	165.12 ± 8.29	205.38 ± 11.02
4	Bambasi-S4	53.88 ± 2.68	83.2 ± 4.76	233.92 ± 11.58	190.7 ± 10.37
5	Bambasi-S5	56.05 ± 2.99	86.6 ± 5.2	216.08 ± 11.6	196.5 ± 11.28
6	Bambasi-S6	60.95 ± 3.14	85 ± 5.01	235.93 ± 12.13	200.6 ± 11.17
7	Bambasi-S7	46.2 ± 2.25	73.4 ± 4.12	176.78 ± 8.63	164.6 ± 15
8	Bambasi-S8	65.49 ± 3.30	92.25 ± 5.33	252.39 ± 12.54	102.39 ± 11.86
	Mean value	61 ± 3.2	89.2 ± 5.3	237.7 ± 12.7	192.5 ± 11.2

Table 3: Results of radiation hazard indexes for the collected soil samples.

No.	Sample code	D (nGy/h)	E (mSv/y)$_{Indoor}$	E (mSv/y)$_{Outdoor}$	I_γ
1	Bambasi-S1	129.3 ± 8.6	3.74 ± 0.24	0.94 ± 0.05	1.02 ± 0.04
2	Bambasi-S2	84.2 ± 4.6	2.44 ± 0.13	0.61 ± 0.63	0.67 ± 0.02
3	Bambasi-S3	90.5 ± 4.8	2.62 ± 0.13	0.66 ± 0.03	0.71 ± 0.02
4	Bambasi-S4	84.58 ± 4.4	2.45 ± 0.127	0.61 ± 0.032	0.67 ± 0.025
5	Bambasi-S5	86.9 ± 4.8	2.52 ± 0.13	0.63 ± 0.034	0.69 ± 0.028
6	Bambasi-S6	89 ± 4.9	2.58 ± 0.14	0.64 ± 0.035	0.70 ± 0.027
7	Bambasi-S7	72.7 ± 3.7	2.10 ± 0.10	0.53 ± 0.026	0.57 ± 0.022
8	Bambasi-S8	96.2 ± 5.22	2.78 ± 0.15	0.70 ± 0.037	0.76 ± 0.029
	Mean value	91.6 ± 5.1	2.65 ± 0.14	0.66 ± 0.1	0.72 ± 0.02

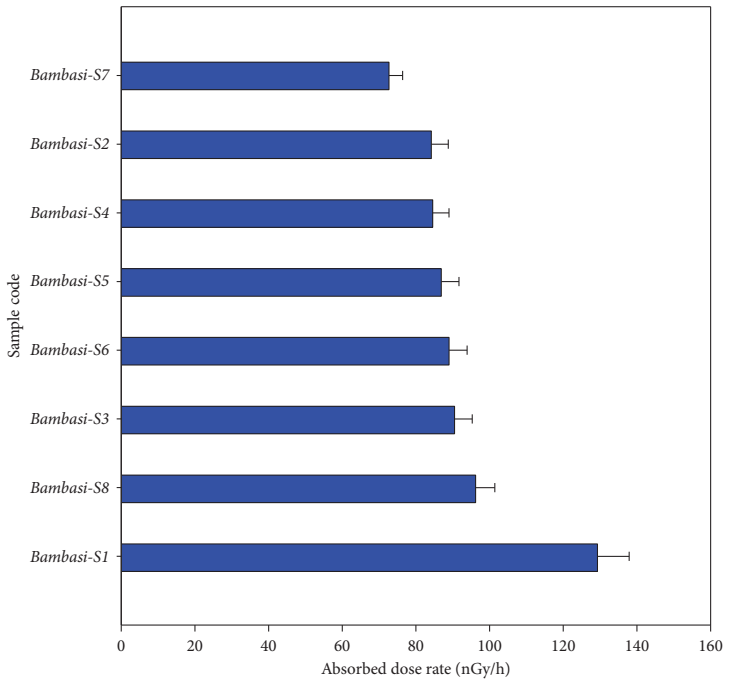

Figure 5: The absorbed dose rate values of the soil samples.

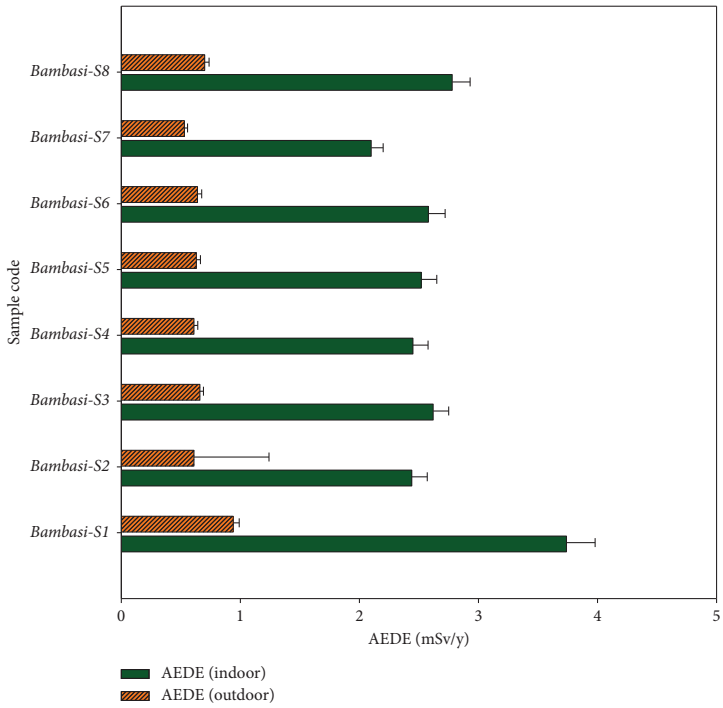

Figure 6: The comparison of indoor and outdoor annual effective dose equivalent values.

Table 4: The external hazard index, internal hazard indexes, and excessive lifetime cancer risk values of the collected soil samples.

No.	Sample code	H_{ex}	H_{in}	ELCR ($\times 10^{-3}$)
1	Bambasi-S1	0.78 ± 0.03	1.022 ± 0.045	3.29 ± 0.175
2	Bambasi-S2	0.51 ± 0.02	0.66 ± 0.024	2.13 ± 2.2
3	Bambasi-S3	0.55 ± 0.02	0.72 ± 0.026	2.31 ± 0.105
4	Bambasi-S4	0.51 ± 0.019	0.66 ± 0.23	2.13 ± 2.2
5	Bambasi-S5	0.53 ± 0.02	0.68 ± 0.025	2.205 ± 0.119
6	Bambasi-S6	0.54 ± 0.02	0.70 ± 0.025	2.24 ± 0.12
7	Bambasi-S7	0.44 ± 0.017	0.56 ± 0.02	1.85 ± 0.09
8	Bambasi-S8	0.58 ± 0.02	0.76 ± 0.027	2.45 ± 0.12
	Mean value	0.55 ± 0.02	0.72 ± 0.05	2.3 ± 0.6

As shown in Figure 6, the values of the indoor annual effective dose rate signify a substantial annual radiation exposure for human tissues. Therefore, implementing safety measures for individuals residing in this environment is advisable. Additionally, Figure 7 shown that the values of the internal hazard indexes exceed those of the external hazard indexes. The gamma index values ranged from 0.57 ± 0.022 to 1.02 ± 0.04, with an average of 0.72 ± 0.02, which is below the recommended safe value of one. The mean values for the gamma index (I_γ), internal hazard index (H_{in}), and external hazard index (H_{ex}) for all soil samples fall below the safe threshold of one. This indicates that the levels of radon and its short-lived daughters in the soils do not pose significant health risks to the respiratory organs of individuals living in the Bambasi district. However, the excessive lifetime cancer risk (ELCR) values ranged from $(1.85 \pm 0.09) \times 10^{-3}$ to $(3.29 \pm 0.175) \times 10^{-3}$, with a mean value of $(2.3 \pm 0.6) \times 10^{-3}$, surpassed the threshold value of 0.29×10^{-3} (Table 4).

3.2. Comparison of Activity Concentration with Similar Studies. As shown in Table 5, a comparison was made between the radioactivity concentration of soils in the Bambasi district and similar studies conducted in other countries. The results reveal that Bambasi soils exhibit an average activity concentration of 61 ± 3.2 Bq/kg for ^{238}U, 89.2 ± 5.3 Bq/kg for ^{232}Th, and 237.7 ± 12.7 Bq/kg for ^{40}K. The mean activity concentrations of ^{238}U, ^{232}Th, and ^{40}K in

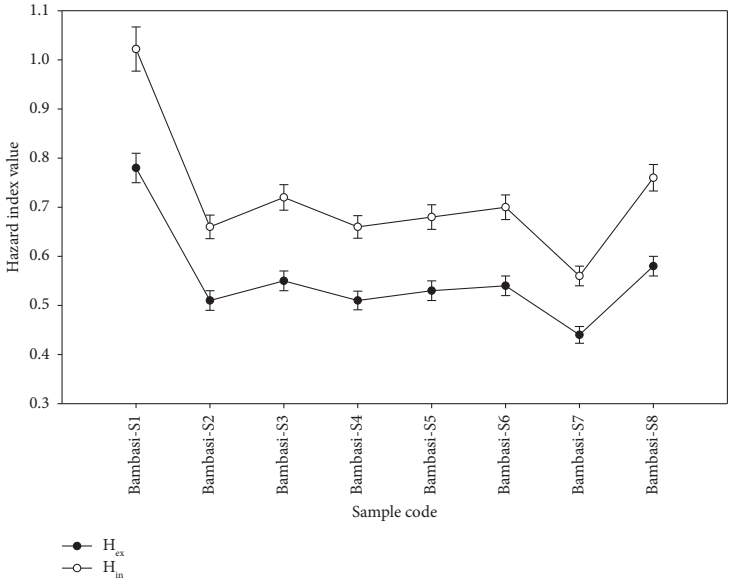

Figure 7: The comparison of internal and external hazard index values of the soil samples.

Table 5: Comparison of the mean activity concentration of ^{238}U,^{232}Th, and^{40}K within Bambasi soils in Ethiopia with other countries' province soils.

No.	Country	Average radioactivity concentrations (Bq/kg)			Reference
		$^{238}U/^{226}Ra$	^{232}Th	^{40}K	
1	Ethiopia (Bambasi)	61 ± 3.2	89.2 ± 5.3	237.7 ± 12.7	Present study
2	Algeria (Mila)	46.7	26.7	246.5	[22]
3	Brazil (Espirito Santo)	30	94	48	[23]
4	China (Guangdong)	79.3	101	535.8	[24]
5	Georgia (Mtskheta-Mtianeti)	25.4	26.9	464	[25]
6	India (Pinapet)	30.24 ± 0.53	29.89 ± 0.61	291.06 ± 0.57	[26]
7	Ireland	60	26	350	[1]
8	Iraq (Baba Gurgur dome)	57.8	25.4	479.9	[27]
9	Italy (Lombardia)	72	48	617	[28]
10	Nigeria (Imo state)	4.15	1.64	134.13	[29]
11	Poland (Kampinoski park)	8.54	6.65	206	[30]
12	Russian Federation	27	30	520	[1]
13	South Africa (Richards Bay)	28.26 ± 11.40	29.64 ± 11.50	146.77 ± 63.30	[31]
14	Türkiye (Ardahan province)	29.9 ± 6.2	36.7 ± 6.8	435.1 ± 23.9	[32]
15	Türkiye (Rize province)	24.5	51.8	344.9	[33]
16	United States	40	35	370	[1]
17	UNSCEAR value	32	45	420	[1]

Bambasi soils are lower than those observed in soils from the Guangdong province of China [24] and Lombardia region of Italy [28], as shown in Figure 8. However, when compared to similar studies, as shown in Figure 8, the measured mean activity concentrations of ^{238}U, ^{232}Th, and ^{40}K in Bambasi soils are higher than those in soils from the Kedah region of Malaysia [13], Mila region of Algeria [22], Panipet region of India [26], Baba Gurgur dome of Kirkuk oil field in Iraq [27], Imo state of Nigeria [29], Kampinos park of Poland [30], and Richard Bay of South Africa [31]. Also, the measured radioactivity concentrations found in Bambasi district soil shows that it have higher concentrations than Assosa City soil, which is the capital city of Benishangul Gumuz region. Assosa City soil has a mean activity concentration of 45.2 ± 2.3, 70 ± 3.8, and 238.8 ± 11.6 Bq/kg for ^{238}U, ^{232}Th, and ^{40}K, respectively [34]. This research provides valuable

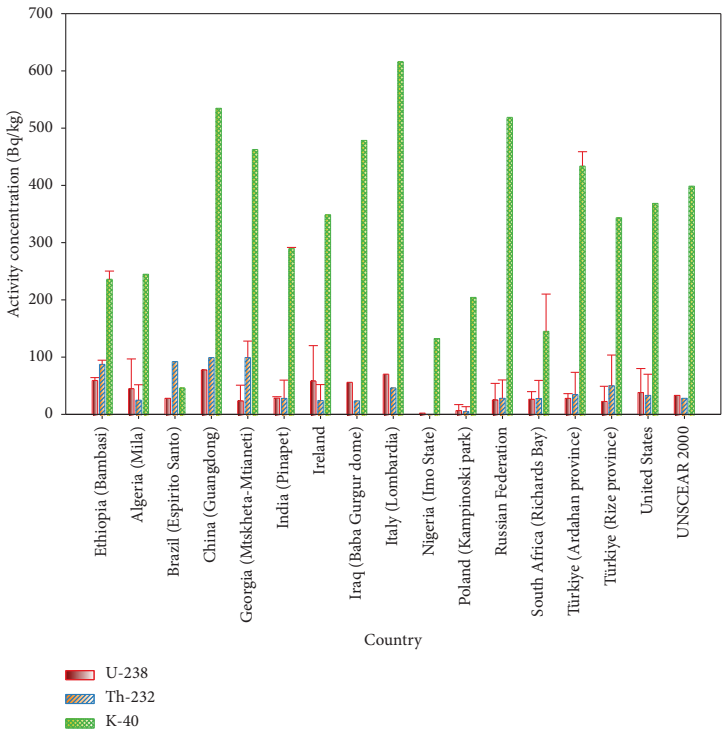

Figure 8: The comparison of radioactivity concentration with different countries province soils.

Table 6: Pearson correlation matrix values between ^{238}U, ^{232}Th, and ^{40}K, radium equivalent, absorbed dose rate, and indoor annual effective dose rate of the Bambasi soil samples.

	^{238}U	^{232}Th	^{40}K	Ra_{eq}	*D*	AEDE
^{238}U	1	0.98	0.86	0.59	0.99	0.99
^{232}Th		1	0.87	0.63	0.99	0.99
^{40}K			1	0.58	0.91	0.91
Ra_{eq}				1	0.626	0.629
D					1	0.99
AEDE						1

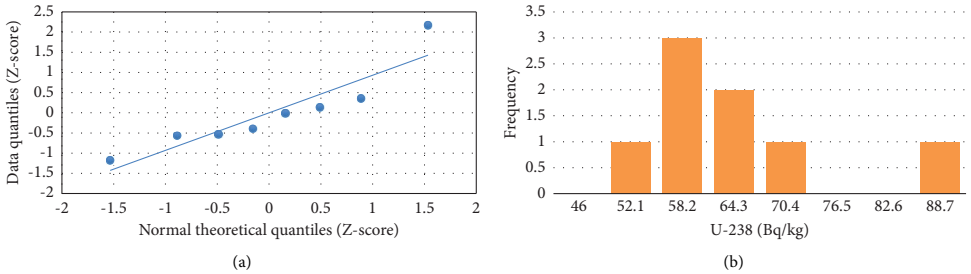

Figure 9: Plots for ^{238}U. (a) Quantile-quantile and (b) frequency distribution.

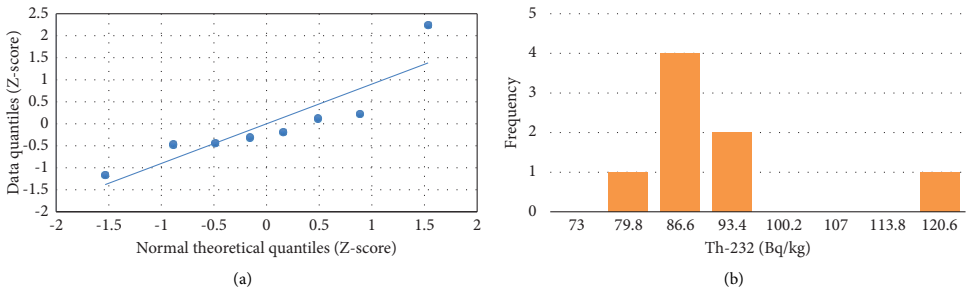

Figure 10: Plots for ^{232}Th. (a) Quantile-quantile and (b) frequency distribution.

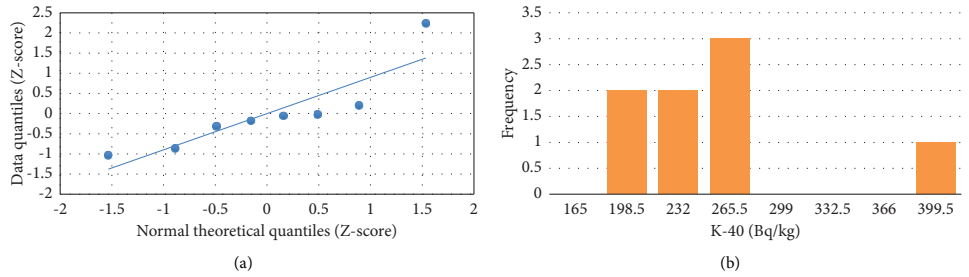

Figure 11: Plots for ^{40}K. (a) Quantile-quantile and (b) frequency distribution.

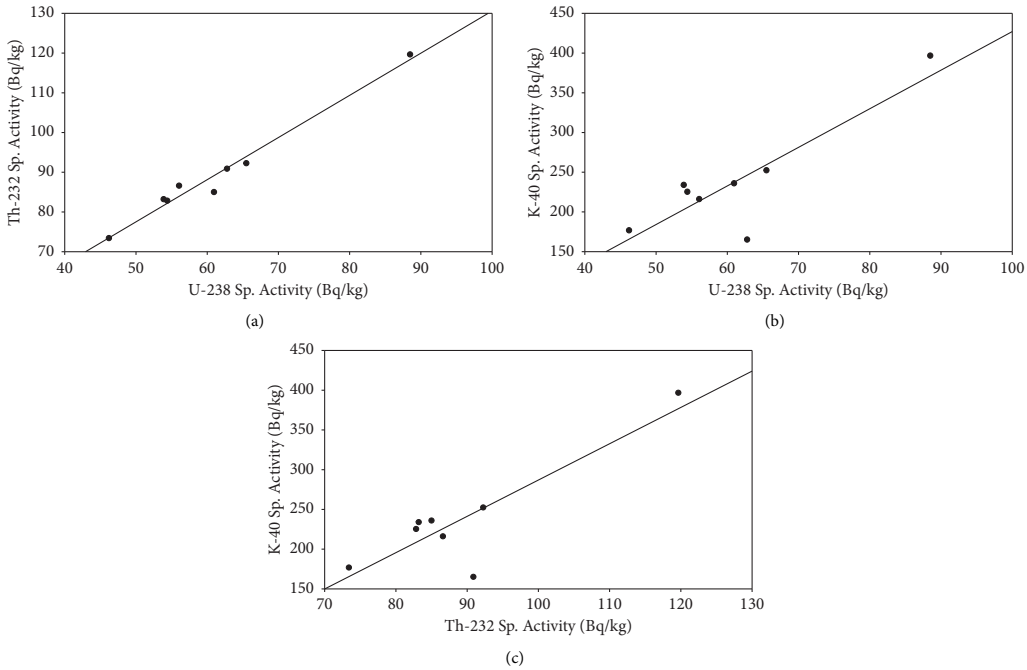

Figure 12: The Pearson correlation between (a) ^{238}U and ^{232}Th, (b) ^{238}U and ^{40}K, and (c) ^{232}Th and ^{40}K.

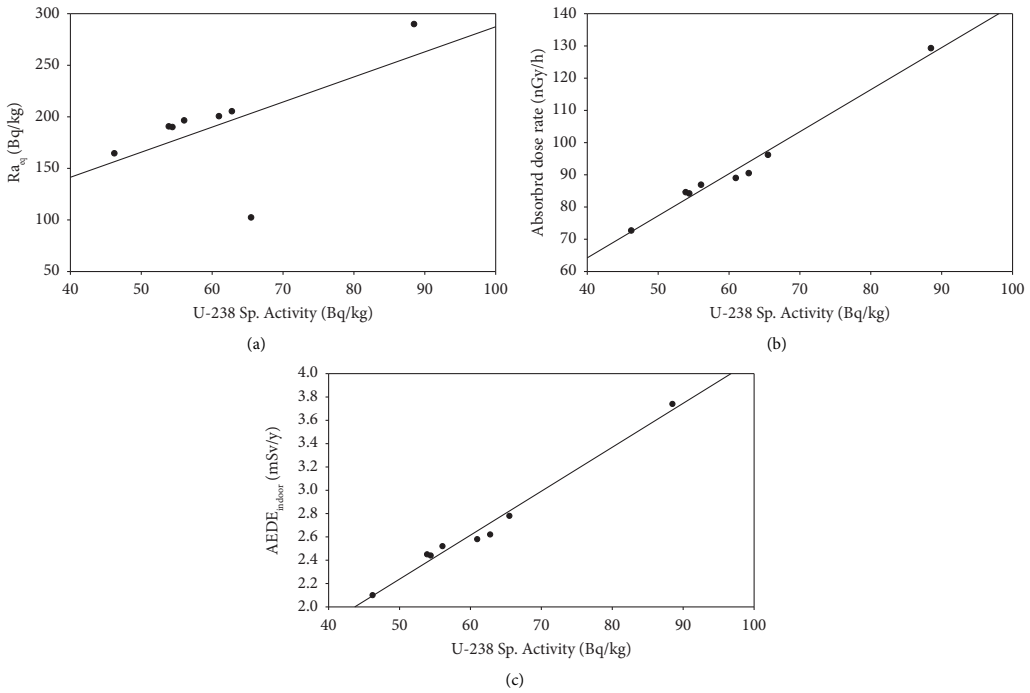

FIGURE 13: The Pearson correlation between (a) ^{238}U and radium equivalent (Ra_{eq}), (b) ^{238}U and absorbed dose rate (D), and (c) ^{238}U and indoor annual effective dose equivalent (AEDE).

insights for future investigations due to its findings of elevated radioactivity concentrations, which are higher than international safety standards set by UNSCEAR. Numerous studies in the past have explored various aspects related to radionuclide concentration in soil, investigations into the transfer of radioactive nuclides to vegetation plants from the soil, external exposures, deposition and distribution of radionuclides in minerals and rocks, as well as radionuclides in medicinal plants, rocks as sources of raw materials for building materials, and environmental assessments [35–42].

3.3. Statistical Analysis. In this study, the analysis of the statistical data was performed using an Excel workbook sheet. The statistical correlation among ^{238}U, ^{232}Th, ^{40}K, and radiological dose index values was examined using a Quantile-Quantile (Q-Q) plot, frequency distribution, and Pearson correlation (Table 6).

3.3.1. Q-Q Plot and Frequency Distribution. The Q-Q plot uses as indicator of whether the linearity of the points or data points lies on the axis, which is related to normal distribution. When data points follow nonlinear, suggesting that the data are not normal distribution. The frequency distributions illustrate the frequency of occurrences for each possible value in a dataset. As shown in Figures 9(a), 10(a), and 11(a), the Q-Q plots suggest that the concentrations follow a normal distribution while the frequency distributions for ^{238}U and ^{232}Th activity concentrations exhibit multimodality, as shown in Figures 9(b) and 10(b). The activity concentration of ^{40}K indicates a normal distribution (Figure 11(b)).

3.3.2. Pearson's Correlation Coefficient Analysis. One of the statistical analysis methods that measures the strength and direction of a linear relationship between two variables is the Pearson correlation coefficient (PCC). By using this method, the degree of association among the measured radiological parameters was determined. The PCC result value r is found in the range of −1 to 1 [27, 43]. Using the Pearson correlation matrix, the correlation between ^{238}U and ^{232}Th, ^{238}U and ^{40}K, and ^{232}Th and ^{40}K, along with their correlations with hazard indexes of D, Ra_{eq}, and AEDR, was estimated.

The Pearson correlation result for ^{238}U and ^{232}Th is close to one, which is $r = 0.98$, indicate that the two radioactive nuclides have strongly positive correlations (Figure 12(a)). For ^{238}U and ^{40}K, the Pearson correlation value is 0.86, indicate a strong positive relation (Figure 12(b)). As shown in Figure 12(c), for ^{226}Th and ^{40}K, the correlated value is $r = 0.87$, indicate a strong positive direction relation. In general, the radionuclides of the ^{238}U, ^{232}Th, and ^{40}K decay

series exhibit strong positive proportional correlation over the given decay time.

As shown in Figures 12(a), 12(b), and 12(c), the Pearson correlation plots have shown a normal distribution of ^{238}U, ^{232}Th, and ^{40}K in Bambasi soil. Their quantities by concentration are directly proportional, especially for ^{238}U and ^{232}Th at soil collected sites in the Bambasi district. The correlated values between uranium (^{238}U) with radium equivalent (Ra_{eq}), absorbed dose rate (D), and annual effective dose equivalent (AEDE) are 0.59, 0.99, and 0.99, respectively, indicate a strong positive directional correlations (Figures 13(a), 13(b), and 13(c)).

4. Conclusions

The mean activity concentration of ^{238}U and ^{232}Th and the absorbed dose rate values of all soil samples exceed their respected safe values; therefore, the natural radioactivity concentrations found in Bambasi district soils need further investigations. Also, the indoor annual effective dose rate values critically surpassed the recommended world annual average safe values. From the measured values, natural radioactivity concentration level of ^{238}U and ^{232}Th in all soil samples exceeds the recommended safe values, and precautions or safety measures are necessary around Bambasi district to avoid significant health problems on the community. From comparison of the radioactivity levels of Bambasi district soil samples with similar studies from different countries provinces, it can be concluded that continuous monitoring is necessary for Bambasi district soil.

Data Availability

Data are available upon reasonable request to the corresponding author.

Conflicts of Interest

The authors declare that they have no conflicts of interest.

Authors' Contributions

Yared Birhane has done sample preparation, data analysis, data interpretation, and manuscript writing. Yared Birhane and Dr. Tilahun Tesfaye have contributed to the study's conception, design, and manuscript revision. Both Yared Birhane and Guadie Degu have contributed to the selection of the study area and sample collection.

Acknowledgments

The authors would like to thank Assosa University and Addis Ababa University for supporting the research and also Ethiopian Conformity Assessment Enterprise (ECAE) staff members and Ethiopian Technology Authority (ETA) for the experimental work using the HPGe detector. The research was partly funded by Assosa University and Addis Ababa University.

References

[1] United Nations Scientific Committee on the Effects of Atomic Radiations-Unscear, "Sources and effects of ionizing radiation," Report to General Assembly, with Scientific Annexes United Nations, New York, 2000, https://pubmed.ncbi.nlm.nih.gov/11281539/.

[2] J. Singh, H. Singh, S. Singh, B. S. Bajwa, and R. G. Sonkawade, "Comparative study of natural radioactivity levels in soil samples from the Upper Siwaliks and Punjab, India using gamma-ray spectrometry," *Journal of Environmental Radioactivity*, vol. 100, no. 1, pp. 94–98, 2009.

[3] M. A. M. Uosif and A. El-Taher, "Radiological assessment of abu-tartur phosphate, western desert Egypt," *Radiation Protection Dosimetry*, vol. 130, no. 2, pp. 228–235, 2007.

[4] International Atomic Energy Agency-Iaea, "Measurement of radionuclides in food and the environment," 1989.

[5] R. Elsaman, M. A. A. Omer, El-M. Mahmoud Seleem, and A. El Taher, "Natural radioactivity levels and radiological hazards in soil samples around abu karqas sugar factory," *Journal of Environmental Science and Technology*, vol. 11, pp. 28–38, 2018.

[6] O. A. Ebyan, H. A. Khamis, A. R. Baghdady, M. G. El-Feky, and N. S. Abed, "Low-temperature alteration of uranium–thorium bearing minerals and its significance in neoformation of radioactive minerals in stream sediments of Wadi El-Reddah, Northeastern Desert, Egypt," *Acta Geochimica*, vol. 39, no. 1, pp. 96–115, 2019.

[7] H. Samia and Taha Osama Sallam Abd Elhadi A Abbas Neveen Abed, "Radioactivity and environmental impacts of ferruginous sandstone and its associating soil," *International Journal of Environmental Analytical Chemistry*, 2022.

[8] L. Ntsohi, I. Usman, R. Mavunda, and O. Kureba, "Characterization of uranium in soil samples from a prospective uranium mining in Serule, Botswana for nuclear forensic application," *Journal of Radiation Research and Applied Sciences*, vol. 14, no. 1, pp. 23–33, 2021.

[9] C. Smith, *Routledge Introductions to Environment Environmental Physics*, Routledge, Taylor and Francis Group, London, UK, 2001.

[10] J. Markovic and S. Stevovic, "Radioactive isotopes in soils and their impact on plant growth," 2018, Metals in Soil - Contamination and Remediation.

[11] S. Tikuye Yalew and B. Fantahun, "Prevalence of bovine trypanosomosis and its associated risk factors in Bambasi woreda, Western Ethiopia," *Journal of Dairy, Veterinary and Animal Research*, vol. 5, no. 2, pp. 44–49, 2017.

[12] L. A. Bullock and O. Morgan, "The geologists' association and the geological society of london," *Geology Today*, vol. 34, p. 1, 2018.

[13] G. Alzubaidi, F. B. S. Hamid, and I. Abdul Rahman, "Assessment of natural radioactivity levels and radiation hazards in agricultural and virgin soil in the state of Kedah, North of Malaysia," *The Scientific World Journal*, vol. 2016, no. 9, pp. 1–9, 2016.

[14] J. Beretka and P. Mathew, "Natural radioactivity of Australian building materials, industrial wastes and by-products," *Health Physics*, vol. 48, no. 1, pp. 87–95, 1985.

[15] International Atomic Energy Agency-Iaea, "Nuclear medicine physics: a handbook for students and teachers," 2014.

[16] Organization for Economic Cooperation and Development-Oecd, *Nuclear Energy Agency (NEA-OECD)*, Exposure to Radiation from Natural Radioactivity in Building Materials, Paris, France, 1979.

[17] European Commission-Ec, *Radiological Protection Principles Concerning the Natural Radioactivity of Building Materials*, Radiation Protection Report—RP-112, European Commission, Brussels, Luxembourg, 1999.

[18] M. Rafique, A. Jabbar, A. R. Khan et al., "Radiometric analysis of rock and soil samples of Leepa valley; Azad Kashmir, Pakistan," *Journal of Radioanalytical and Nuclear Chemistry*, vol. 298, no. 3, pp. 2049–2056, 2013.

[19] G. O. Avwiri, S. A. Olatubosun, and C. P. Ononugbu, "Evaluation of radiation hazard indices for selected dumpsites in Port Harcourt, Rivers State, Nigeria," *International Journal of Science and Technology*, vol. 3, no. 10, 2014.

[20] H. M. Taskin, M. Karavus, P. Ay, A. Topuzoglu, S. Hidiroglu, and G. Karahan, "Radionuclide concentrations in soil and lifetime cancer risk due to gamma radioactivity in Kirklareli, Turkey," *Journal of Environmental Radioactivity*, vol. 100, no. 1, pp. 49–53, 2009.

[21] International Cooperation for Radiation Protection-ICRP, "International commission on radiological protection," *Annals of the ICRP*, no. 37, pp. 2–4, 2007, https://www.icrp.org/page.asp.

[22] A. Bramki, M. Ramdhane, and F. Benrachi, "Natural radioelement concentrations in fertilizers and the soil of the Mila region of Algeria," *Journal of Radiation Research and Applied Sciences*, vol. 11, no. 1, pp. 49–55, 2018.

[23] R. W. Dutra Garcêz, J. Marques Lopes, S. da Silva Perez et al., "Activity concentration and mapping of radionuclides in Espírito Santo State soils, Brazil," *Radiation Physics and Chemistry*, vol. 167, 2020.

[24] J. Yang and Y. Sun, "Natural radioactivity and dose assessment in surface soil from Guangdong, a high background radiation province in China," *Journal of Radiation Research and Applied Sciences*, vol. 15, no. 1, pp. 145–151, 2022.

[25] N. Kekelidze, T. Jakhutashvili, B. Tutberidze, E. Tulashvili, M. Akhalkatsishvili, and L. Mtsariashvili, "Radioactivity of soils in Mtskheta-Mtianeti region (Georgia)," *Annals of Agrarian Science*, vol. 15, no. 3, pp. 304–311, 2017.

[26] A. K. Amanjeet, A. Kumar, S. Kumar, J. Singh, P. Singh, and B. Bajwa, "Assessment of natural radioactivity levels and associated dose rates in soil samples from historical city Panipat, India," *Journal of Radiation Research and Applied Sciences*, vol. 10, no. 3, pp. 283–288, 2017.

[27] A. H. Taqi and B. F. Namq, "Radioactivity distribution in soil samples of the Baba Gurgur dome of Kirkuk oil field in Iraq," *International Journal of Environmental Analytical Chemistry*, pp. 1–19, 2022.

[28] L. Guidotti, F. Carini, R. Rossi, M. Gatti, R. M. Cenci, and G. M. Beone, "Gamma-spectrometric measurement of radioactivity in agricultural soils of the Lombardia region, Northern Italy," *Journal of Environmental Radioactivity*, vol. 142, pp. 36–44, 2015.

[29] C. C. Mbonu and U. C. Ben, "Assessment of radiation hazard indices due to natural radioactivity in soil samples from Orlu, Imo State, Nigeria," *Heliyon*, vol. 7, no. 8, 2021.

[30] A. Łukaszek-Chmielewska, M. Girard, O. Stawarz, B. Piotrowska, K. Wojtkowski, and K. Isajenko, "Measurements of natural radioactivity in soil samples collected in the Kampinoski National Park," *E3S Web of Conferences*, vol. 100, Article ID 00052, 2019.

[31] F. B. Masok, P. L. Masiteng, R. D. Mavunda, P. P. Maleka, and H. Winkler, "Measurement of radioactivity concentration in soil samples around phosphate rock storage facility in Richards Bay, South Africa," *Journal of Radiation Research and Applied Sciences*, vol. 11, no. 1, pp. 29–36, 2018.

[32] G. Bilgici Cengiz, "Natural radioactivity analysis in soil samples of Ardahan province, Turkey for the assessment of the average effective dose," *Sakarya Üniversitesi Fen Bilimleri Enstitüsü Dergisi*, vol. 2, no. 6, pp. 1583–1590, 2017.

[33] A. Durusoy and M. Yildirim, "Determination of radioactivity concentrations in soil samples and dose assessment for Rize Province, Turkey," *Journal of Radiation Research and Applied Sciences*, vol. 10, no. 4, pp. 348–352, 2017.

[34] B. K. Yared, D. Tilahun Tesfaye, and B. Guadie Degu, "Evaluation of radioactivity level in soil samples from Assosa city in Benishangul Gumuz region, Ethiopia," *Environmental Forensics*, 2024.

[35] S. Turhan, "Assessment of the natural radioactivity and radiological hazards in Turkish cement and its raw materials," *Journal of Environmental Radioactivity*, vol. 99, no. 2, pp. 404–414, 2008.

[36] H. El-Gamal, E. Sidique, and M. El-Haddad, "Spatial distributions and risk assessment of the natural radionuclides in the granitic rocks from the Eastern Desert, Egypt," *Minerals*, vol. 9, no. 7, p. 386, 2019.

[37] N. S. Abed, M. G. El Feky, A. El-Taher et al., "Geochemical conditions and factors controlling the distribution of major, trace, and rare elements in sul hamed granitic rocks, Southeastern Desert, Egypt," *Minerals*, vol. 12, no. 10, p. 1245, 2022.

[38] S. A. Okasha, A. A. Faheim, M. H. E. Monged, M. R. Khattab, N. S. Abed, and A. A. Salman, "Radiochemical technique as a tool for determination and characterisation of El Sela ore grade uranium deposits," *International Journal of Environmental Analytical Chemistry*, vol. 103, no. 4, pp. 737–746, 2023.

[39] A. El-Taher, "INAA and DNAA for uranium determination in geological samples from Egypt," *Applied Radiation and Isotopes: Including Data, Instrumentation and Methods for Use in Agriculture, Industry and Medicine*, vol. 68, no. 6, pp. 1189–1192, 2010.

[40] A. I. Amasi, K. M. Mtei, I. J. Nathan, P. Jodłowski, and C. N. Dinh, "Natural radioactivity in Tanzania Cements and their raw materials," *Research Journal of Environmental and Earth Sciences*, vol. 6, no. 10, pp. 469–474, 2014.

[41] F. Steinhausler, "The natural radiation environment: future perspective," *Radiation Protection Dosimetry*, vol. 45, no. 1-4, pp. 19–23, 1992.

[42] C. C. Arwui, G. Emi-Reynolds, and E. O. Darko, "Natural radioactivity and its associated radiological hazards in Ghanaian cement," *Research Journal of Environmental and Earth Sciences*, vol. 3, no. 2, pp. 161–167, 2018.

[43] S. Turney, "Pearson correlation coefficient (r) guide and examples," 2023.

DECLARATION

ADDIS ABABA UNIVERSITY
COLLEGE OF NATURAL AND COMPUTATIONAL SCIENCES
DEPARTMENT OF PHYSICS

PhD Dissertation

Measurement of Radioactivity Concentrations
and Analysis of Radiation Hazards
for Environmental and Industrial Samples
Collected from Different Parts of Ethiopia

Name of Candidate: Yared Birhane Kidane

I the under signed declare that the thesis is my original work and no part of it can be claimed as an intellectual property of anybody else except me and my advisors.

Signature: _____